Stress Analysis and Fabrication of Composite Monocoque Bicycle Frames

By:

Patrick L. Lizotte
Department of Mechanical Engineering
McGill University, Montréal

A Thesis Submitted to the Faculty of Graduate Studies and Research in Partial Fulfillment of the Requirements of the Degree of Master of Engineering

ISBN 0-612-19874-X

Canada

To my parents, Lise and Georges...

Abstract

An analytical and experimental investigation was conducted to study the design and fabrication of carbon fiber track bicycle frames. A finite element software was used for the geometry development, laminate configuration, and for predicting failure using the maximum stress criteria. A load case and boundary conditions simulating actual riding conditions were developed. The stresses in each of the composite layers were found to be lower than the allowable stresses because of a properly designed geometry and laminate. Two composite frames were fabricated using the hand lay-up technique, using unidirectional and woven carbon fiber pre-preg material over an internal foam core. Using static testing techniques and comparisons with traditional tubular frames, the carbon fiber prototypes were shown to be better in all rigidity aspects. Combining the experimental and theoretical results, a good understanding of the critical problems related to composite monocoque bicycle frame design was obtained.

Résumé

Une étude analytique et expérimentale a été faite pour étudier la conception et la fabrication de vélos de piste faits de fibre de carbone conçus et fabriqués au terme de cette recherche. Un logiciel d'éléments finis a été utilisé pour le developpement de la géométrie, du laminé et pour prédire la rupture en utilisant le critère de contrainte maximale. Un système d'efforts et d'encastrements simulant des conditions d'utilisation a été développé et utilisé. Les contraintes dans chacuns des plis sont ainsi obtenus et sont inférieures aux containtes permises grâce à une géométrie et un laminé bien conçus. Les cadres de composite sont fabriqués en utilisant le moulage à la main du préimprégné de fibre de carbone unidirectionnel et tissé sur un moule interne de mousse. Les prototypes de fibre de carbone sont ensuite testés de façon statique et comparés à des cadres traditionnels. Les résultats de ces tests montrent que les cadres de carbone sont supérieurs sur tous les plans de la rigidité. En combinant les résultats expérimentaux et théoriques, on obtient une bonne connaissance des problèmes critiques reliés aux cadres de vélos monocoques faits de composite.

Acknowledgments

I wish to thank my thesis supervisor Prof. Larry Lessard for his constant help and insight through this work. Also special thanks to Prof. James Nemes for his availability and guidance. I am also grateful to the technicians George Dedik, George Tewfik, Gary Savard and Louis Hueppin for their generous and rapid help in the many situations which arose. I wish to thank the exchange students Fabrice Gattone, Christian Bourget, Jean-Philippe Tizi and Richard Devallé of the Ecole Nationale d'Ingénieurs de Metz (ENIM) in France for their help in model development using finite-element analysis. My gratitude also extends to Philip White for his help in the construction of the 2 prototypes and to Richard Langlois of the Centre des Matériaux Composites de St-Jérome for allowing us to use their facilities for the final composite layup and curing of the two prototypes. Also my sincere thanks to the many undergraduate students who worked on various aspects of this project such as the curing jig construction, and the static jig construction, and to Jerry Chabot for his work on the static testing of metallic frames. I also wish to thank Mahmood Shokrieh, Hamid Eskandari, Louis Brunet, Gérard Vroomen, Jean-François Milette, Sylvain Riendeau, Ann-Louise Lock and all the other past and present members of the Composites Materials Group for their continued help, laughter and support. I would also like to thank all my friends: Martin, Nicolas, Louis, Yvan, Pierre, Pierre-André, Stéphane, Nathalie, Francois, Mathieu, Matthieu, Paul, Benoit, Zaz, Dave, Sébastien, Claude, Marie-Josée, Jocelyn, and all the ones I forget, who during the time I have spent doing this work, stood by closely and continually helped me to move forward. Et merci particulièrement à toi Julie qui a illuminé ma vie durant le sprint final. Last but certainly not least, sincere thanks to my parents Lise and Georges, my sister Martine and the rest of my family who have continually encouraged and supported me in anything I dived into. Thanks again to everyone.

Table of Contents

List of Symbols

ε : Strain
σ : Stress
σ_{100N} : Stress at 100N force
ω : Angular velocity
A : Area
C : Couple at the bottom bracket
C_x : Aerodynamic drag coefficient
E : Young's Modulus
E_o : Wheatstone bridge output
$E_{o,\,total}$: Wheatstone bridge total output
E_x : Supply voltage
F : Force
F_1 : Load applied by the front wheel on the frame
F_2 : Load applied by the rear wheel on the frame
F_p : Downward force on pedals
F_t : Upward force on the pedals
F_{wind} : Wind resistance
p : Air density
P : Power
P_{air} : Power lost due to air resistance
$P_{cyclist}$: Power input from cyclist
P_{total} : Total power
r : Radius
R_1 : Load on front wheel
R_2 : Load on rear wheel
S : Bike + cyclist frontal area
t : Time
T : Pulling force on handlebars
T_1 : Pulling force from the rider's right hand
T_2 : Pulling force from the rider's left hand
W : Weight of the rider

List of Figures

Chapter 2

Chapter 3

Chapter 4

Chapter 5

List of tables

Chapter 3

Chapter 4

Chapter 5

Chapter 1

Introduction

The use of advanced composite materials is becoming increasingly common. They are used in numerous applications ranging from aerospace products to sports equipment. The sporting goods industry in particular has turned to advanced composites recently in sports such as cycling, hockey, and golf. The cycling industry adopted composites more than 10 years ago in the construction of high performance frames. The use of advanced composites materials in this industry has led to changes in the materials, geometry and construction technique of bicycle frames. Advanced composites are being used in frame construction because they allow improvements in weight, stiffness, strength, and aerodynamics.

Bicycles have been part of everyday life for more than 100 years now. They constitute a vital means of transportation for some, a pastime for others, and a high level competition machine for a few. International racers are continually seeking frames which perform better in order to ultimately achieve higher speeds for the same amount of frame energy input. To achieve this goal, advanced composite materials have been used in the making of high tech frames for some years now. However, in order to design and manufacture a frame with these materials, a thorough engineering knowledge of composite materials, combined with a means of analyzing a structure as complex as a bicycle frame, is essential.

1.1 Objective

The first main goal of the research was to understand composite frame design through finite element analysis. This analysis was helpful for the determination of strength and stiffness parameters for a frame without actually building it. The stiffness results were then

compared with a data bank of existing traditional diamond shape frames made of steel and aluminum in order to make sure that the stiffnesses (torsion, in-plane, out-of-plane) were improved. The second main goal was the development of a manufacturing technique for composite prototype frames. Two monocoque carbon fiber frames were constructed using this technique. After the composite frames were constructed, they were statically tested to compare their respective stiffnesses with their finite element models.

Chapter 2

Literature Review

2.1 Review of Bicycle Frame History

It is believed that people have been thinking about building human powered vehicles since the fifteenth century. A sketch named *Codex Atlanticus* [1] shown in Figure 2.1 and attributed to Leonardo Da Vinci shows a device resembling a bicycle with pedals, a crank and a chain drive connected to the rear wheel. This vehicle however did not have steering, hence would have been unstable and thus could not have been ridden.

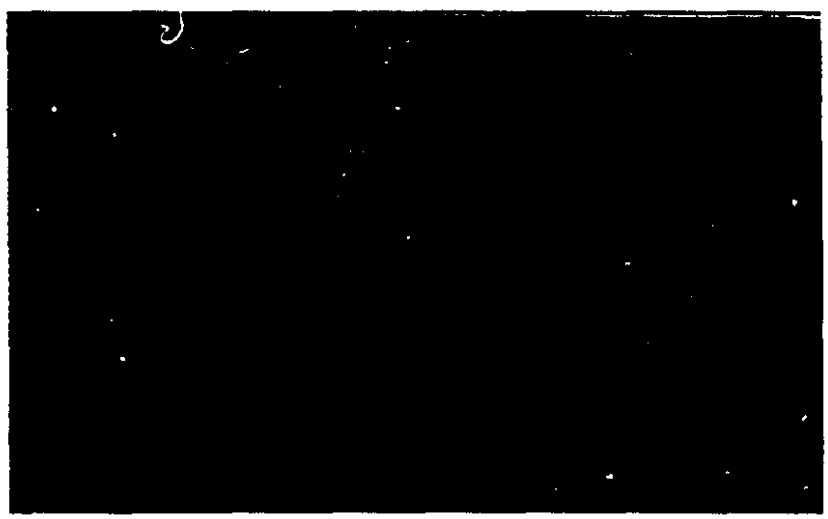

Figure 2.1 : Leonardo Da Vinci's Bicycle from the *Codex Atlanticus* [1]

By the beginning of the 1800's, unsteerable two-wheelers referred to as hobby horses appeared in England [2]. The problem with these machines is that they could not be balanced going down a hill at high speed as they could not be steered. Thus possibly the most important invention in bicycle frame design was made by the German Karl Von Drais

who discovered (possibly by error) that a front steering hobby horse could be balanced going down a hill at high speed. In 1817 he built the *Draisienne* shown in Figure 2.2 [3].

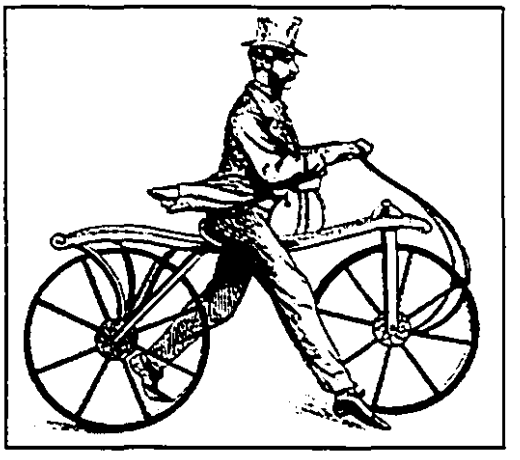

Figure 2.2 The *Draisienne* [3]

The ensuing evolution in bicycle design was driven by the need to use the legs in an efficient way in order to propel the rider at the highest speed possible. The lack of an appropriate chain drive combined with the road conditions at the time (which would have made a chain drive unusable even if it existed), led to the appearance of the *Ordinary* bicycle (high wheeler) shown in Figure 2.3 [4].

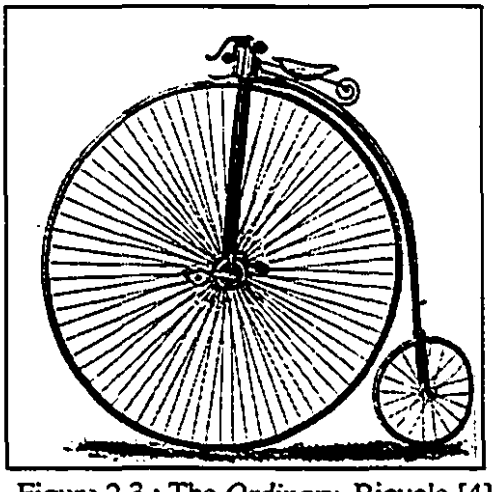

Figure 2.3 : The *Ordinary* Bicycle [4]

The driving front wheel was made as large as comfortable pedaling would allow in order to provide the maximum distance for each pedaling revolution and hence the highest speed possible. The size of the front wheel was dictated by the length of one's legs. A large *Ordinary* could have a driving wheel in excess of 1.5m in diameter. The 1870's were the years of dominance of these high wheelers. But severe injuries to those who fell and the impracticalities that prevented women with dresses and short or unathletic people to ride these machine combined with the appearance of suitable chain drives led to the more

conventional *Safety* bicycle. The *Safety* bicycle was called as such because it was much safer than the *Ordinary*. The first *Safety* bicycle was introduced in 1869 at the first Paris velocipede show by Andre Guilment [5]. However the direct descendants of today's bicycles were built and presented in the early 1880's at Britain's Annual Stanley Bicycle Show by Starley. By 1886, these Starley *Safety* bicycles had ball bearing direct steering, rubber tires and a diamond geometry very close to what we know today. Figure 2.4 shows the Starley *Safety* bicycle [6]. The decades that followed led to refinement in the materials, design, components and construction methods up to what we know today.

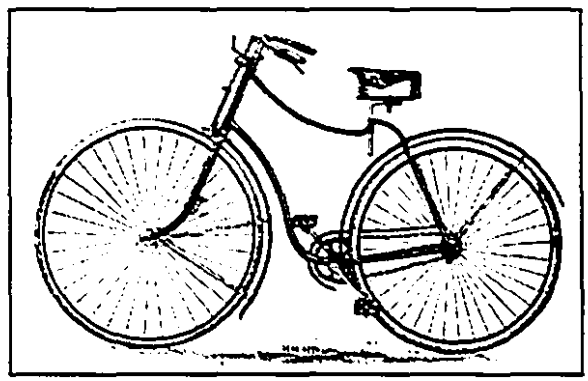

Figure 2.4 : Starley *Safety* Bicycle [6]

After the appearance of cars and motorcycles relying on the internal combustion engine, bicycle popularity as a means of transportation decreased in some countries, including Canada and the United States. But in the 1960's, North-America experienced the early signs of a bicycle revolution. Sport bikes with multiple gearing were introduced into the adult market. Cycling was then promoted as an adult activity and as a legitimate sport that would foster cardiovascular health. This revolution gave every indication of being broad-based, deep, and diverse. Millions of people are now riding bikes for exercise and transportation, and the market is alive with inventiveness. Large and small scale manufacturers are introducing new bicycle frames, components, and systems at a rapid rate. Cities are building more and more bicycle paths in order to accommodate the increasing traffic and the sales of bicycles are ever increasing. We are thus in the middle of a "cycling frenzy" that the world has never experienced before which is favorable to research into bicycle design.

2.2 Review of Frame Building Materials

Throughout the years, frame building materials have evolved from what we now think as very primitive materials to space age materials which were unknown to our society only 30 years ago. It is this improvement in materials which allowed to the greatest extent the evolution in bicycle frame design. This section will review most of the frame building materials which have been used in the past. It will show the advantages and disadvantages of the different materials and explain the apparition and disappearance of some of them. This analysis will help to rationalize the use of carbon fiber material for use in this project.

2.2.1 Wood

Wood was used in the very first bicycle frames produced. Von Drais' *Draisienne* and most other hobby horses in the 1800's were made of wood [7]. Since a minimum stiffness was required in order to prevent enormous bending and potential collapse, heavy wood was often used resulting in very heavy structures. This combined with the tremendous work required to shape the wood made designers and builders quickly realize that this material was not the solution, even though some good wood frames were successfully built. Around the 1870's, metal construction became dominant, but wood continued to be used sporadically in the construction of frames, rims, and mudguards even until the 1930's. At some point, bamboo was used in the construction of frames [7]. Figure 2.5 shows a bamboo frame from 1870. However because of the scarcity of this wood in the cities, and the increasing use and understanding of steel, wood and bamboo frames have completely disappeared.

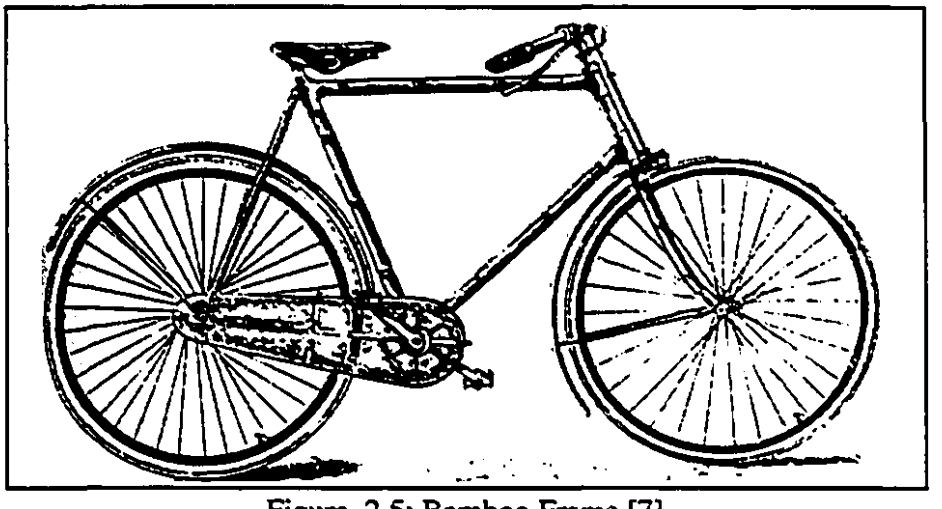

Figure. 2.5: Bamboo Frame [7]

2.2.2 Steel

Without question, the use of steel in the past century of bicycle frame construction has been dominant. Many different alloys of steel ranging from low-carbon steels for inexpensive frames to proprietary steel alloys of chrome-molybdenum-manganese for the best competition frames have been used. Currently, inexpensive frames are made from straight-gauge tubes formed from steel strips, rolled and welded along the seam and later welded to the other tubes of the frame. Better frames are made from seamless tubes, drawn thinner in the middle than at the ends (butting) and silver brazed into close fittings tapered at the tube intersections. The butting of tubes is now considered a science and tube manufacturers have developed double and triple-butted tubes as well as circumferentially butted tubes (differential shape butting) [8] in order to allow material to be present only where it is really required. Frame builders appreciate steel's user-friendliness. It offers so many variables of diameter, wall thickness, shape and metallurgy that it is almost possible to tune the riding of a steel frame to the rider's desire. Tubing manufacturers such as Tange, Reynolds, and Columbus have a complete selection of tube sets of different cross section and using different alloys. As in the case of other metallic materials, the rigidity and weight of a frameset is driven by the shape of the tubes while the strength is dictated by metallurgy, heat treatment, and/or mechanical cold working. The strongest bicycle steel available is the French-made EXCELL. It has a tensile strength of more than 1380MPa.

Among the advantages of using steel includes the fact that it is ideal for custom design, as different tubesets can be chosen to provide different riding characteristics for each rider. Steel also possesses traditional beauty and can in certain cases highlight beautiful craftsmanship. Also, steel has remained relatively inexpensive and readily available over the years. Steel frames do not fail catastrophically without indication and they possess the attractive property of having a *fatigue limit*. A *fatigue limit* is defined as the stress level below which a material will never fail under fatigue loading. It reveals the region close to failure with cracks that widen slowly in order to allow for an early detection of possible failure. If it does break, it is very easily repaired by heating a few joints, popping out the damaged tube and replacing it with a new one. All in all steel is a very convenient frame building material, but because of its high density, it is tied to the diamond shape frame design and in this way is condemned to frame shapes and geometries that go back to the 19th century. Figure 2.6 shows the traditional diamond shape structure and Figure 2.7 the

basic dimensions of a bicycle frame. Steel does not allow frame designers to depart from the diamond shape geometry and experiment with new shapes.

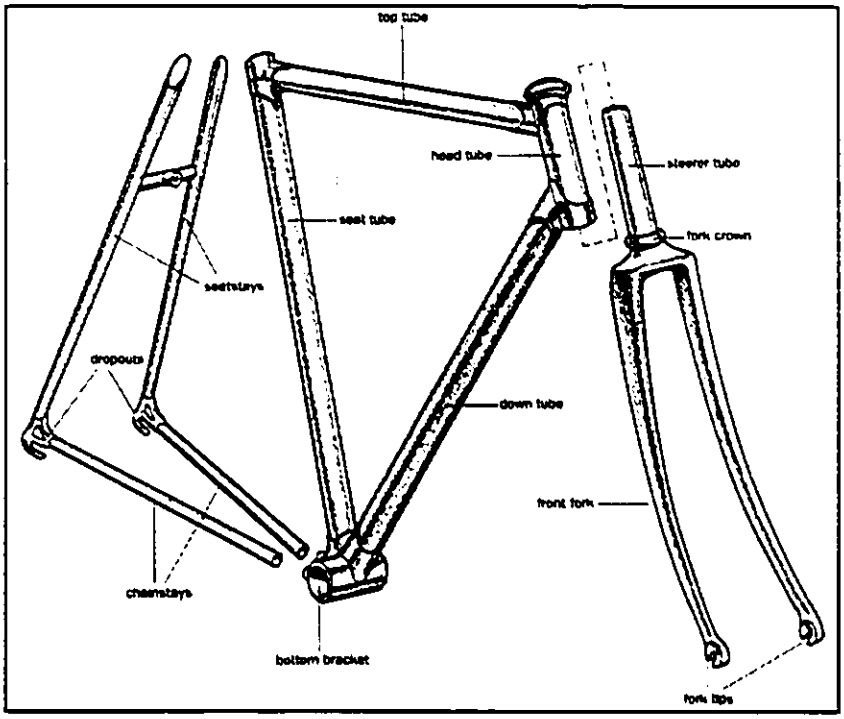

Figure 2.6: Traditional Diamond Shape Structure [9]

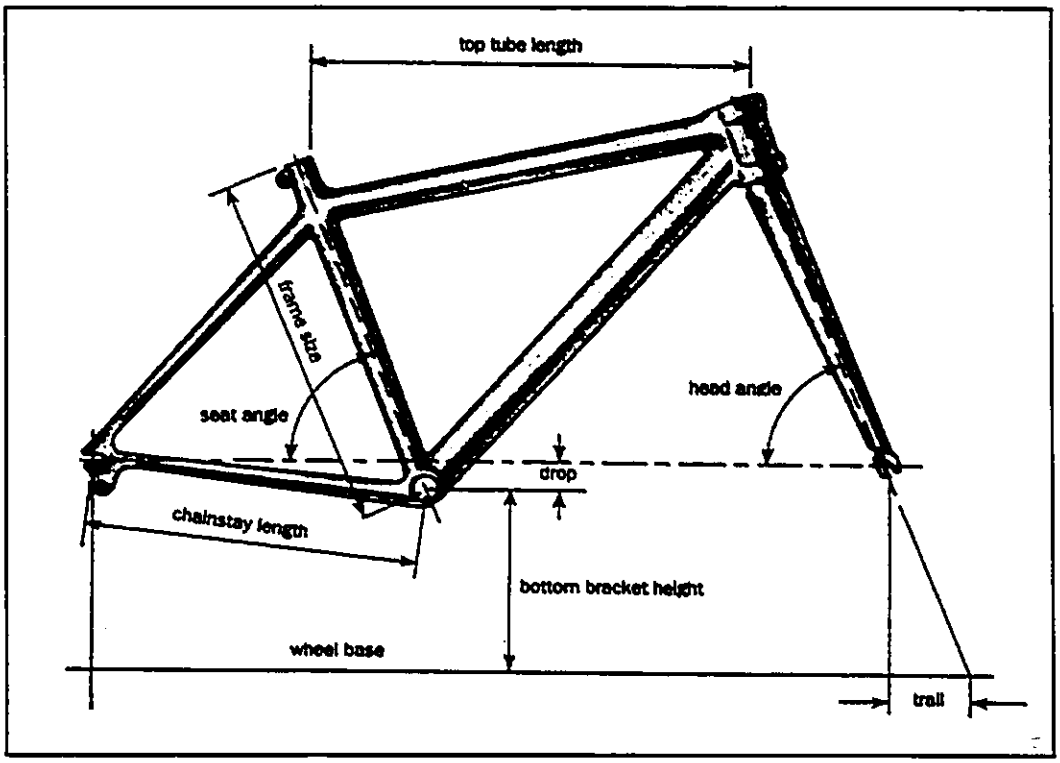

Figure 2.7 : Basic Dimensions of Traditional Frames [10]

2.2.3 Aluminum

The first experimentation with aluminum frames occurred in the 1890's [11]. The early frames were made from cast aluminum. The tubes were joined together with lugs as the welding of aluminum was not well known at that time. Aluminum tubes are now brazed, welded or adhesivelly bonded together. Since aluminum has a modulus lower than steel, oversize tubes may be required in order to provide a rigidity comparable to a steel frame [12]. However because of its lower density, even larger diameters and wall thicknesses do not result in a heavier frame. As we increase the diameter of the tube the rigidity increases to the 4th power of the diameter while the weight increases following the square of the diameter. Hence it is possible to ootain a rigid and light frame with aluminum. Early, poorly designed aluminum frames helped to build a bad reputation for aluminum frames. In fact, early aluminum frames tended to fail at the tube joints from improper welding or bonding and also from fatigue failures as aluminum has no *fatigue limit* as is the case with steel and titanium. The fact that this material does not have a *fatigue limit* requires the frames to be slightly overdesigned in order to compensate for this property of the material. Aluminum is relatively inexpensive, light and adequately strong. One of the major advantages of aluminum over steel frames is that it is non-corrosive. If properly designed and built, aluminum frames can be as stiff and lively as steel frames and are now among the lightest frames on the market. However, as opposed to steel frames, these frames are not easily repaired and do not look traditional with their often oversized tubes. As with steel, aluminum is relatively dense compared to composites and is thus tied to the traditional diamond shape structure. It would be practically impossible to depart from the traditional diamond shape structure while still using aluminum.

2.2.4 Titanium

The first use of titanium in frame construction occurred in the early 1970's. Titanium offers bicycle designers a material 62% stiffer than aluminum but 42% lighter than steel [12]. Titanium frames are amongst the lightest frames on the market at the present time. Titanium frames are usually made from commercially pure titanium (0.2% oxygen added to pure titanium) or from 3Al/2.5V (3% aluminum and 2.5% vanadium) alloy tubes. These tubes are usually bought from aircraft and chemical company suppliers which sell these tubes usually as corrosion resistant plumbing for these industries [13]. Figures 2.8, 2.9,

2.10 and 2.11 show the densities, specific moduli, and specific strength and price of 5 of the most popular frame building materials.

The high cost of titanium (see Figure 2.11) comes from the difficulty in extracting the material out of the rutile ore (TiO_2) as well as the stringent quality control procedures for components destined for the aircraft industry. However, some tubing manufacturers are now producing "recreational grade" titanium alloy tubes. This grade has only the applicable properties sufficient for use of the material in bicycles. Another factor which adds to the high price of titanium frames is that titanium can only be welded in an inert atmosphere (typically argon) since molten titanium instantly reacts with oxygen [14]. The availability of the tubes still being somewhat limited, the designs are limited by the available tubes.

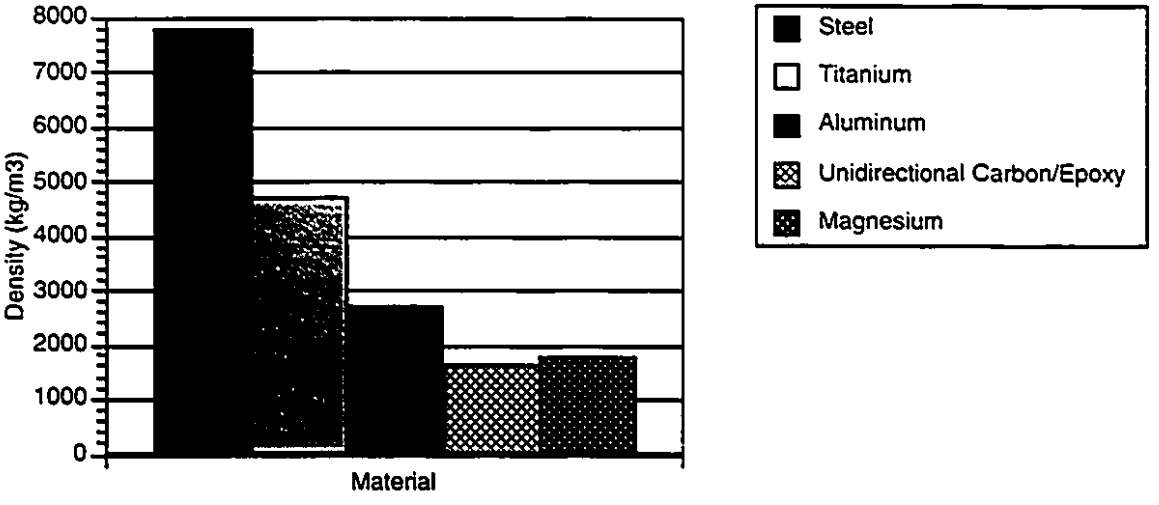

Figure 2.8: Material Densities of 5 Frame Building Materials [15]

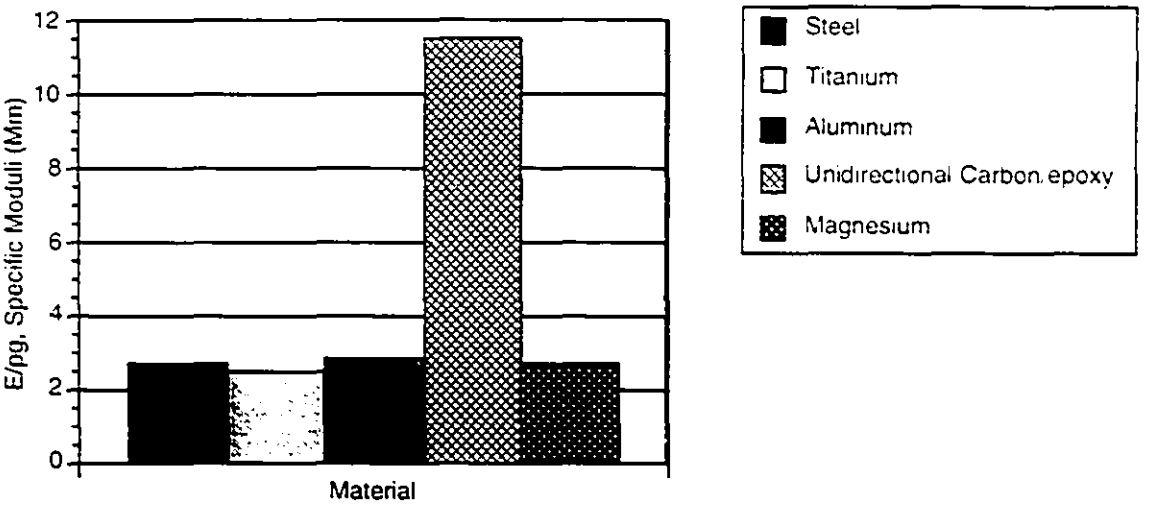

Figure 2.9: Specific Moduli of 5 Frame Building Materials [15]

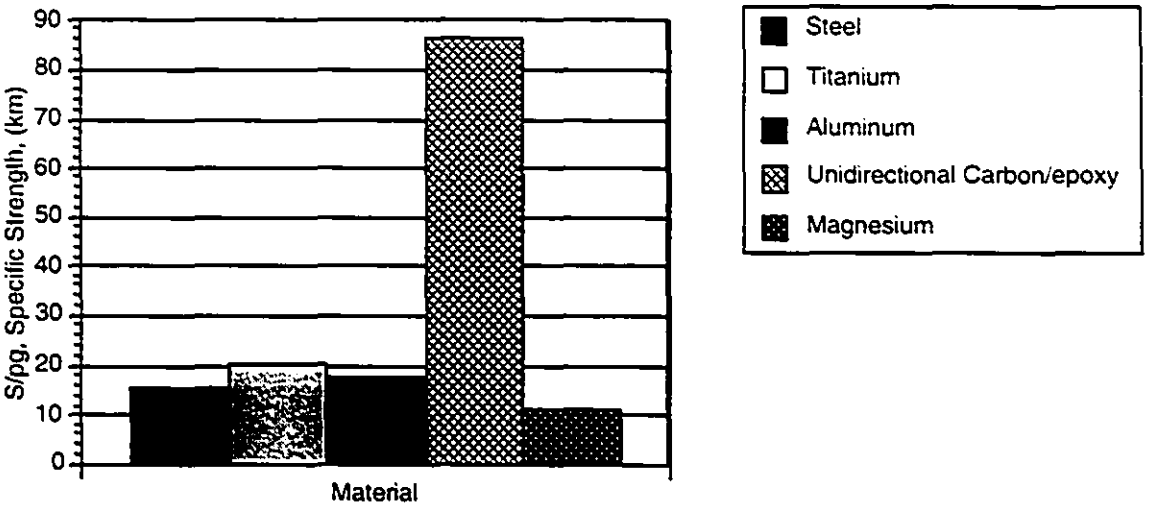

Figure 2.10: Specific Yield Strength of 5 Frame Building Materials [16]

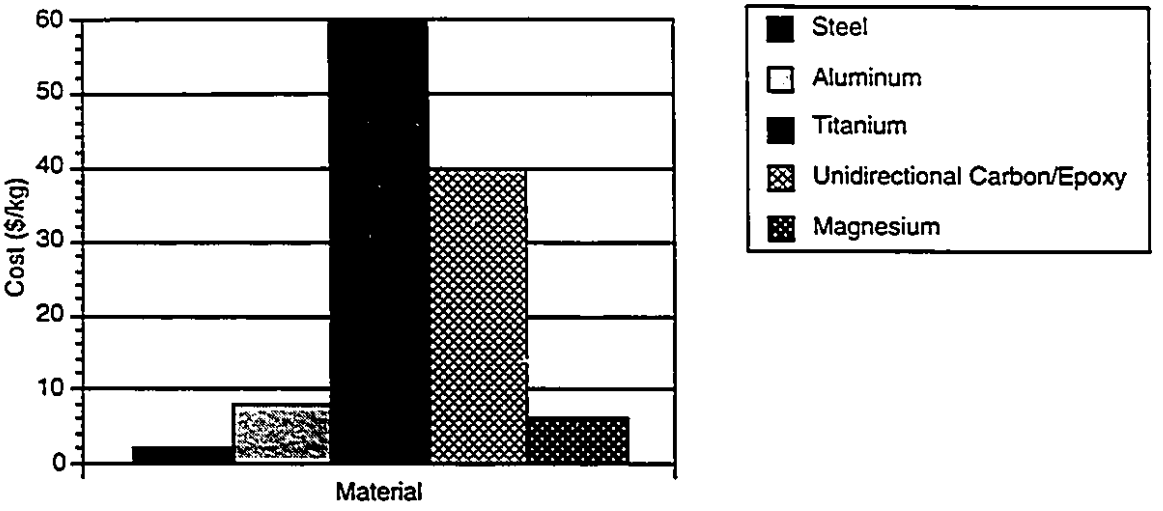

Figure 2.11 Price per Kilogram of Material of 5 Frame Building Materials

Since the stiffness of titanium is moderate (between that of steel and aluminum), tubes of larger diameter than steel are often used in the design of rigid frame structures. Although the structure is rigid, a nice property of titanium is that it still offers a very comfortable and lively ride. Like steel, titanium has a defined *fatigue limit* and thus at stress levels below this limit, the frame will never degrade. If they do wear out, they are not easily repaired because welding of titanium is a difficult process. Although many describe titanium as being corrosion resistant, this notion is somewhat misleading. Actually it reacts very easily with oxygen (hence oxides, or corrodes), but the titanium oxide actually forms a tenacious surface layer that coats the underlying material against further intrusion [14] thus it needs no paint and always looks new. The qualities of titanium in frame construction has prompted many riders to adopt titanium as the material of choice for their frames.

2.2.5 Magnesium

Magnesium is the only other metallic material likely to be considered for bicycle frame construction. The attractive property that lures designers to use magnesium is its low density (66% of that of aluminum), but equivalently its modulus is only 63% of aluminum. Hence if tubular sections are chosen for a magnesium frame they will tend to be of very large diameter. Magnesium has been used in the production of frames by KIRK Precision Racing Bikes [17]. They designed a cast magnesium frame with the "tubes" shaped as I-beams for increased rigidity due to the low modulus of the material [18]. It is interesting to note that the availability of magnesium is quasi-infinite as it can be extracted from sea water at a cost which is very reasonable. One KIRK frame uses the magnesium extracted from 1

cubic meter of sea water and costs half as much to make as an aluminum, steel, or composite frame [17]. But as the modulus and strength of magnesium is quite low, this material will possibly never be used extensively as a frame building material.

2.2.6 Plastics

Since the advent of large molding capability for plastics, there have been several attempts to mold plastic bicycle frames. The Itera plastic bicycle from Sweden was commercialized in 1982 [19]. Although this injection-molded bicycle had high projected sales, the project failed completely because people were not ready for a radical change in bicycle shape and riding feel, as plastic allowed a departure from the traditional diamond frame geometry. The Itera bicycle did not feel like a steel frame and its bulky appearance was never accepted by the community. In addition, early unreinforced plastics had very low modulus and hence resulted in very bulky structures with relatively high weight. As new polymers and polymer-based composites become readily available, traditional plastics did not stand a chance as a frame building material for bicycle frames. They do however retain their potential as matrix materials for composite structures.

2.2.7 Composites

Fiber reinforced polymeric composites are relatively new to the bicycle frame market. Since many composites offer higher strength-to-weight and stiffness-to-weight ratios than most metallic materials used in frame construction (see 2.8,2.9,2.10), it is logical that designers have turned to these materials in order to fabricate lighter, stronger and stiffer frames. The anisotropic nature of composites is very beneficial for improving the weight of frames as reinforcement can be placed along the structural load paths rather than other regions where low loads exist. The number of possible fiber and matrix combinations allows the choice of exactly the desired property in a certain frame region. Different fibers may be chosen, e.g. carbon, Kevlar and boron, and these fibers may be used in combination in the same material. In this case each fiber's specific properties could be used in an optimized way in order to give the structure desired properties. In the past, fiber materials used for bicycle construction have included carbon, aramid (Kevlar, Technora), boron, glass and Spectra fibers. These fibers were incorporated with either epoxy, polyester, or vinylester thermosetting resins. New fibers and matrix materials appear on the market each year with new and improved properties. The matrix material in all frame

constructions in the past has been thermosetting (heat-cured) resin whereas no documentation on the use of thermoplastic (heat melting) matrix material could be found in the literature. Thermoplastic matrices allow easy molding with excellent material properties especially related to the increase in fracture toughness in the order of 50-100 times with respect to thermosetting matrices [20]. Thermoplastic composites have found their way into some new bike handlebars, and may revolutionize the frame building market in the years to come. Also when the price of ceramic and Vectran fibers and metal matrix composites will have come down to reasonable levels, they could be used successfully for frame building.

Because the traditional diamond shape structure was so deeply entrenched in designers' and manufacturers' minds, the only way to introduce new advanced composite materials into the cycling industry was to use composite tubes to replace the steel and aluminum ones. Composite tubes can be manufactured using the filament winding process, by rolling woven material over a mandrel to make a tube, or by using dry woven braid with a resin infusion process such as resin transfer moulding (RTM). Finished tubes are then assembled in the traditional diamond shape structure using lugs which are made out of steel, aluminum, titanium, or composite materials. However, this tube and lug approach does not use one of the advantages of composites over metals which is their formability. The tube and lug design is less than optimum and has created many problems in the past which have given composite frames a very bad reputation. Depending on the lug material used, problems such as galvanic corrosion at the tube-lug interface, different thermal expansion coefficients of the dissimilar materials and uneven distribution of stresses creating poor load paths at the tube intersection can occur [21]. The improper joining of the composite tubes has also led to many failures [21]. Composite material frames should evolve as monocoque structures because of the great formability associated with the material and also in order to alleviate problems related to the joining of tubes. The way to prevent this problem is to make a monocoque structure where the riding loads are carried by a structure without any joints. This proposition is better than the original solution and gives designers unlimited creativity for the shape of the frame.

The freedom of choice for frame shape will allow development of very different structures, which after research, may reveal qualities which could never be achieved with diamond shape designs. Traditionally, composite frames made with carbon, Kevlar or another fiber type have been very expensive. But material and labor costs associated with composite frames will become lower as the fibers and resins are much more readily available than in

the past and the manufacturing aspect is better known and well understood by the manufacturers. One problem with monocoque frames is that a new mold is required for each frame size, which represents additional costs to the manufacturer. In order to be marketable, a bicycle frame must be available in different sizes to match the needs of the rider. Composites do not corrode under normal atmospheric conditions and also possess very good fatigue properties. Carbon fibers in particular are fatigue resistant even at high stress levels. The reason for using carbon fiber as a composite material stems from the fact that carbon fiber composites offer very high modulus at a very high strength and low weight (see Figures 2.8,2.9,2.10). It is now readily available in many different weaves as a preimpregnated material and is relatively inexpensive compared with other fibers such as boron and spectra for example. Carbon fibers are U.V. resistant. All in all carbon/epoxy composites are very well suited for this type of high performance structure.

2.3 Review of Carbon Fiber Frames

Since the early 1970's, carbon fiber frames have been constructed and sold by different manufacturers. This section will attempt to review all important carbon fiber road bikes on the market now in order to have an idea of what the industry has striven for in composite construction. Current carbon fiber frames are very different from each other. Carbon fiber frames on the market can be separated into 4 different categories in order to be more easily described. The categories include 1) diamond shape structures with lugs, 2) monocoque diamond shape structures, 3) Beam type designs and 4) other monocoque structures. This classification will help in the description of existing carbon fiber frames.

2.3.1 Carbon Fiber Tube and Lug Designs

As described earlier, the most intuitive way to introduce carbon fiber in the construction of frames is to make carbon fiber tubes and to join them together using some sort of lug. Many manufacturers still adopt this alternative. Specialized uses titanium lugs in its S WORKS [22] while TREK uses carbon fiber lugs in its 9000 series [22], and the Mongoose Iboc Pro SX uses aluminum inserts [22]. The Aegis carbon frame also uses aluminum lugs bonded to carbon tubes [23]. Carbonframe's Tetra pro uses a patented technology to laminate carbon fiber material to prefabricated carbon tubes through the use of high pressure matched metal dies [24]. This technique does not yield a truly monocoque

structure but attempts to minimize the effect of using dissimilar materials at the tube intersections. The tube and lug method for manufacturing a composite frame is by far the simplest. Some manufacturers will produce these frames in order to allow the cycling enthusiast to possess a carbon frame at a relatively low cost (possibly in the $800 range). However, these frames still constitute the low end of carbon fiber bicycles. Figure 2.12 shows a TREK carbon tube and aluminum lug design [25].

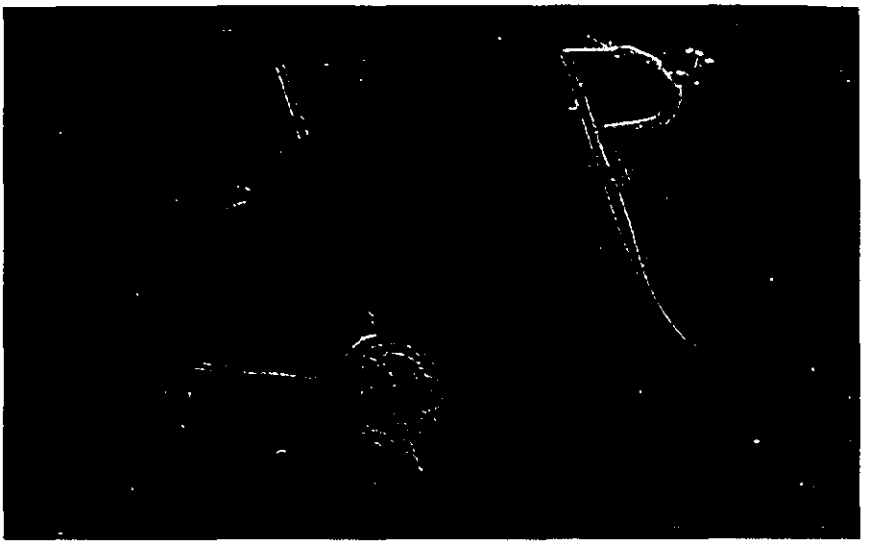

Figure 2.12 : TREK Carbon Tube and Aluminum Lug Design [25]

2.3.2 Monocoque Diamond Shape Carbon Fiber Frames

This second category includes frames which still possess a diamond shape structure or one very close to it but which are constructed as a monocoque structure. These attempt to take full advantage of the benefits of composite materials while still relying on a geometry dating back to the last century. These frames thus constitute a paradox. Perhaps they are made for traditionalist bikers who want to obtain the maximum out of the new materials while still retaining the look of the structure he/she rode all his/her life. Possibly the first manufacturer to use this method was Kestrel with Brent Trimble as designer [26]. Trimble holds most of the patents concerning carbon fiber frame monocoque construction [27,28,29,30]. Kestrel first deviated from the pure diamond geometry in the construction of a monocoque frame without a seat tube [26]. This was done in order to further reduce the weight and to offer the rider more comfort from road perturbations. The increased stiffness of the carbon fiber material undoubtedly allowed for this special feature. Trek also uses monocoque construction in its OLCV carbon series both for mountain and road bikes [22]. Figure 2.13 shows the Kestrel 500SCI frame without a seat tube [26].

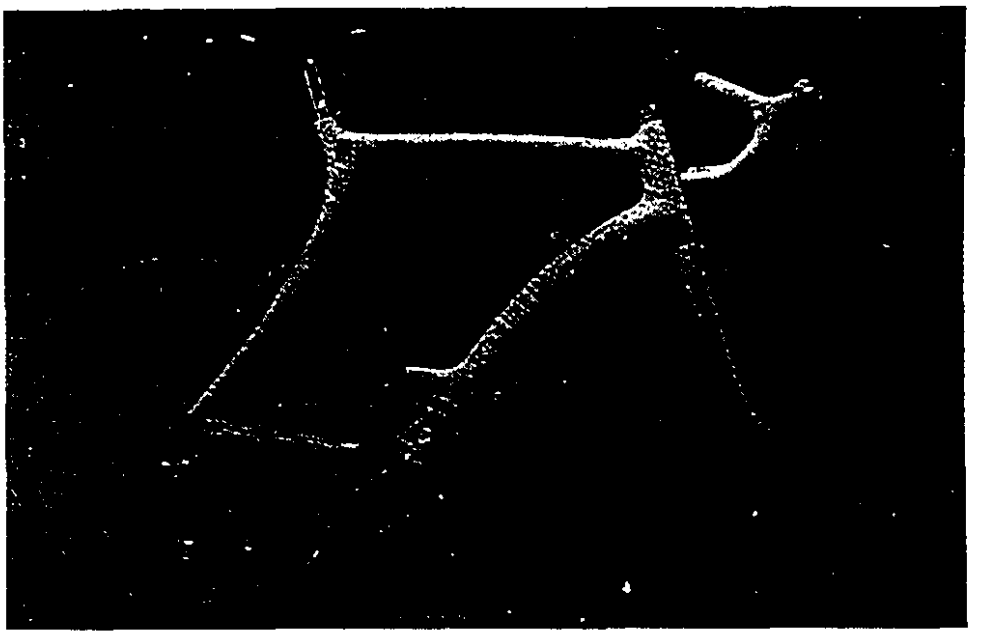

Figure 2.13 : Kestrel 500SCI Bicycle Frame Without Seat Tube [26]

Graphite Technology Racingbik also uses a mold to manufacture its carbon fiber monocoque road frame [31]. They use both aluminum and steel inserts in the different locations where the frame is attached to the external components. This frame has the distinctive attribute of having a curved seat tube in order to allow for the seat tube angle to be quite shallow without hitting the rear wheel.

The Huffy corporation of Dayton, Ohio also has a monocoque frame on the market. This frame is constructed with titanium inserts and has aerodynamic tubing [32]. This frame was priced in the $8,000-$10,000 range in 1990 depending on if a road, mountain or track version was desired. This frame is almost an identical copy of the frames that Huffy built for the American cycling team.

Another frame which possesses characteristics similar to a diamond geometry is the Corima road frame. The Corima frame emerged as a fast and efficient frame in July 1993 when Chris Boardman piloted his bicycle to a world hour record of 52.270 kilometers [33]. Although this record has been broken since this date, the Corima remains a very highly respected composite frame. The bicycle's design, the selection of its material and the thickness' in the different frame locations was dictated mainly by finite-element analysis [34]. Corima claims that the use of finite-element analysis has increased the stiffness of the frame by 30% while achieving a weight reduction of 33% [34]. The Corima frame reveals a very aesthetic design and has incorporated features such as internal cable routing and

aerodynamically shaped tubes. Nevertheless its geometry is based roughly on the double triangle structure which gives the design limited variables and complex tube joining regions where stresses might be high. Figure 2.14 shows the Corima frame [33].

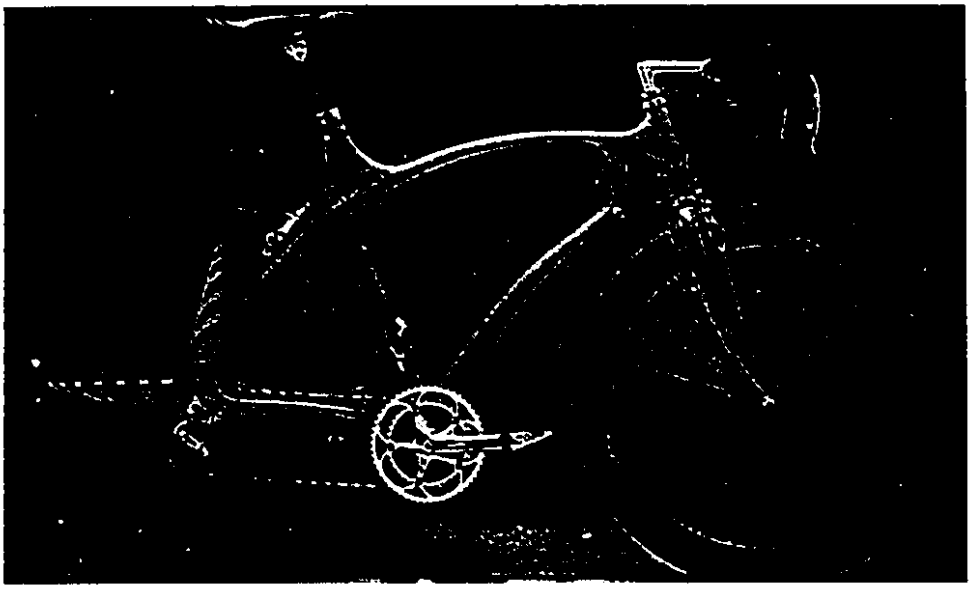

Figure 2.14 : Corima Bicycle Frame [33]

2.3.3 Beam Bikes

The next category of bicycle to be studied and categorized are the carbon fiber monocoque structures which do not rely on the diamond shape structure and which are often referred to as *beam bikes*. This geometry is again a paradox between a diamond shape structure and a true monocoque composite frame. Beam bikes are those which possess a down tube, chain stays and a top tube while eliminating the seat tube and the seat stays. The ZIPP [35] and the Lemond V^2 Boomerang [36] are beam bikes. They both have a thick V-shaped beam running from the head tube to the bottom bracket and continuing on towards the rear dropout. The term beam bike comes from the fact that the seat is suspended at the end of a cantilever beam running from the head tube to the seat (which could be referred as a top tube if the normal diamond shape terminology is used). The main difference between the ZIPP and the Lemond design is in the way the beam is fixed to the rest of the frame. The Lemond design has a fixed beam position while the ZIPP beam has a pivoting point near the head set which allows vertical movement of the seat. The desired amount of movement can be adjusted from almost zero displacement to almost 1.5 inches of vertical seat travel when riding. These frames are surprisingly light in the 1.2 kg range. They use a minimal

amount of material as they only incorporate frame parts which are necessary to keep all the frame components together. The ZIPP has an adjusTable and even exchangeable beam which adapts to riders of size ranging from 1.60m to 1.93m. The advantage of this design is that only one size of bicycle need be made and the actual size of the frame is adjusted for each rider by changing only the beam. Unfortunately, these beam designs also have disadvantages. As the beam acts as a cantilever structure and is unsupported at the seat end, it allows for both vertical movement of the seat and lateral sway. The vertical movement is relatively limited since the beam is deep with respect to its width, giving it good rigidity in the vertical direction but not in the lateral one. This lateral sway has been noted as a problem in the riding of these bikes [35]. However, it seems that the main problem with this design is the actual geometry of the frame. The load transfer from the rider's weight on the seat must be transferred in shear at the joint from the head tube to the main down tube. The head tube region may already be highly loaded by road forces and moments induced by the riders arms, so it seems unwise that the introduction of the rider's body weight to the rest of the frame be done at that location. The stand over height (height of the frame at the front end of the seat) being quite high, these beam bikes are often difficult to mount, even for experienced riders. Although they have interesting characteristics, such as their excellent aerodynamics and low weight, the beam bikes have had mixed success since their early inception into the market. Their limited popularity might be linked to their non-conventional shape and relatively high price. They have been used mostly by triathlon riders. Figure 2.15 shows an example of the ZIPP beam bike [37].

Figure 2.15 : ZIPP Beam Bike [37]

2.3.4 True Monocoque Shapes

This last group of carbon fiber frames are among the most state-of-the-art carbon fiber frames. They are structures which truly depart from the traditional diamond shape structure.

The first frame to be examined is Mike Burroughs Giant prototype [38]. It includes some of the basic components of the traditional diamond geometry, but like the beam bikes with some parts omitted. This frame has the same backbone as the beam bikes, going from the head tube to the bottom bracket and then to the rear dropouts. However, instead of holding the seat with a cantilever top tube, Burrough's decided to attach the seat to a seemingly ordinary seat tube which extends to the bottom bracket. Hence this frame does not have any top tube nor seat stays. This design is much more intuitively correct than the beam bike because the rider's weight is transferred to a bulky bottom bracket area which forms the core of the frame. Also the load transfer is through a compression member (the seat tube) instead of a cantilever beam as in the case of a beam bike. This prototype, which will most likely become a production model, combines extreme rigidity with other practical concerns such as a low stand-over height (a feature which the beam bikes do not have), light weight and aesthetic design. It includes internal cable routing and a monoblade front fork.

In 1994, five-time winner of the prestigious*Tour de France* Miguel Indurain mounted the *Sword* and succesfully broke the world hour record. Even though the record has since been broken by Tony Rominger, Indurain's performance on that day was exceptional. The Spaniard was riding on a carbon fiber monocoque frame with titanium inserts built by Pinarello [39,40,41]. This structure is truly unique and original as it really shows the inventiveness of the designer. An interesting feature of this frame is the hole in the right side of the structure to allow the chain to go from the front chainring to the rear derailleur. The *Sword* dictated new standards in aerodynamics because the frame was only 15mm thick (smaller than the width of a tire) at its narrowest point while the area of higher stresses in the bottom bracket, head set and rear dropout regions were built up to 30mm. Relatively heavy at 1.7kg, this custom frame may never be commercialized but is believed to be both very aerodynamic and stiff and hence a good statement of what can be achieved with composites in bicycle frame construction. Figure 2.16 shows the Pinarello *Sword* [41].

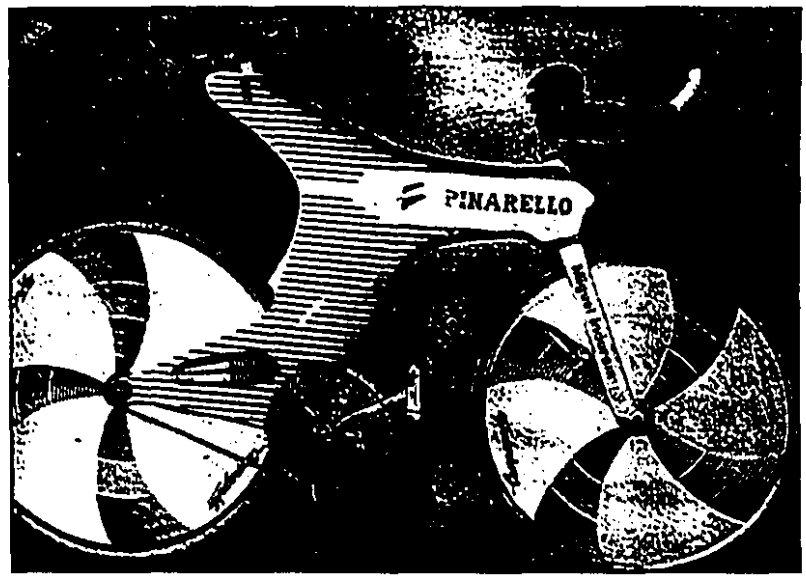

Figure 2.16: Pinarello *Sword* [41]

The original Lotus frame which was used by Chris Boardman to win the gold medal in the 1992 Barcelona Olympics has evolved, with many changes to the production *Lotus Sport 110*. This monocoque carbon fiber frame has a Z-shaped structure [42]. Some of the original Lotus frame features, such as the monofork and the single chainstay have been abandoned. The *Lotus Sport 110* has interesting features such as internal cable routing and the efficient rear section of the frame which is closely faired to the rear wheel. On the other hand, the Z-shaped structure is far from being structurally efficient. There is no direct load path for the weight of the rider to the ground. This load path must twist around the bottom bracket location, where other torsion loads also exist, to reach the rear vertical reaction point at the rear dropouts. Hence, although this frame is very popular, it does not seem so well-designed structurally. Figure 2.17 Shows the *Lotus Sport 110* frame [42].

The *Hotta* frame is a carbon fiber monocoque frame which uses an X-shape [42]. From a structural point-of-view, this X-shape structure is very efficient for distributing the applied loads. It provides a direct path from the headset to the rear dropouts which provides an excellent torsional stiffness. This design also incorporates efficient fairing of the rear wheel with the frame. This frame is of very low weight at 1.29kg because it adopts a structurally efficient design and thus requires a minimum amount of material. A frame of this type allows very easy internal cable routing along the main beam. Figure 2.18 Shows the *Hotta* bicycle [43].

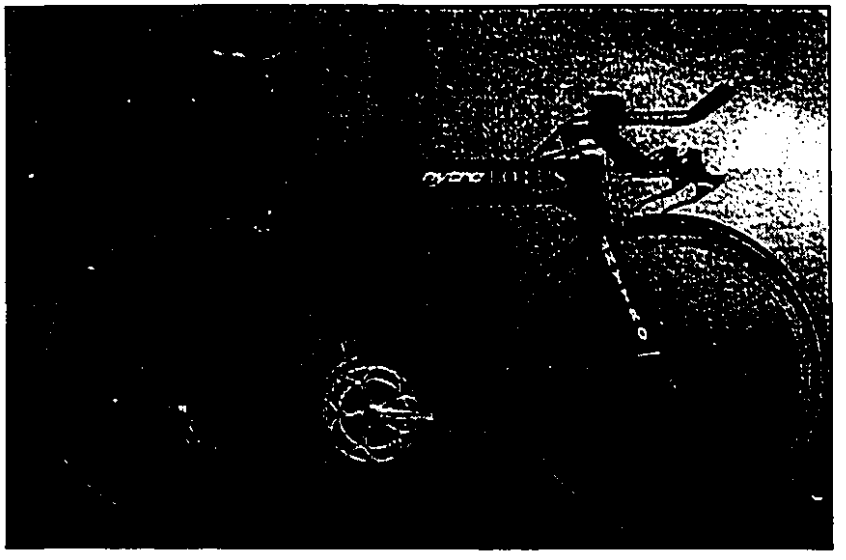

Figure 2.17 : *Lotus Sport 110* Frame [42]

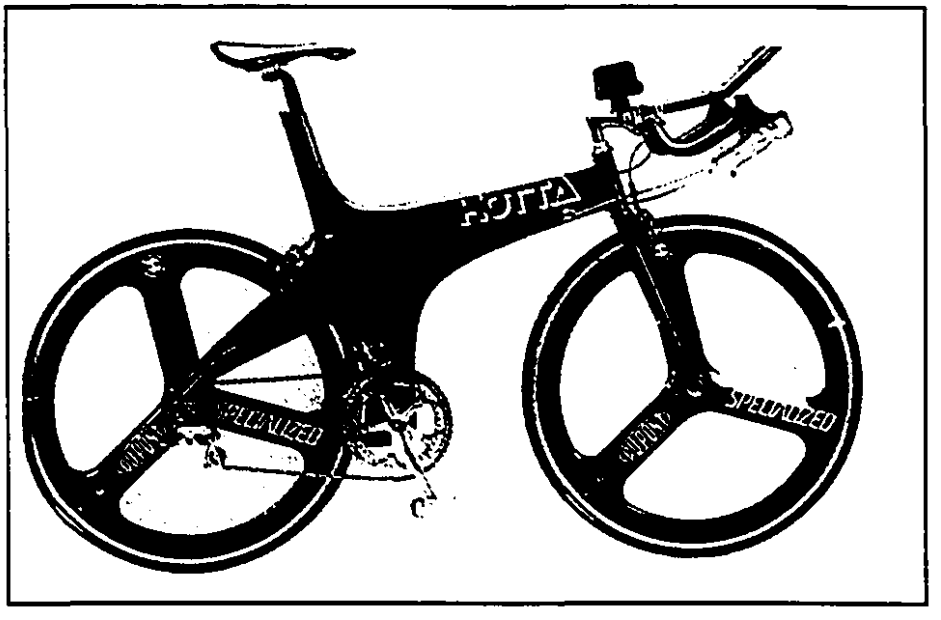

Figure 2.18 : *Hotta* Bicycle [43]

2.3.5 Summary of Current Carbon Fiber Frames

This review of carbon fiber frames on the market is far from being complete, but it helps to understand why current diamond shape frames or monocoque structures are used. It also provides a framework for comparison with the prototypes which will be developed during this project.

2.4 Review of Bicycle Frame Stress Analysis

Stress analysis using finite-element techniques is a good way to analyze a complex composite structure. Many published studies document the use of finite-element analysis in the design of traditional tubular frames [44,45,46,47]. The simplest way to perform a finite-element analysis on the traditional diamond structure is to use beam elements to model the tubes. The beam element can accurately account for the tube parameters of thickness, outside diameter and material properties. If sufficient number of elements are utilized, double butting of tubes can also be easily incorporated into the model.

Using the beam element method and a load case where a cyclist is in a sprint out of the pedals on a traditional metallic diamond frame, it was found that the maximum stress was at the intersection of the down tube and the seat tube at the bottom bracket [48]. A study of the same type, but considering rider induced loads at different crank angles combined with handlebar and seat loads, found that the maximum stress is at the top and seat tube intersection [44]. The beam model approach is approximate as it does not consider the actual tube joining regions where large stresses and failure usually occurs and could not model a composite structure consisting of many plies of material. This is why the use of shell elements to model the tubes themselves and the joints has also been considered [45]. Shell models allow the determination of the different tube stresses around the circumference, something that beam models cannot provide. However, it was shown that deflection measurements on both shell and beam finite-element models were very similar for static loading cases [47]. Therefore, if deflections are the main concern and not failure, a beam model is sufficient.

In a good design, the strengths of the different tubes must be high enough to prevent failure, coupled with a design goal that the frame be stiff in certain regions and compliant in others. It is desirable to have a stiff head tube and bottom bracket region in order to prevent excessive deformations during cases of high loading during intense riding. On the other hand, a vertically compliant frame would be desirable for riding comfort. Hence, characterization of bicycle frames must be done in terms of strength in order to assure structural integrity, but also must be done in terms of stiffness in order to produce a good frame. Frames can also be characterized by the strain energy absorbed into the frame during pedaling. As energy is most effectively transferred through a stiff structure from the

rider's body to the back wheel, a minimum of strain energy stored by the frame under loading is desirable [46].

It is difficult to compare bicycle frames since each researcher and manufacturer utilizes a different loading case or test method to characterize their frames. This is so because there are very few standards for the determination of performance of bicycle frames. The existing standards are mostly for security and structural integrity and cannot be used directly to compare performance and rigidity of different frames. These standards offer only static and dynamic testing where one load is applied to one point whereas this is not what happens in actual riding situations. Hence the standards are sometime only useful to make sure that bicycles respect a certain baseline of structural integrity but not as a design tool for high performance racing bicycles. However, new initiatives in bicycle standards from ISO [49], JSA [50] and ASTM [51] will greatly contribute to the standardization of test methods in the near future.

Since it is believed that high performance track and time trial composite bicycles should evolve into the shape of monocoque tubeless frames, the lessons learned from the finite-element analysis of tubular frames may not be relevant. This research is thus aimed at using finite-element methods to perform stress analysis on monocoque composite frames rather than on conventional tubular frames. Another study on monocoque composite material frames has been performed but concentrates mainly on the construction process and testing, and no finite-element analysis was performed [52]. Also a study of a composite mountain bike was performed but only considers finite-element static loading at one location to be compared with the actual prototype, and does not review the stresses during actual riding conditions [53]. The use of a geometrically efficient structure combined with the desirable properties of composites, a correct understanding of the loading and boundary conditions, as well as stress and failure analysis are all important factors for the development of a good composite bicycle frame.

2.5 Review of Manufacturing Methods

Many methods can be employed to manufacture a composite structure. For the case of a composite monocoque bicycle frame, more than one fabrication method exists. Each method has its advantages and disadvantages. Hence, for a certain application, it is important to know which method to use. This section will provide a quick non-exhaustive

overview of the possible fabrication methods for the construction of a composite bicycle frame.

2.5.1 Wet Layup

This method involves the application of dry fabric wetted with an appropriate resin over a previously shaped foam core. The fibers and resin are purchased separately, as opposed to preimpregnated material where the appropriate quantity of resin is already mixed with the fibers. In the wet layup process, each layer of material is wetted with the resin and placed on the structure. It is then allowed to room temperature cure. The main advantage of buying the fibers and resin separately is that it is less expensive. Also it allows, up to a certain extent, the choice of any fibers to be used with any resin. There are also many disadvantages with this method. Although it is a reliable process, it is by nature very slow and labour intensive. Since no pressure is used during the curing process, the plies are not forced together in any way. This prevents the correct consolidation of the unbonded plies into a bonded laminate. For this reason, this method is often limited to low-tech applications where the interply bonding is not critical. Since this method uses an internal open mould, it will create a surface finish that may not be perfect. Extensive sanding and fairing will be required in order to obtain the proper surface quality. Also in order to assure a good bonding between layers, it is often required to sand in between each layer again increasing the labor time. But the main disadvantage with this method is the fact that it often results in heavy pieces as the volume fraction of fiber and resin is difficult to control. For structural considerations, it is better to have a resin rich structure than a resin deficient one where it will be easier for cracks to form and propagate. For this reason, more resin than required is often added, resulting in a heavier structure.

2.5.2 Prepreg with Internal Bladder

This fabrication method involves a re-usable 2 or 3-part external mould, inside which an internal bladder is used to create pressure on the preimpregnated material against the mould. This fabrication method thus requires a re-usable mould made of aluminum, epoxy, fiberglass or any other mould making material. The appropriate layup is placed on the mould with the preimpregnated material. After the layup is finished, a nylon/polyethylene bladder is placed on one half of the mould. The mould is then closed and the bladder inflated to a proper pressure. The mould is then placed in an oven for curing to take place.

This method produces an excellent surface finish because the external layer of the structure is forced against the finished surface of the mould. This method has successfully been used in the production of bicycle frames for some time now [54]. It is appropriate for medium to large scale production, but not for small scale prototyping. It is thus an expensive fabrication method for small quantities, but rapidly becomes worthwhile if many pieces are to be produced. It provides a very light structure as it is internally filled with air instead of the internal foam used in some other methods. The thin nylon/polyethylene film remains part of the structure after the curing has taken place. This method is quick and clean. A frame can be produced in 2-3 hours with this method compared with 2-3 days using the wet layup technique. This method cannot be completely automated, because it still requires the hand layup of the composite prepreg in the mould. The internal bladder technique is used in the construction of bikes such as the Antelope [54], the TREK OLCV Carbon Series [26] and many other carbon frames. Figure 2.19 shows a schematic of the internal bladder technique.

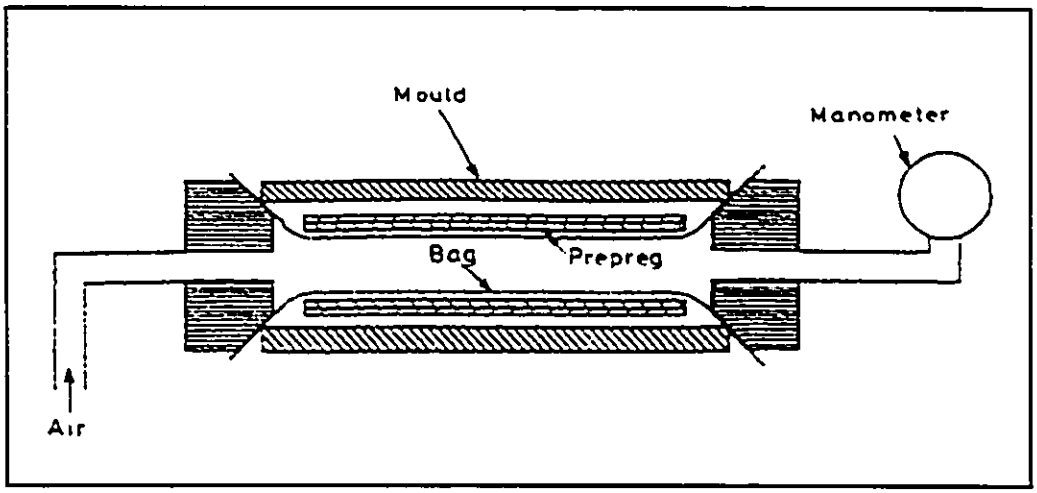

Figure 2.19: Internal Bladder Technique [55]

2.5.3 Resin Transfer Moulding (RTM)

In Resin Transfer Moulding (RTM), dry reinforcement is placed inside a 2 or 3 part mould. The mould is then closed and a catalyzed resin is injected into the mould via a centrally located injection point. The resin injection point is located so as to provide equal wetting of the fibers everywhere in the mould. As the resin spreads through the mould, it displaces the entrapped air through the air vents and impregnates the fibers. Depending on the resin system used, the curing can be done at room temperature or in a controlled temperature

oven. Similar to the internal bladder method, this construction technique uses an external mould which may be improper for a small production. However it provides a very good surface finish. In order to produce a bicycle frame with this method, it might be necessary to use an internal foam core in the mould in order to provide the required wall thickness. But for the making of a very thin bicycle frame such as the ones often used in time trials, composites with no internal core may be used. Figure 2.20 shows a schematic of the RTM process.

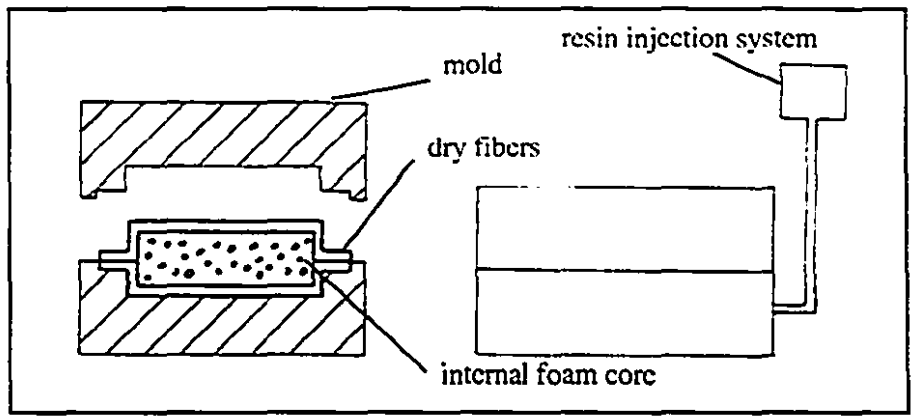

Figure 2.20: RTM Process [20]

2.5.4 Thermoset Prepreg - Vacuum Bagging

Like the wet layup method, the vacuum bagging method involves the fabrication of an internal core over which the composite material is placed. Foam or other materials with appropriate properties can be used as a core. Aluminum inserts are then secured at the appropriate locations on the core with glue. The frame is then ready to be covered with composite material. The material has a tacky feel and thus adheres well directly on the foam. The layers are applied one after the other in a specified sequence. After the composite material layup is done, a layer of release film and breather material is added. A large vacuum bag is then made over the part. The bagging material is very resistant to tears and stretching. A vacuum is then drawn from under the bag, creating pressure on the part. This pressure has many uses such as assuring that there are no air bubbles trapped between layers. This problem often occurs in the wet layup technique, because there is nothing forcing the layers together during curing, so the compaction is often very poor. The vacuum bagged part is then placed in a controlled temperature oven for a specified time to allow full curing. The second use of pressure is to allow the resin to flow before the actual curing. As the resin heats up, it flows from resin rich to resin poor areas. The vaccum bagging-prepreg technique does not yield a perfect surface finish. The quality of the finish

is very much dependent on the quality of the vacuum bag. Often sanding is required after the curing in order to remove resin wrinkles. A primer and paint can then be applied so as to improve the surface finish.

2.5.4 Thermoplastic

Instead of using a thermosetting composite, it is possible to use a thermoplastic material. The thermoplastic matrix (PEEK, PPS, Polysulfone, Polyimide, etc.) can be used with almost all of the conventional fibers in order to make a prepreg. This prepreg is dry and can be kept at room temperature. The method of using the thermoplastic prepreg is the same as the thermoset prepregs and thus could be used in the internal bladder or vaccum bagging method. Thermoplastic prepregs are not as well known as the conventionnal thermosets as they are newer and have not been used in as many applications. They are often used in high-tech applications were fracture toughness is important. This property is very important for bicycle frames, hence they could be used in the near future. The problem with thermoplastics is that they are not tacky at room temperature and hence it may be difficult to construct a layup of many superimposed layers on an intricate shape.

Chapter 3

Traditional Frames

3.1 Rationale for Modeling and Testing Traditional Frames

Although this research concentrates on composite frames, it is important to understand how and why traditional frames should be improved upon. Thus, as part of this research, a summary investigation of traditional metallic bicycle frames was performed. Some traditional frames were modeled using finite element analysis (FEA) and then tested using a specially built testing jig in order to quantify their stiffness in different directions and to correlate results with the FEA models. The results also provide baseline values for frame stiffness, so that valid conclusions can be made for the new composite structures. This preliminary static testing of traditional frames also permitted to establish the experimental procedure required for the static testing of the composite frames.

3.2 Finite Element Analysis of Traditional Frames

The finite element analysis of traditional frames was performed in order to quantify the stiffness of these frames, and also to show that correlation between the finite element results and the testing jig could be obtained. The finite element analysis was performed using SRDC'S I-DEAS software [56] at McGill University. This finite element software combines good 3-D graphics, element library and pre- and post-processing.

In order to model traditional bicycle frames, two approaches were utilized. The first one considered each tube of the frame as a beam element, thus creating a beam frame structure. The inside and outside diameters of the beams were cross-section material properties of the beam elements. Thus the beam elements could be defined by their end-point locations in 3-

D space. This procedure is simple but, as will be seen later, does not yield all the necessary results. A typical frame modeled using this technique may contain only 10 elements and be readily solved requiring minimal computer time. The other approach is to model the whole frame using shell elements. This procedure models each tube with rectangular and triangular thin shell elements. The tubes may contain 6-8 such elements around their circumferences, and an appropriate amount along their length resulting in models with over 1000 shell elements and thus requiring more extensive computer time. The geometry of the junction between the tubes is achieved manually by creating triangular or rectangular thin shell elements connecting the intersecting tubes. It is obviously much simpler to model a frame using beam elements but a better analysis is done by understanding the tube intersection stress analysis. Depending on the results required (stiffness or strength) an appropriate choice of modeling technique can be chosen. The modeling of a frame using beam elements can yield fairly accurate displacements and thus stiffness parameters. However, it is difficult to obtain an accurate account of the stress levels and patterns associated with the structure. On the other hand, if we use thin shell elements, in addition to accurate displacement results, the longitudinal and circumferential stresses present in the tubes can also be obtained. Hence if a stiffness-only study is required, beam elements modeling the frame might be sufficient for certain stiffness measurements. On the other hand, if a complete stiffness and strength study is required, thin shell finite elements should be used to model a traditional tubular frame.

3.3 Experimental description

In order to effectively compare different frames, a series of static tests were developed. Each test corresponds to a different loading case where forces are applied to different parts of the frames and where other parts of the frames are restrained. The different static tests are shown in Figure 3.1.

The individual tests are aimed at measuring a different characteristic that may or may not be beneficial to the rider and thus characterizes a good or a bad frame. A description of each test from figure 3.1 will give a preliminary qualitative explanation of what kind of result is desirable.

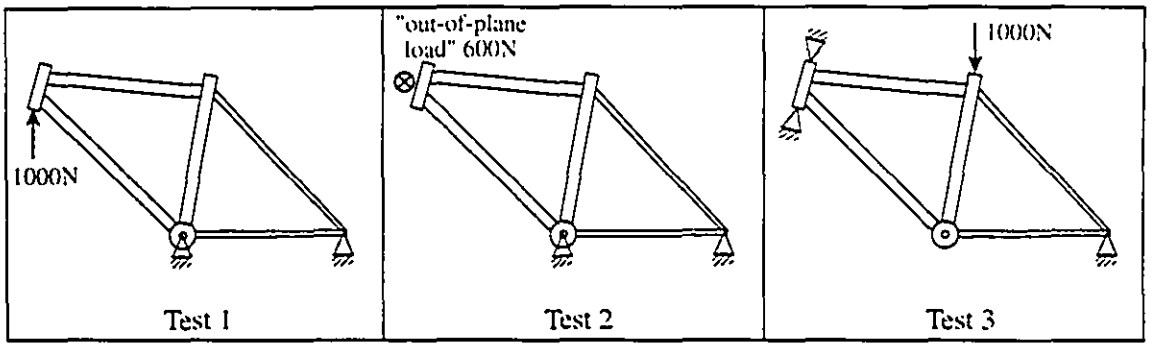

(a) (b) (c)

Figure 3.1 - Loading Cases

Test 1 consists of a 1000N in-plane force applied vertically up on the bottom of the head tube while the bottom bracket and the rear dropouts are rigidly fixed, as shown in figure 3.1(a). Test 1 gives a measure of the static response of a frame under loading from the front fork due to a bump in the road. A satisfactory result for this test would be a relatively compliant movement that would help minimize the force generated by the impact of the front wheel on a bump in the road which is subsequently transmitted to the rider's arms. Attempts to minimize this input force have been implemented in recent years by the installation of front spring or hydraulic suspensions on the front forks of mountain bikes. Although this type of suspension would not be necessary for a road frame used in normal conditions, a moderate in-plane resiliency is desirable.

Test 2 consists of a 600N load applied at the head tube in the out-of-plane direction while the bottom bracket and the rear dropouts are rigidly restrained, as shown in figure 3.1(b). Test 2 is a measure of the lateral stiffness of the frame, whereby a small deflection indicates a laterally stiff frame, which is desirable. This is desirable as under intense riding there is out of plane, or twisting loads which are applied to the frame due to the rider's pedaling action. Lateral or out of plane rigidity will prevent extreme deformation of the frame and is thus desirable. This test may also be called the "torsional rigidity of the front triangle".

Test 3 consists of a 1000N in-plane load applied vertically down at the seatpost. In this scenario, the head tube and rear dropouts are fixed, as shown in Figure 3.1(c). The displacement measurement is done in the direction of the applied load at the point of application of the force. Test 3 is a vertical compliance test. A relatively large displacement is favorable in this case as we again want to minimize the road-induced loads to the cyclist.

In a modified triangular diamond shape structure, a way to appease the rider from a surface bump could be to build a frame like the Kestrel 500SCI (see figure 2.13) which eliminates the seat tube and thus would result in a more vertically compliant structure. Also, many touring bicycle frames have seat mounted springs for the same reasons.

Since all the tests are performed within the elastic limit of the material, the choice of load to be applied is arbitrary as the load-displacement curve is linear in the elastic region. The above loads were chosen in order to obtain measurable deflections for the appropriate tests. This series of tests is a satisfactory but non-exhaustive list that may be modified or updated in order to provide for a more complex and complete analysis in the future.

3.4 Experimental and Theoretical Techniques for Traditional Frames

The 3 tests described in section 3.3 were simulated on 3 different models using FEA in order to obtain stiffness values for traditional geometry frames. The 3 models consisted of one classical diamond shape frame that was modeled using isotropic shell elements, and two classical frames modeled using beam elements. A 52 cm chromium-molybdenum steel frame built using Reynolds 501 tubing was modeled using isotropic shell elements and also using beam elements. Also, a 58 cm Trek 1100 frame made of 6061 aluminum tubing was modeled using beam elements only.

The experimental measurements on both the steel and aluminum frames were performed on a specially built testing jig developed at McGill University. The jig consists of a rigid box structure made of rectangular members with a large cross sectional area in order to restrict the jig to minimal deflections compared to those of the bicycle frame. Different points of a bicycle frame can be fixed to the structure using attachments, thus creating fixed boundary conditions for the test. Hydraulic cylinders were attached to the testing jig in order to apply loads to the bicycle frame. By varying the placement of these hydraulic cylinders, load can be applied in any axis, and at almost any point on the bicycle frame. The applied load is measured by calibrated load cells placed between the hydraulic cylinders and the load application points on the frame. The displacements at the different locations are measured using dial gages. Figure 3.2 shows the testing jig used to test the frames.

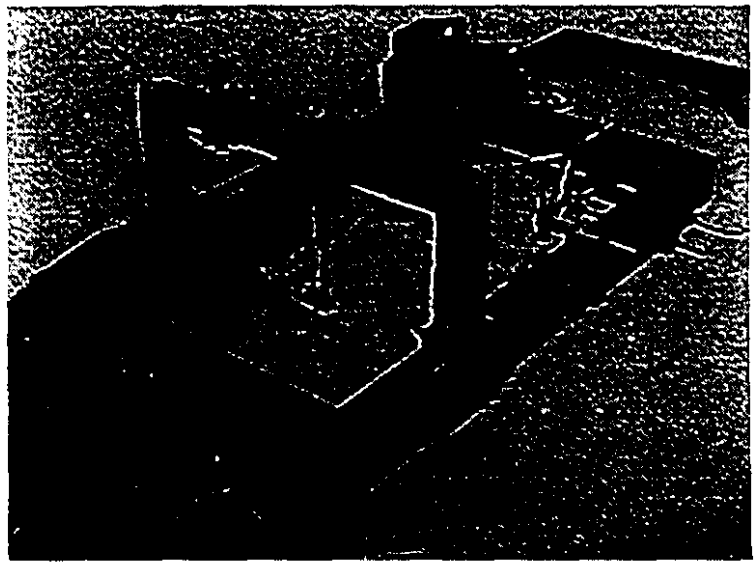

Figure 3.2 - Static Bicycle Frame Testing Jig.

The load cells consisted of 4 strain gauges mounted to form a wheatstone bridge on a rectangular piece of steel. The size of the steel piece was chosen so that at the minimum expected load the steel would strain enough to generate an appropriate bridge output. Also, the steel cross section was chosen to be sufficient so that the induced stresses would be below the yield stress at the highest expected load. The load cell dimensions were 13mm by 13mm with a 6mm hole drilled through it. Hence at a load of 2000N (twice as high as the highest load expected with these tests) the stress in the steel will be:

$$\sigma = \frac{F}{A} = \frac{2000}{13^2 - \left(\frac{\pi * 6^2}{4}\right)} = 14.2MPa \qquad (3.1)$$

From equation 3.1, the value of 14.2 MPa is well below the 250 MPa yield of low grade steel. The next step is to make sure that the bridge output will be sufficient, even in the low range of the loads to be used. An analysis for the determination of the bridge output at a load of 100N is performed, as 100N will be considered as the lowest load required to be measured during the tests.

$$\sigma_{100N} = \frac{100N}{140.7mm^2} = 0.71MPa \qquad (3.2)$$

The approximate strain value is:

$$\varepsilon = \frac{\sigma}{E} = \frac{0.71MPa}{207GPa} = 3.43 \times 10^{-06} \tag{3.3}$$

Using the wheatstone bridge formulas [57],

$$\frac{dR}{R} = gaugefactor \times \varepsilon \tag{3.4}$$

For this bridge the gauge factor is 2, hence

$$\frac{dR}{R} = 2.0 \times \varepsilon = 6.86 \times 10^{-06} \tag{3.5}$$

and

$$E_0 = 0.25 \times \frac{dR}{R} \times E \tag{3.6}$$

where E is the supply voltage. Hence assuming a 5.0 volt source,

$$E_0 = 0.25 \times 6.86 \times 10^{-06} \times 5.0 = 8.575 \times 10^{-06} Volts \tag{3.7}$$

and the bridge output signal will be:

$$E_{0,total} = 2 \times (1 + \mu) \times E_0 \tag{3.8}$$

The resulting voltage is thus

$$E_{0,total} = 2 \times (1 + 0.3) \times 8.575 \times 10^{-06} = 2.23 \times 10^{-05} volts = 0.022mV \tag{3.9}$$

From equation 3.9 a wheatstone bridge output of 0.022 mV is expected at 100N, hence 0.220 mV at 1000 N. These voltages can easily be measured using a conventional voltmeter. If the wheatstone output would have been insufficient, it would have been possible to amplify the signal, but this was not necessary.

Although the above analysis provides an approximation of the expected output from the load cell, the cell required calibration before accurate load measurements could be performed. The load cell calibration was done with a Chatillon TCM 200 tensile tester equipped with a calibrated load cell. The cells were powered by a constant 5.0 volts DC voltage and the resulting wheatstone bridge output was read from a Keithley 195A digital multimeter. Figure 3.3 shows the calibration curve used for the load cell. This curve gives an average transfer function of 4350 N/mV. This transfer function gives a bridge output of 0.023 mV for a 100 N load compared with the 0.022 mV, found analytically.

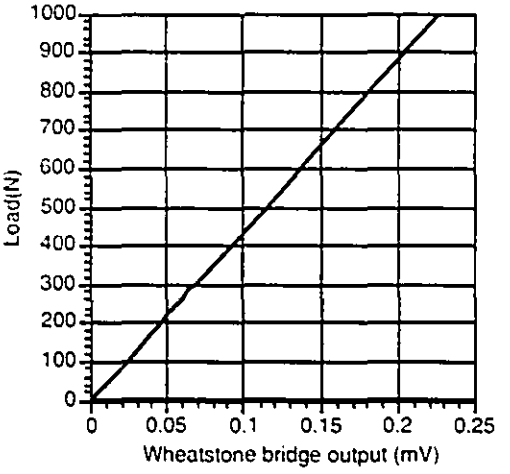

Figure 3.3 - Load Cell Calibration Curve

3.5 Finite Element and Experimental Results

Table 3.1 shows the finite element and experimental results as obtained for the 3 different tests on the different frames. For the experimental results, the values obtained are an average of 3 runs which were done for each test.

	F.E.A.			Experimental	
	Steel - beam	Steel - shell	Al. - beam	Steel	Aluminum
No. of elements	10	1800	10	N.A.	N.A.
Weight (kg)	1.46	1.53	1.28	2.08	1.80
TEST 1 (mm)	0.27	0.32	1.00	0.40	1.14
TEST 2 (mm)	22.9	25.6	32.0	24.9	34.1
TEST 3 (mm)	0.05	0.08	0.001	-	-

Table 3.1 - Finite Element and Experimental Results for Metallic Frames

	% error between experimental and Steel-beam model	% error between experimental and Steel-shell model	% error between experimental and Al.-beam model
TEST 1	59	25	14
TEST 2	8.7	2.7	6.5

Table 3.2 - Errors Between the Finite Element and Experimental Results

Numerous observations can be made from tables 3.1 and 3.2. In test 2, the difference between the experimental and FEA results is less than 7% for both the steel and the aluminum frame. However, for test 1, the FEA and experimental results differ by a larger amount. Errors up to 20% can be detected between the finite element and experimental results. An interesting aspect to note is that the experimental results are consistently higher than the FEA results. A possible explanation for this would be a slight lack of rigidity in some parts of the jig (possibly the boundary conditions) which would contribute in giving a larger displacement for the same load in the experimental results compared with the finite element ones. This effect is much more important for test 1 than for test 2 as the displacement for the former are much smaller. The movement of some of the components of the jig (retaining plates, bolts, nuts) is suspected to take place at the initial load application strengthening this possibility. Test 3 was impossible to perform experimentally because of the geometry of the jig. However, it seems that the difference in the FEA results are much more evident than for the other tests. The most probable explanation for this behaviour is that the beam element models are not suitable for this particular in-plane load. Also, the larger diameter of the aluminum tubes compared with the steel ones might lead to a much stiffer structure for this type of load and mesh, yielding results for test 3 which are very different for each model.

The comparison between the FEA and experimental results is good considering the errors that could arise from a number of sources such as the difficulty in modeling the exact intricate shape of a bicycle frame, the modeling of restraints by FEA, and inherent errors involved in experimental measurements. The fact that experimental results match the FEA to some extent gives confidence in other FEA results. As the goal was to compare frames without actually building them, experimental testing on existing frames confirms the idea that FEA testing can replace experimental testing. Another important observation is that the steel frame, which is modeled using both beam and shell elements, gives results which are appreciably close to each other. It could thus be concluded that for a classical frame with

tubular geometry a much simpler and quicker stiffness analysis using beam elements can be done in order to obtain approximate results for some test simulations. Nevertheless, it should be remembered that if a complete stress analysis is required, the beam model would not be sufficient to provide this information.

In addition to comparing actual traditional frames to their finite element models, other traditional steel frames were statically tested on the testing jig. This further testing of steel frames was done in order to obtain baseline values for the different tests in order to compare with the future carbon fiber frames built as a result of this project. Test 1 and 2 were thus performed on two other steel frames. The first one is a Colnago Sport frame which uses Columbus Aelle tubing. This frame is a light and flexible Italian racing frame. The second is a high quality Rocky Mountain frame built from Tange Prestige tubing. This mountain bike frame is made from one of the best steel tubing materials available and thus is considered as one of the best steel mountain bike frames on the market. Table 3.3 shows the results obtained for test 1 and 2 for the two frames described above. Included in the table are results from the other steel frame (Reynold 501) which was earlier compared to its finite element model.

From table 3.3, observe that the Rocky Mountain frame, which uses the Tange Prestige tubing, is by far the stiffest in the out-of-plane direction as confirmed by test 2. An interesting aspect to consider is that, at the same time, this frame still offers the most compliant head tube motion as shown by test 1. This reveals a very well designed frame, as it combines the dual attributes of being compliant in-plane and stiff out-of-plane. It is this trend (high out-of-plane stiffness and low in-plane stiffness) which will be a goal for the design of the carbon fiber frames.

Bicycle frame	Tubing material	Test 1 (mm)	Test 2 (mm)
Chabot Frame	Reynolds 501	.40	24.9
Colnago	Columbus Aelle	.31	27.8
Rocky Mountain	Tange Prestige	.53	18.6

Table 3.3 - Steel Frame Test Results

In chapter 4 these results will be compared with the composite prototypes which will be constructed. Even though these traditional frames are not the best racing frames on the market, they are of reasonable quality so as to provide an adequate baseline upon which the composite frames should be improved upon.

Chapter 4

Composite Frame Design

4.1 Introduction

This chapter will focus on the design and finite-element analysis of the composite frames developed during this project. This is the core of the research. In order to set goals for this study, a number of design criteria were set forward. The first criteria is low weight. A frame weight on the order of 1500g should be sought. This is slightly lower than other composite frames on the market and in the same range as the lightest aluminum frames available. The second design criteria is to obtain a frame with the appropriate stiffness at the appropriate locations. The head tube and bottom bracket stiffnesses should be as high as the stiffest frames on the market (such as the ones sampled in chapter 3). The frame should also be compliant in the vertical direction in order to help dissipate road irregularities. These criteria will guide the design and construction of the composite monocoque frames.

4.2 Finite-Element Analysis of the Composite Frames

The finite-element analysis of the monocoque bicycle frames was performed using SDRC's I-DEAS finite-element software [58]. This software is particularly appropriate for this type of structure as it incorporates both a very good composite laminate modeling section with advanced geometric modeling capabilities. I-DEAS uses a standard classical laminated plate theory with an option to calculate additional interlaminar shear stresses. The laminate modeling section directly computes all of the stiffness matrices which are inherent to the use of materials with orthotropic material properties (i.e., composite materials). The calculations and manipulations of the stiffness matrices for each laminate are very tedious,

so detailed analysis of a composite bicycle frame using any method other than using finite-element analysis is practically unthinkable. The following sections will describe the important considerations of the finite-element analysis, namely geometry, laminate configuration, loading, boundary conditions and results.

4.2.1 Geometry

The geometry of the frames was the first parameter to be studied. The first step in geometry development was to invent as many possible geometries based on observation and engineering intuition. From the initial geometries, three were kept after preliminary stress and deflection analysis was performed [59]. The three frame geometries studied are shown in Figure 4.1

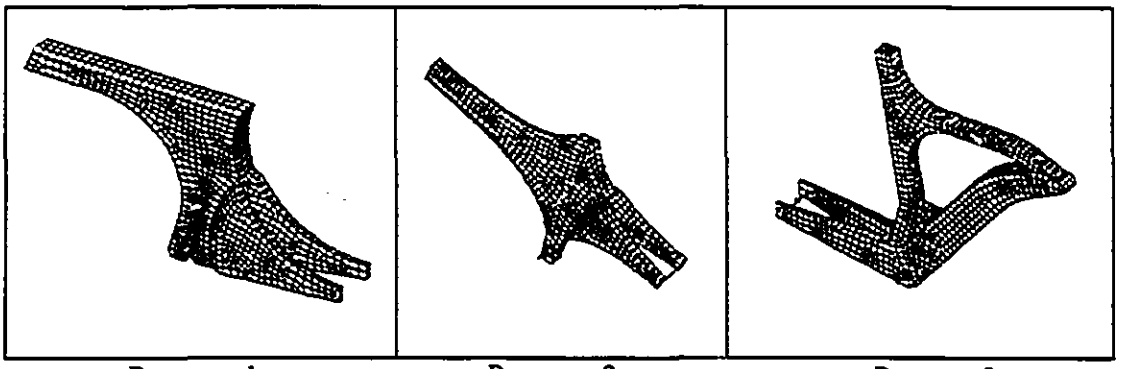

Prototype 1 Prototype 2 Prototype3

Figure 4.1: Frame Geometries of Three Composite Monocoque Prototypes

The geometry of the frames must also respect rule 49 of the Union Cycliste Internationale (UCI) which sets forth technical specifications for bicycle frames for use in international cycling competitions [60]. Figure 4.2 shows the specific dimensions which are regulated by rule 49 and Table 4.1 shows the dimensions of the 3 composite frames and how they obeyed the rules.

In addition to the specifications outlined in Figure 4.2 and Table 4.1, no features on the frame should serve as to reduce the drag or to accelerate the propulsion by any means, such as a wind protection shield, or other devices that serve only an aerodynamic purpose without being structural. The other restrictions of rule 49 are automatically met by the use of normally available bicycle components.

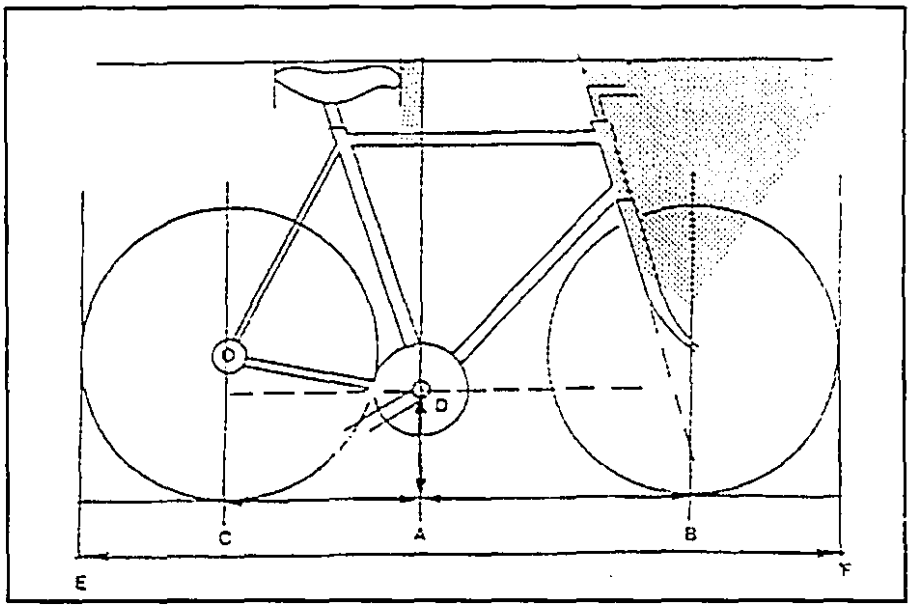

Figure 4.2 : UCI Regulated Dimensions

	UCI Rule	Prototype 1	Prototype 2	Prototype 3
AB (cm)	54-75	58	57	64
AD (cm)	24-30	30	28.5	27
AC (cm)	35-55	46	41	44
EF (cm)	<200	173	168	178

Table 4.1 : Prototype Dimensions

The shape of prototype 1 was chosen because it possesses a similar geometry to that of the *LOTUS* (see Figure 2.17). The thickness of the main part of this frame was 75 mm. This results in a structure which is quite bulky, but provides excellent torsional and out-of-plane rigidity. Prototype 2 models a beam which extends from the rear dropouts to the top of the head tube. This geometry is new and original and no other composite frame on the market possesses a geometry similar to it. The frame thickness is 50 mm. This reduction in thickness was made in order to lower the aerodynamic drag and make the frame more aesthetic. The reduction in thickness from 75 mm to 50 mm will reduce the inherent rigidity but with an increase in number of plies, the lateral rigidity may be made equivalent. Prototype 3 is actually a modification of the *Beam* bike (see Figure 2.15) which is on the market now. The modification is that prototype 3 contains a seat beam; a feature which is not part of the original design. This modification allows a reduction of the lateral sway and vertical movement associated with the cantilevered seat design of the beam frames. A

stress and failure analysis was performed on these three models. The three frames were modeled using thin shell triangular and quadrilateral elements. Thin shell elements were used as they are appropriate for modeling the thin structure of a composite of large surface area. Also, thin shell elements are used by default by the laminate modeling section of the software as they best represent a thin composite layup. The FEA models do not contain an internal core that constructed prototypes have. The introduction of the internal core was done as an aid to fabrication and should have only a small influence on the stress state thus it can be ignored in the model. Prototype 1, 2 and 3 contain respectively 2260, 1558, and 2156 thin shell elements. The different prototypes also used other types of elements in order to model the frame. For example rigid elements were used in order to apply forces or restraints at locations where they actually occur. These rigid beam elements represented handlebars, pedals, and fork stems. This permits the complete transmission of actual loads to the frame without any losses through the members.

4.2.2 Material and Laminate Configuration

The materials used for the modeling and construction of the frames are unidirectional and woven high strength carbon/epoxy prepreg. The woven material was modeled in the finite-element software as being one layer with equal material properties in the x and y-planar material directions. The unidirectional layer was modeled with orthotropic properties. The material properties used for the finite-element and failure analysis are shown in Table 4.2 [61]. Laminates for different elements of the 3 prototypes were modeled using the laminate modeling capability of the software. The 0° direction, i.e., the x-axis of a local coordinate system coinciding with material orientation used for the laminate construction, is taken to be the direction of a vector going from the rear dropouts to the top of the head tube. From the given 0° vector, the finite-element software automatically generates a corresponding vector for each element on the surface of the frame. The x-direction, corresponding to material orientation, is thus different for each element of the frame. The 90° direction, i.e., the y-direction for the local material orientation, is again in the plane of the elements, perpendicular to the x-axis according to the right hand rule with the z-axis pointing outward from the surface. Note that throughout this research the stresses are given in terms of this coordinate system. Hence, for example, the x-direction stress is a stress along a direction corresponding to the 0° vector of a certain element, and the shear stress is in the plane of the element. A global cartesian coordinate system will also be used and will have its -x-axis along the direction of motion of a frame with wheels, with its y-axis vertically up. Figure

4.3 shows the global x-y axes, the global 0° vector and the local 0° vector for a certain element of prototype 1.

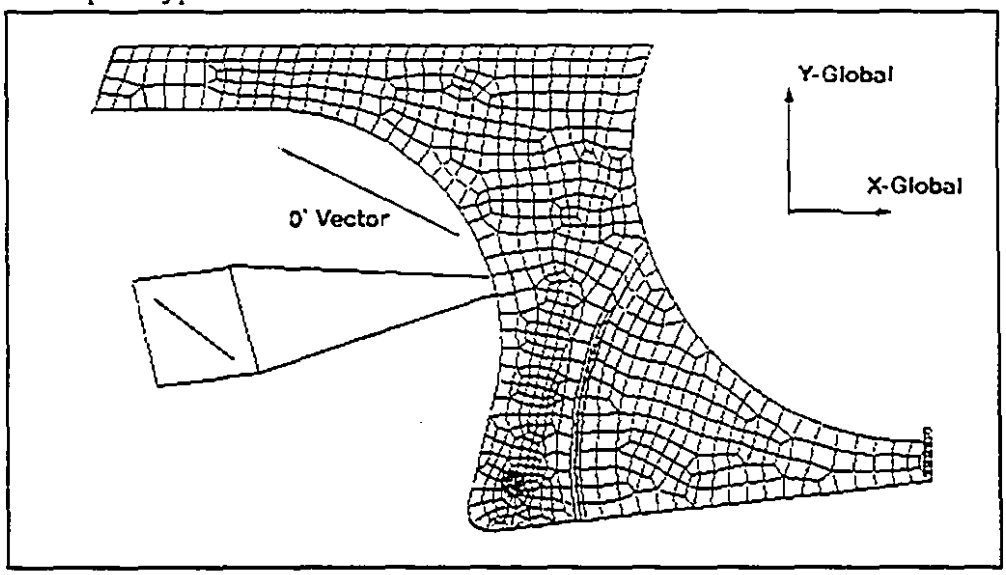

Figure 4.3: Direction of the 0° Vector.

The laminates discussed in the following subsections are the result of an evolutive study in which many types of laminates were attempted in order to develop a close to optimum fiber orientation for each case in terms of strength, stiffness and ease of fabrication.

	Unidirectional carbon/epoxy AKZO HTA7-LTM20	Woven carbon/epoxy CFS 001-LTM22
Cured ply thickness	0.17 mm	0.28 mm
Tensile modulus	126 GPa	65.6 GPa
In-plane shear modulus	2.14 GPa	3.17 GPa
Interlaminar shear strength	82.7 MPa	67.0 MPa
Compressive strength	1055 MPa	405 MPa
Tensile strength	1724 MPa	562 MPa
In-plane shear strength	93.1 MPa	78.2 MPa
Weight	0.263 kg/m^2	0.435 kg/m^2

Table 4.2 : Material Properties for Unidirectional and Woven Materials Used in this Study [61]

4.2.2.1 Laminate Configuration of Prototype 1

Prototype 1 includes 5 different laminates containing woven and unidirectional material and corresponding to layups used at different locations. It should be noted that this particular prototype was modeled and constructed only as a verification of the finite-element analysis results and construction method. Hence this particular frame could not be used in a riding or racing situation as it was not designed nor conceived to do so. Unidirectional material was used in conjunction with the woven material in certain high load areas as reinforcement. The regions of high loads were matched with the regions of material overlap since those regions have more material to support the load. The overlap regions were at least 25mm which well exceeds the required load transfer length of only several millimeters. Hence overlaps actually worked as reinforcement. The main front part of the frame was modeled and made of 2 layers of woven material. The layup changed to 4 layers in the overlap regions. Also unidirectional reinforcement was added to regions where 2 and 4 layers of woven material was already present. The last layup is in the rear region of the frame inside the well where the rear wheel is located. This region contains only one layer of woven material. Hence, for this frame, the 5 different laminates include:

1- 1 layer of woven material
2- 2 layers of woven material
3- 2 layers of woven material + overlap (4 layers woven)
4- 2 layers of woven + unidirectional
5- 2 layers of woven + overlap + unidirectional

Figure 4.4 shows the mesh and the different laminate locations for prototype 1. The numbers in Figure 4.4 correspond to the laminate numbers enumerated above.

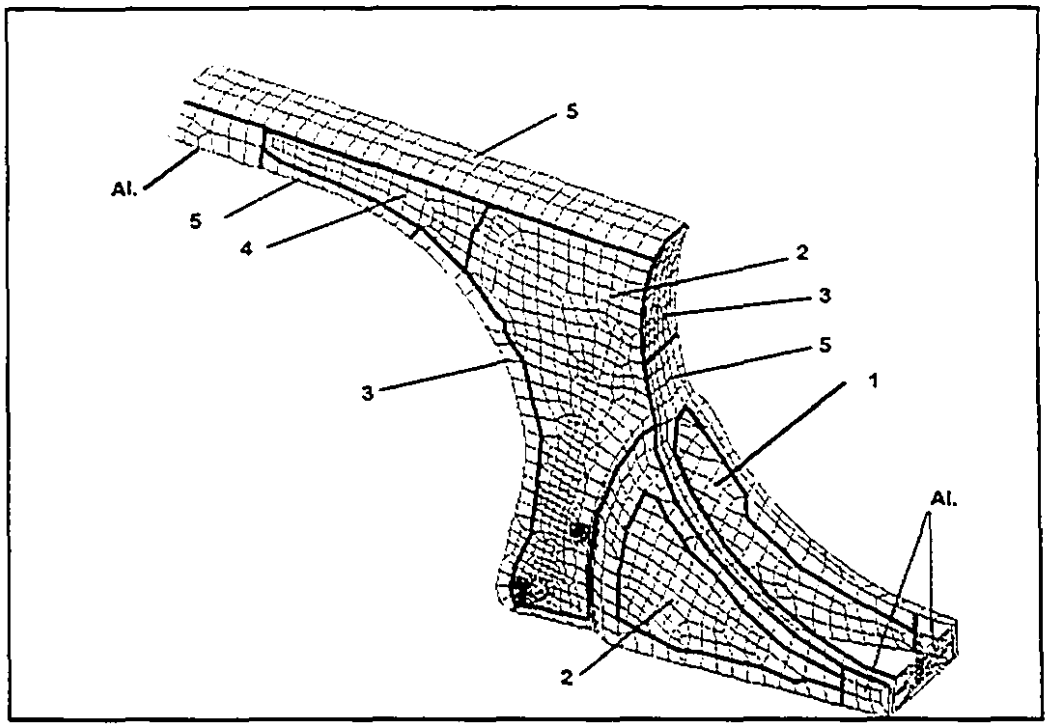

Figure 4.4 - Finite-Element Mesh and Laminate Regions for Prototype 1

4.2.2.2 Laminate Configuration of Prototype 2

Two sets laminates were considered for prototype 2. The first laminate used only unidirectional material applied on the model. It contained a $[0_2/90]_s$ 6-layer laminate in the low load regions built up with overlaps to a 10-layer $[0_2/90_2/0]_s$ laminate in higher load areas. This laminate was not adopted for construction because after the construction of prototype 1, it was realized that the use of unidirectional material on a structure as complex as a bicycle frame was very problematic. The unidirectional material did not conform well to double curvatures and hence cannot be used exclusively in the construction of a frame. It was thus attempted to model prototype 2 with woven material only, because even if the unidirectional reinforcement provides better stiffness and strength, it is believed that the construction process would be accelerated with the use of only woven fabric. Hence another laminate using woven material was developed. The laminate modeled for this prototype was made of 3 layers of woven material in low stress areas and a buildup to 6 layers in the overlap regions. Again the overlap regions were made to correspond to higher load areas. Prototype 2 was also modeled using 45° woven reinforcement in some areas as will be discussed later. The 45° reinforcement in the head tube, bottom bracket and rear

dropout regions was used in order to provide reinforcement in those critical areas as well as increasing the torsional rigidity in those regions. Figure 4.4 shows the finite-element mesh and different laminate regions for prototype 2. Hence for Figure 4.5, the 3 different laminates on the frame correspond to the following code:

1- 3 layers woven

2- 3 layers woven + overlap (6 layers woven)

3- 3 layers woven + overlap + reinforcement (8 layers woven)

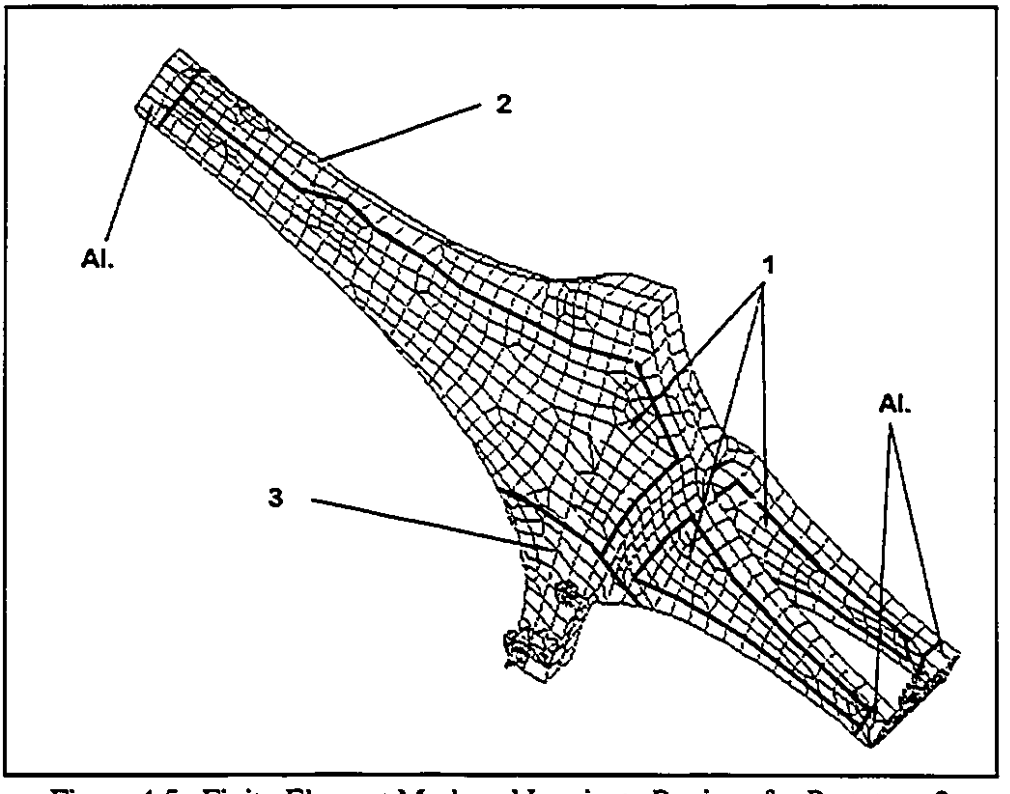

Figure 4.5 : Finite-Element Mesh and Laminate Regions for Prototype 2

4.2.2.3 Laminate Configuration for Prototype 3

The laminate for prototype 3 was modeled using unidirectional material only. A $[0_2/90]_s$ laminate is used with overlap reinforcement making the laminate a $[0_2/90/0_2]_s$ in critical regions. Figure 4.6 shows the location of the two laminates applied to prototype 3. Region 1 on Figure 4.6 has a $[0_2/90]_s$ laminate while region 2 has a $[0_2/90/0_2]_s$ laminate. This frame was only designed and developed on computer and was not constructed as part of this research project.

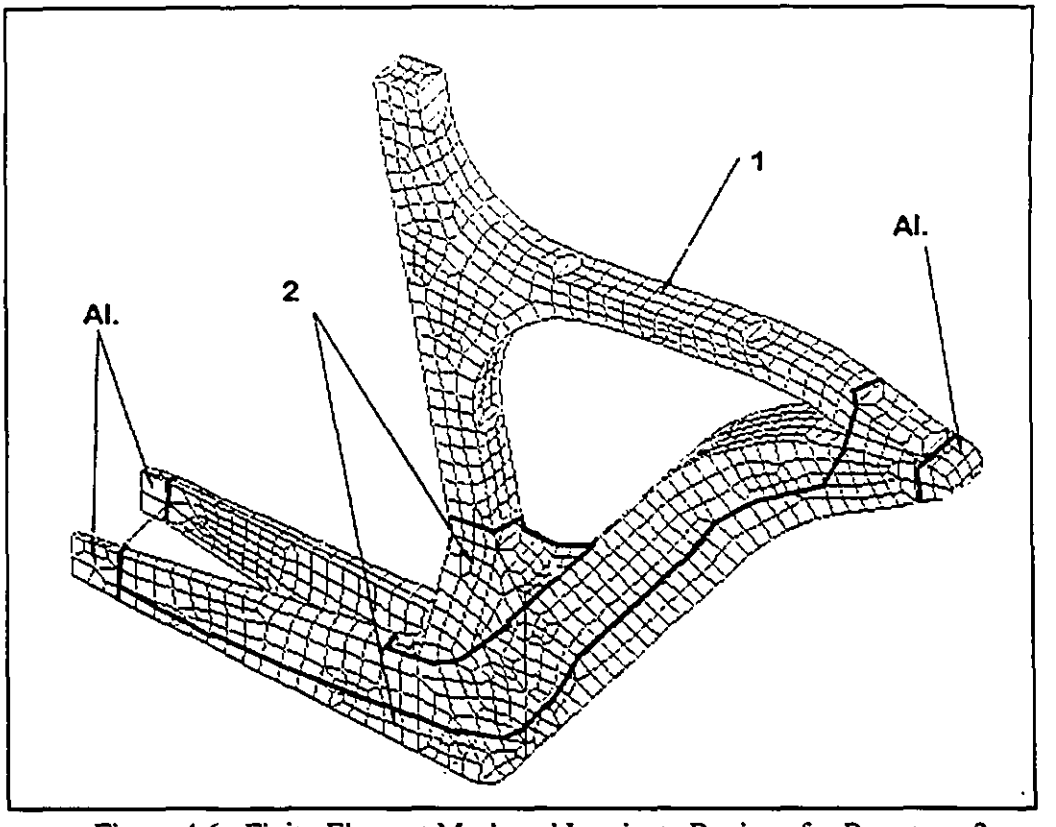

Figure 4.6 : Finite-Element Mesh and Laminate Regions for Prototype 3

4.2.3 Loading and Boundary Conditions

The loading and boundary conditions for a study of this type are very important in order to obtain realistic and useable results. A bicycle frame in motion is a complex loaded structure. In order to perform a reasonable stress analysis, it is important to choose a load case which closely represents true riding conditions. As track racing or time trial racing is the discipline of interest, and is performed under controlled road conditions, only rider induced loads were considered here. Although this assumption is quite valid for track racing, it certainly is not for mountain biking. Also, a load case where only one load is applied at a specific location, for example at the pedals, with stress and displacement patterns obtained throughout the frame is too simplistic and cannot realistically be used for design. An analysis of this type would only inform the designer about the specific response to a certain load and not the response of the frame to a riding situation. The load case chosen for this study contains loads applied to the frame by a racer riding on a flat surface at 50km/hr developing an average power of 400W. This load case is a static load case obtained at the point during the pedaling stroke where the loads are at a maximum,

hence this study is for the worst case static scenario. No dynamic analysis was performed during this research. This load case was calculated analytically and corresponds closely to what has been measured for the maximum loads in another study where loads at different application points were measured as a function of crank angle [62]. Loads during this study were calculated for a conventional geometry 56 cm frame, thus small corrections would have to be made in order to use it for a different size bike. This particular load case is different from those used in other studies as it considers the non-negligible effect of the chain and thus renders the loading situation non-symmetric with respect to the major vertical plane of the bicycle. Hence it is not possible to use symmetry to reduce the number of elements on the frame. It is believed that this load case reflects reality and is a good starting point for design. The following is a complete description of the load case derivation.

4.2.3.1: Starting Hypothesis of Load Case Derivation

-Mass of cyclist: 80 kg hence W=785 N
-Loads on the handlebars by the arms are unknown
-Angle of the arms with the handlebars is 45°
-Speed of the bike is 50km/hr = 13.88m/s
-Aerodynamic coefficient: $C_x = 0.83$ [63]
-Surface of the bike-cyclist assembly $S = 0.3m^2$ [63]
-Flat terrain
-Wind speed=0

4.2.3.2: Problem Steps

-Calculate the power expenditure of the cyclist
-Calculate the loads on the pedals from the input power
-Isolate the bicycle and calculate the loads on the wheels
-Isolate each wheel
-Calculate the loads on the frame

4.3.3.3: Powers Involved

-Power developed by the cyclist: $P_{cyclist}$

-Power dissipated by the chain transmission is neglected (a chain transmission is typically 98% efficient) [64]

-Power lost due to air resistance is P_{air}

-Power dissipated by rolling resistance is neglected

-Power dissipated by the contact forces perpendicular to the roads are neglected

Then at constant speed applying the kinetic energy theorem

$$P_{total} = dE_c/dt = 0 \qquad (4.1)$$

$$\text{hence } P_{cyclist} + P_{air} = 0 \qquad (4.2)$$

$$P_{cyclist} = -P_{air} = F_{air} V$$

$$= 0.5\, p\, C_x\, S\, V^2\, V$$

$$= 0.5 \times 1.19 \times 0.83 \times 0.3 \times 13.88^2 \times 13.88$$

$$= 400 \text{ W}$$

Where V= Riding Velocity= 50 km/h = 13.88 m/s

C_x = Aerodynamic coefficient = 0.83

S = Frontal area = 0.30 m^2

p = Air density = 1.19 kg/m^3

For comparison, reference [65] shows a racer riding at 12.1m/s (43.6 km/hr) corresponding to a tractive power of 373W and from [66] a time trial power output for a 40.22 km record performance at an average speed of 13.6m/s (49km/hr) produces a power expenditure of more than 373W.

4.2.3.4: Calculation of pedal loads

Isolate the chain drive

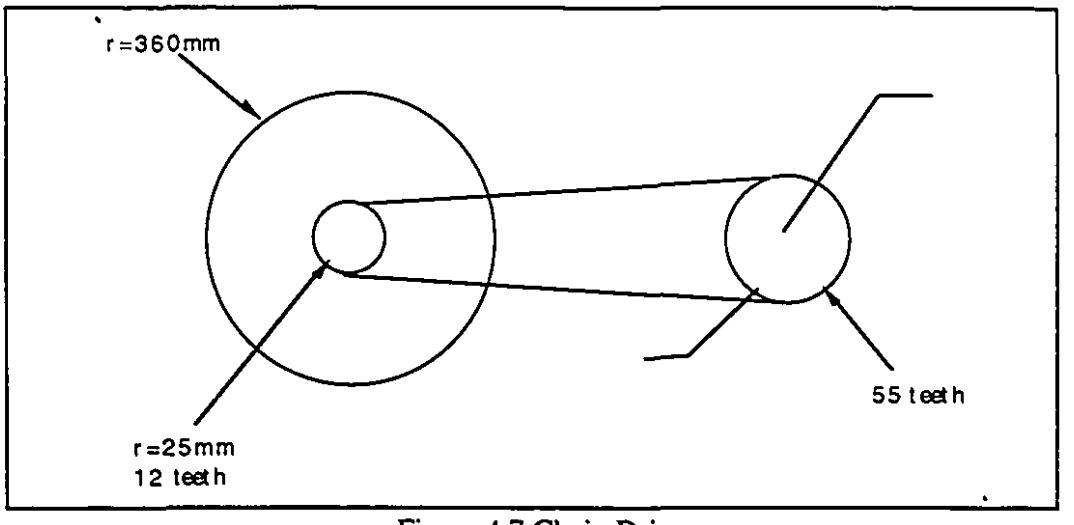

Figure 4.7 Chain Drive

The circumference of the back wheel is 2261 mm, hence at 50km/hr (13.88m/s) the rear 12 teeth cog turns at:

$$V/r = 13880 / 2261 = 6.14 \text{ turns/s} \quad (4.3)$$

hence the front chain ring rotates at

$$(12 \text{ teeth}/ 55 \text{ teeth}) * 6.14 \text{ turns/s} = 1.39 \text{ turns/s}$$
$$\text{or } w = 8.73 \text{ rad/s}$$

From the total power (P) of 400 W, the couple C at the bottom bracket is related to the power delivered by the cyclist by the following relation, where w is the angular velocity

$$P = C\,w = 400 \text{ W} \quad (4.4)$$
$$\text{or } C = P / w = 400 / 8.73 = 46 \text{ Nm}$$

Again for comparison [67] shows 35Nm for 373W at 105rpm and increasing torque for lower rpm.

If the crank arms have a radius r of 170mm, the total force exerted on the pedals will be:

$$C / r = 46Nm / 0.17m = 271\ N \qquad (4.5)$$

where we assume that the racer pushes down on the right pedal with 75% of his force while pulling up on the left pedal with the remaining 25%. The downward force with the left pedal will be 203N (Fp) while the upward pull is 68N (Ft) as shown in Figure 4.8. This assumption is intuitive but could easily be justified and shown to be close to reality if an appropriate study on this subject were performed.

4.2.3.5 Considering the Complete Bicycle

The forces present are:

-The weight of the rider (**p**)

-The pulling forces on the handlebars (**T**)

-The wind resistance ($\mathbf{F_{wind}}$)

-The loads on the pedals (**Fp** and **Ft**)

-The loads on the wheels ($\mathbf{R_1}$ (front wheel) and $\mathbf{R_2}$ (rear wheel))

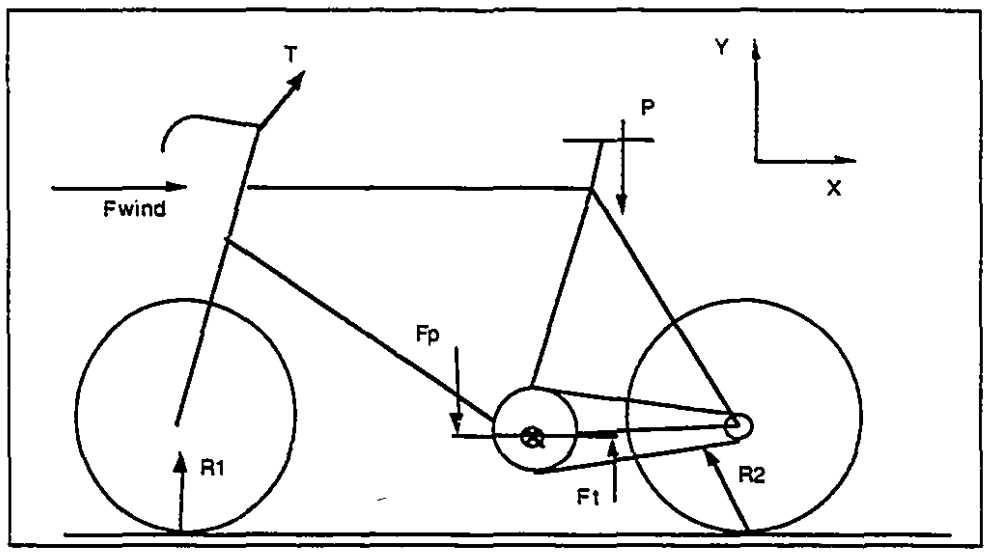

Figure 4.8 : Forces Acting on the Bicycle

$$\mathbf{F = m\,A}$$

$$\mathbf{Fp + Ft + Fwind + T + P + R1 + R2 = 0} \qquad (4.6)$$

$$\text{x-direction} : Tx + R1x + R2x + Fwind\ x = 0$$

$$Tx + R1x + R2x + 29 = 0 \qquad (4.7)$$

y-direction: $Ty + P + Fp + Ft + R1y + R2y = 0$

$$Ty - 785 - 203 + 68 + R1y + R2y = 0$$

$$Ty - 920 + R1y + R2y = 0 \qquad (4.8)$$

And the moment equation, taken about a moment axis in the z-direction at the bottom bracket axis is:

$$-0.1\,P + 0.170\,Ft + 0.170\,Fp + 0.3\,R1x + 0.3\,R2x + 0.42\,R2y - 0.68\,R1y - 0.62\,Tx - 0.49\,Ty - 0.3\,Fwind = 0 \qquad (4.9)$$

$$-33 + 0.3\,R1x + 0.3\,R2x + 0.42\,R2y - 0.68\,R1y - 0.62\,Tx - 0.49\,Ty - 0.3\,Fwind = 0$$

Isolating the front wheel:

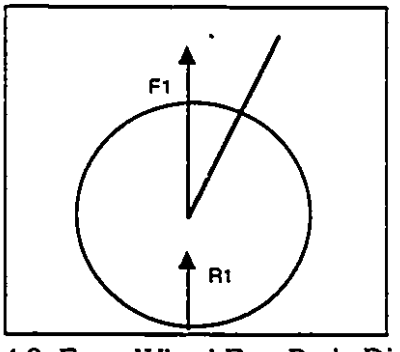

Figure 4.9: Front Wheel Free Body Diagram

where : F1 is the load applied by the wheel on the frame,

R1 is the load applied by the ground on the wheel

$$R1x + F1x = 0 \quad \text{(x-dir.)}$$

$$R1y + F1y = 0 \quad \text{(y dir.)}$$

$$R1x * \text{radius of wheel} = 0 \quad \text{(moment eq.)}$$

$$\text{hence } R1x = 0 \qquad (4.10)$$

Isolating the rear wheel:

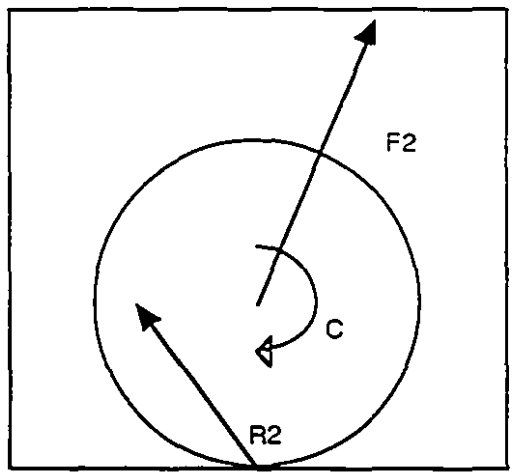

Figure 4.10 : Rear Wheel Free Body Diagram

Where : F2 is the load applied by the wheel on the frame

R2 is the load applied by the ground on the wheel

$$R2x + F2x = 0 \text{ (x-dir.)}$$

$$R2y + F2y = 0 \text{ (y-dir.)}$$

$$R2x * \text{radius of wheel} + C = 0 \text{ (moment eq.)}$$

where C is the chain couple which was found to be equal to 46Nm using equation 4.4, hence:

$$R2x = -46 \text{ Nm} / 350\text{mm}$$

$$R2x = -131 \text{ N}$$

and: $F2x = 131 \text{ N}$ (4.11)

Assuming the force on the handlebars to be at 45° to the horizontal,

$$Tx = Ty \quad (4.12)$$

Using (4.7), (4.8), (4.9), (4.10), (4.11), (4.12) , solve for all the parameters to get:

From (4.7) $Tx + R1x + R2x + 29 = 0$

$Tx + 0 - 131N + 29 = 0$

$Tx = 102 \text{ N}$ (4.13)

From (4.12) $Tx = Ty = 102 \text{ N}$ (4.14)

From (4.8) $Ty - 920\ N + R1y + R2y = 0$

$102\ N - 920\ N + R1y + R2y = 0$

$R1y + R2y = 818\ N$ (4.15)

From (4.9) $-33 + 0.3\ R1x + 0.3\ R2x + 0.42\ R2y - 0.68\ R1y - 0.62\ Tx - 0.49\ Ty - (0.3 * Fwind) = 0$

$-33 + 0 - (131*0.3) + 0.42\ R2y - 0.68\ R1y - (102*0.62) - (102*0.49) - (29*0.3) = 0$

$-33 - 39.3 - 63 - 50 - 8.7 + 0.42\ R2y - 0.68\ R1y = 0$

$-194 + 0.42\ R2y - 0.68\ R1y = 0$ (4.16)

Using 4.14, equation 4.8 becomes $R1y = 818 - R2y$ (4.17)

Using 4.17, equation 4.16 becomes $-194 + 0.42\ R2y - 0.68 * (818 - R2y) = 0$

$-194 + 1.1\ R2y - 556 = 0$

$1.1 * (R2y) = 750$

$R2y = 682\ N$ (4.18)

and from 4.17 and 4.18 $R1y = 818 - R2y$

$R1y = 818 - 682$

$R1y = 136\ N$ (4.19)

Hence in conclusion we have from 4.10, 4.11, 4.14, 4.18 and 4.19

$R1x = 0$ (4.20)

$R2x = -131\ N$ (4.21)

$Tx = 102\ N$ (4.22)

$Ty = 102\ N$ (4.23)

$R2y = 682\ N$ (4.24)

$R1y = 136\ N$ (4.25)

4.2.3.6 Calculation of the Frame Torsion Forces on the Handlebars

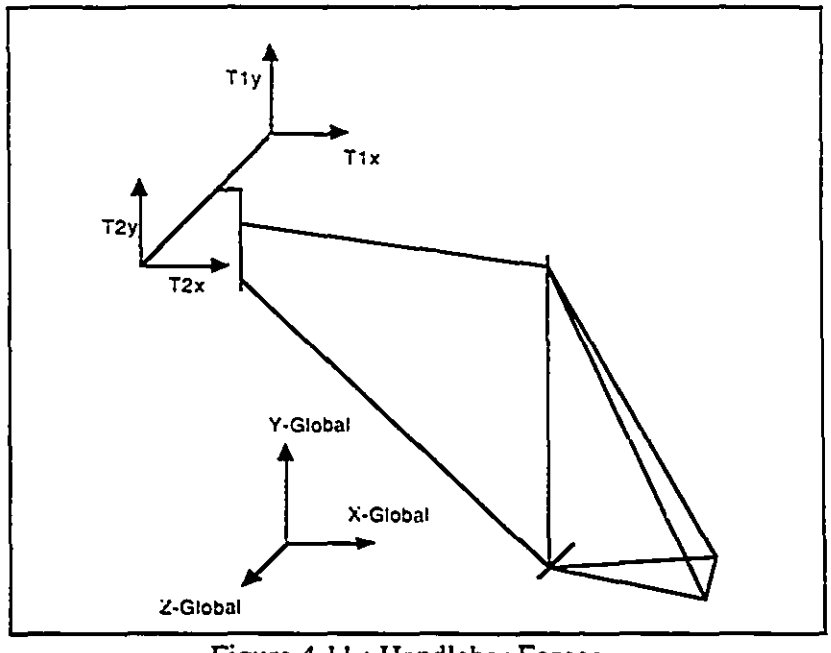

Figure 4.11 : Handlebar Forces

$$T1x + T2x = 102 \quad (4.26)$$

$$T1y + T2y = 102 \quad (4.27)$$

Moment equation about bicycle centerline at pedal axis:

X-dir: $Fp * 80mm - Ft * 80mm - T2y*200mm + T1y*200mm = 0$

$68 * 0.08 + 203 * 0.08 + T2y*0.2 - T1y*0.2 = 0$

$$21.6 + T2y*0.2 - T1y*0.2 = 0 \quad (4.28)$$

Y-dir: $T1x * 0.2 - T2x * 0.2 = 0$

Hence $T1x = T2x$ (4.29)

And from (4.26) and (4.29)

$$T1x = T2x = 51N \quad (4.30)$$

from (4.27) and (4.28),

$21.6 + (102 - T1y) * 0.2 - T1y*0.2 = 0$

$42 - T1y * 0.4 = 0$

hence T1y = 105 N (4.31)

and from (4.27)

T2y = 102 - 105 = -3

T2y = -3N (4.32)

The complete load case is now shown in Figure 4.12.

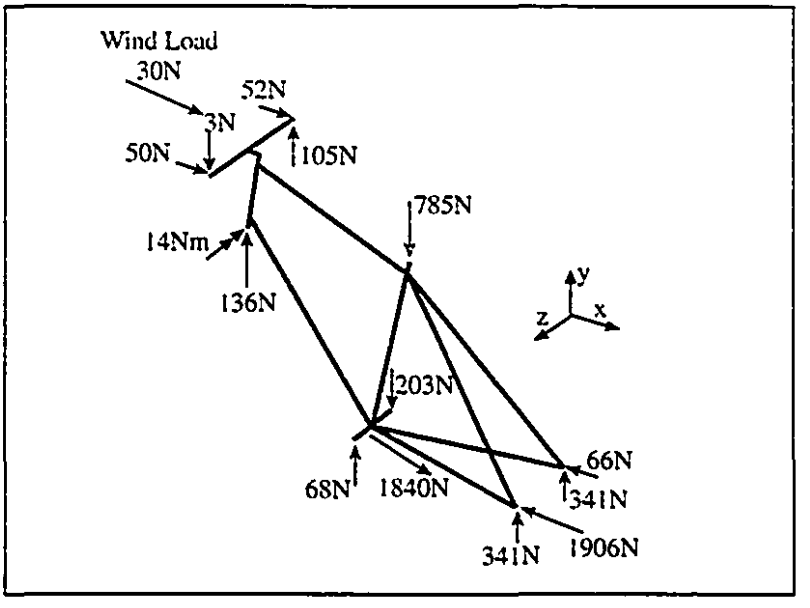

Figure 4.12 - Riding Load Case

The loads shown in Figure 4.12 were applied to the finite-element thin shell nodes either directly or through the rigid beam elements used at the handlebars and pedals. In the regions of the seat and rear dropouts, the loads are divided up and applied to many nodes directly on the shell model.

4.2.3.7 Boundary Conditions

The restraints attempted to model the boundary conditions on a riding bicycle frame as closely as possible. The frame was restrained at the bottom of the front fork as well as the left and right rear dropout. These are the only points where the frame is in contact with components that are directly in contact with the ground. There are no more locations were restraints could be implemented.

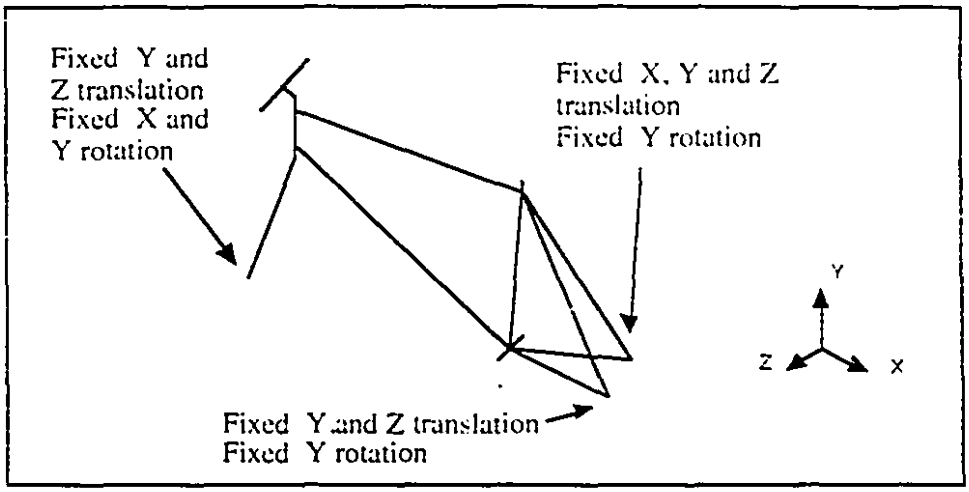

Figure 4.13: Riding Restraint Locations

The restraints shown in Figure 4.13 are summarized in Table 4.3. This restraint set has been previously used in other bicycle frame stress studies [62]. The global coordinate system used is shown in Figure 4.13.

	X	Y	Z	X rot.	Y rot.	Z rot.
Bottom of front fork		*	*	*	*	
Left rear dropout		*	*		*	
Right rear dropout	*	*	*		*	

In the above Table, * denotes a fixed degree of freedom.

Table 4.3 : Riding Restraints

4.2.4 Stress Analysis Results

Stress analysis is essential in many ways. It allows the determination of the stresses in the different layers and thus assures that the stress levels are below the allowables. Also, it allows the visualisation of the different high stress areas so that modifications can be implemented. The stress analysis was performed using the loads and boundary conditions described in section 4.2.3. Classical laminated plate theory was assumed, and stresses were found in each of the laminate layers. Normal stresses in the x- and y-directions as well as the in-plane shear stresses were obtained.

4.2.4.1 Prototype 1

The maximum stresses for prototype 1 were obtained for each layer of each laminate. The stresses are tabulated in failure index form (stress divided by strength as per the maximum stress criteria [68]). The maximum stress criteria is justified in this study because one stress (shear stress) is the dominant stress which may cause failure. A failure index of 1 means failure in the material, while a failure index of 0 means no stress at all. The factor of safety is then the reciprocal of the failure index. The failure index for this prototype was calculated with the failure stress of the material at the location of the maximum stress for each layer. The x-direction refers to the material orientation direction in the plane of the elements that was defined from the rear dropouts to the head tube. The y-direction is a direction perpendicular to the x-direction in the plane of the element. Table 4.4 shows the maximum failure indices for each material failure mode in each ply.

	Xtension	Xcomp.	Ytension	Ycomp.	XYshear
Ply 1	0.092	0.196	0.049	0.080	0.493
Ply 2	0.043	0.168	0.085	0.168	0.628
Ply 3	0.042	0.193	0.082	0.144	**0.633**
Ply 4	0.031	0.067	0.083	0.083	0.494
Ply 5*	0.047	0.225	0.004	0.008	0.280

*Unidirectional layer

Table 4.4 : Maximum Failure Index for Each Layer of Prototype 1

It is interesting to note trends from Table 4.4. The largest failure indices for the first prototype are due to in-plane shear stresses. Figure 4.14 shows the xy-shear stress contours in ply 3.

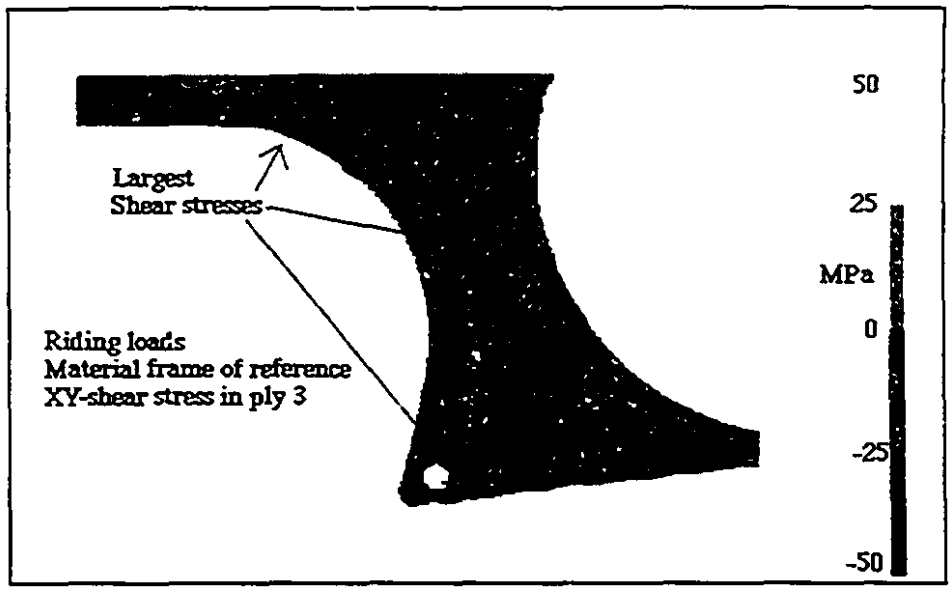

Figure 4.14 : XY-Shear Stress Contours for Prototype 1, Layer 3

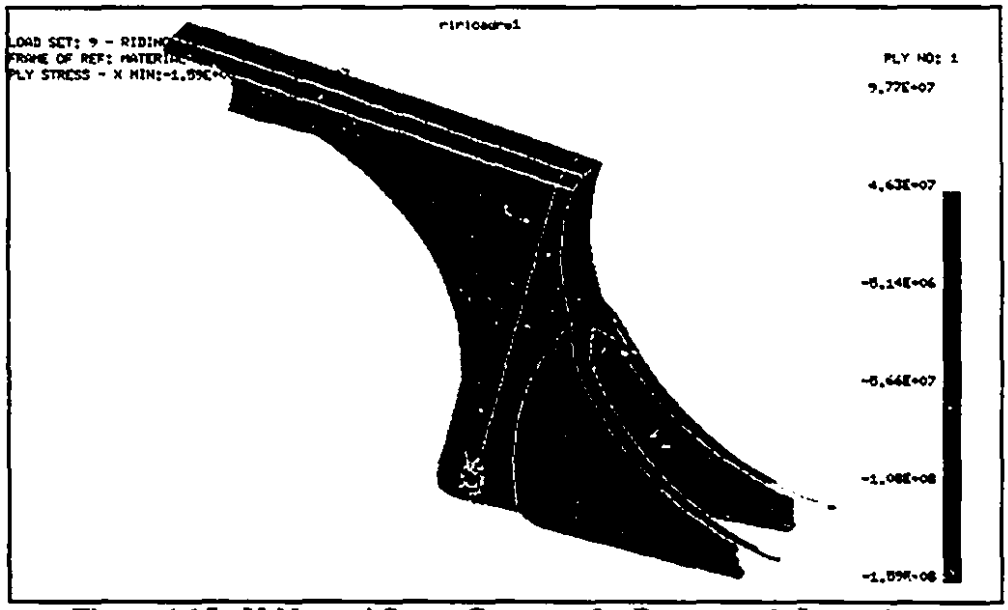

Figure 4.15 : X-Normal Stress Contours for Prototype 1, Layer 1

From Figure 4.14, note that the largest shear stress region occurs near the edge of the front curvature of the frame. Two other large stress regions occur near the bottom bracket and the rear curvature. As shear stress is reduced by the addition of 45° layers, from this analysis, it can be seen that more 45° layers would be needed in the front and back curvature regions. This observation corresponds with existing practice for tubular carbon fiber frames where the down tube is made mostly with 45° layers in order to resist down

tube torsion [21]. Hence for this first prototype, with this particular laminate and under these riding loads, the in-plane shear stresses are the highest.

Figure 4.15 shows the x-direction fiber stress in ply 1. The magnitude of the x-stress on this frame is higher than the xy-stress, but considering the ability of composites for carrying loads in tension, the failure indices for this material direction are much lower. The most important aspect to consider from Figure 4.15 is that the high stress region is concentrated near the bottom bracket and that the rest of the frame is under an almost constant state of low stress. The distribution of the low stress evenly on the frame is a geometric attribute of a specific design. Hence only reinforcing the bottom bracket region (although not necessary in this case for this specific stress component) would be sufficient. It is also interesting to note the thin region of higher stress going diagonally down from the head tube region toward the rear dropouts. This general direction corresponds to the bending load path for a bicycle frame so it is interesting to see that this physically intuitive aspect shows up in the finite-element results.

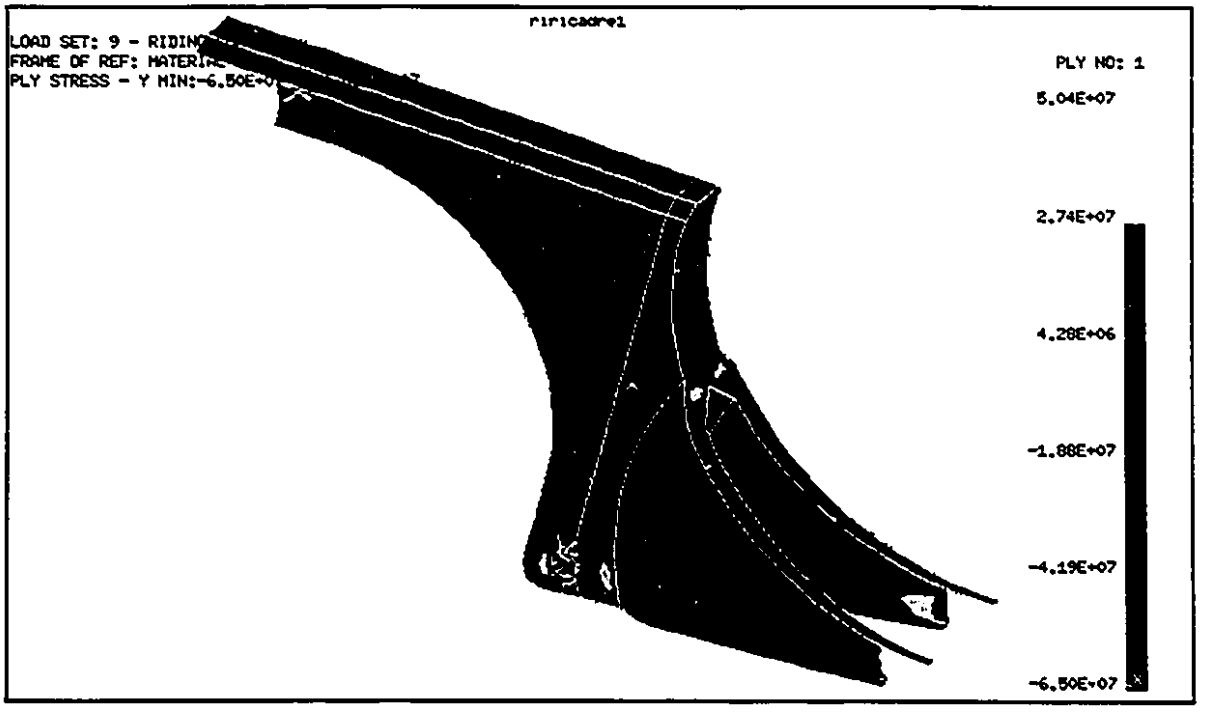

Figure 4.16: Y-Normal Stress Contours for Prototype 1, Layer 1

Figure 4.16 shows the y-stress in ply 1. As ply 1 is made from woven material, the y-stress is again a fiber stress. As seen from Table 4.4, the magnitude of the y-stress is

much less than the x-stress for ply 1 shown in Figure 4.15. Again, a fairly uniform state of stress is observed throughout the frame with larger stress regions observed in the back of the seat region and near the bottom bracket.

Figure 4.17 shows the out-of-plane displacements under the riding loads and boundary conditions. The out-of-plane displacement varies from 1.37mm in the positive z-direction (out of paper) to 3.32mm in the negative z-direction (into paper). The top part of the frame is essentially free of out-of-plane displacement. On the other hand the bottom bracket region and overall lower part of the frame is affected by out-of-plane displacement. As was shown in chapter 3, the out-of-plane displacement should be restricted to a minimum to prevent extreme deformation in the frame, hence if more reinforcement should be added, it should be done in the areas of the frame near the bottom bracket. Hence it is clear that in the bottom bracket region, geometric and laminate design is of utmost importance.

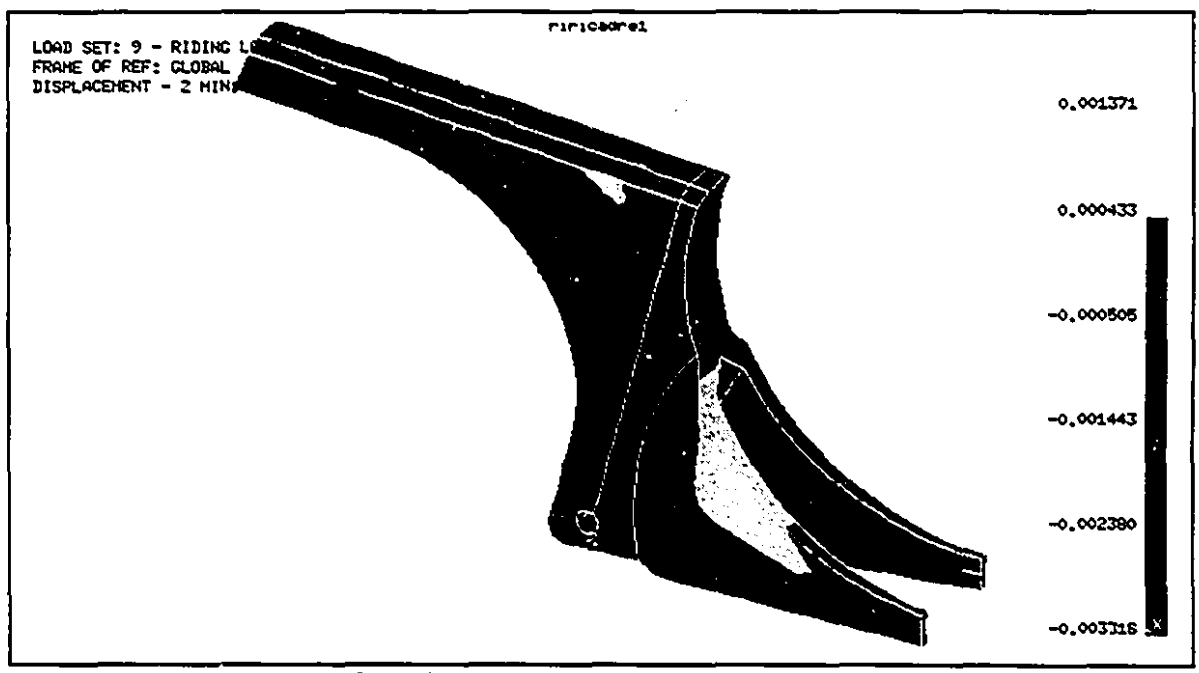

Figure 4.17: Out-of-Plane Displacement Contours for Prototype 1

4.2.4.2 Prototype 2

Table 4.5 shows the maximum failure indices for the second prototype, again subjected to the same loading and restraint set as prototype 1.

	X tension	Xcomp.	Ytension	Ycomp.	XYshear
Ply 1	0.138	0.172	0.075	0.170	0.744
Ply 2	0.124	0.156	0.077	0.170	0.763
Ply 3	0.126	0.169	0.099	0.142	**0.782**
Ply 4	0.043	0.175	0.040	0.114	0.660
Ply 5	0.033	0.122	0.036	0.186	0.679
Ply 6	0.049	0.185	0.067	0.140	0.692

Table 4.5: Maximum Failure Index for Each Layer of Prototype 2

For prototype 2, the highest stresses were again due to shear stresses but only in the region of the bottom bracket, especially on the left side of the bicycle where the chain is located. Figure 4.18 shows the shear stresses in the bottom bracket region. The shear stress varies from a positive value to a negative value within a small region. The magnitude of these shear stresses being very high in this region, careful laminate design has to be implemented. This is why the addition of reinforcement was considered in some specific regions. The addition of reinforcement will be discussed in this section. Except for the large concentrated values of shear stress, the rest of the frame is submitted to very low values of shear stress. The same is observed for the x-stress (fiber stresses) shown for ply 1 in Figure 4.19. Large values of stresses, shown by the darker regions, are located in the bottom bracket region where most of the load (from the rider's legs) is introduced to the composite structure. However, it is clear from the failure indices that this frame will not fail due to tensile or compressive loading of the fibers.

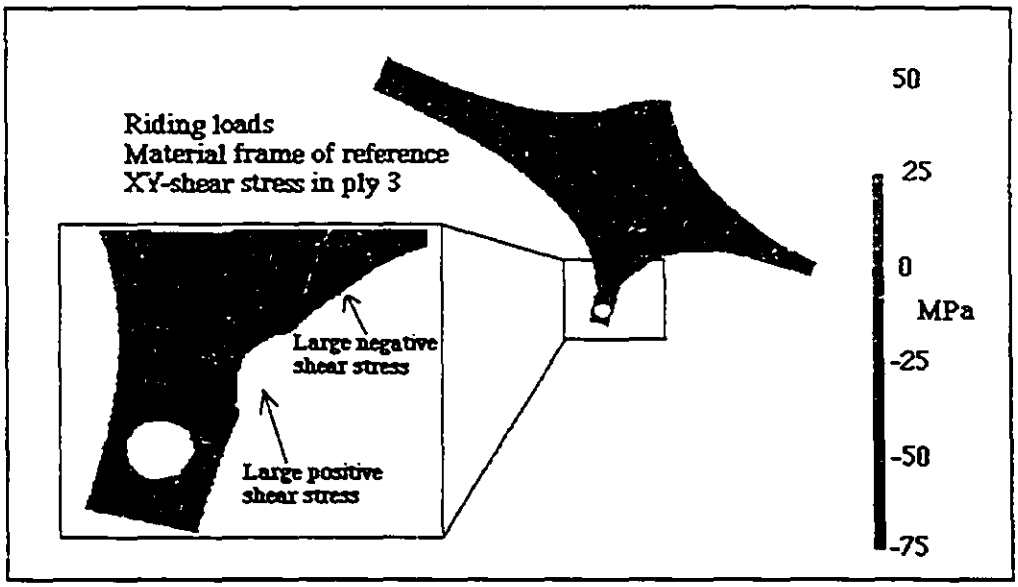

Figure 4.18: Prototype 2 - XY-Shear Stresses at Bottom Bracket Region, Layer 3

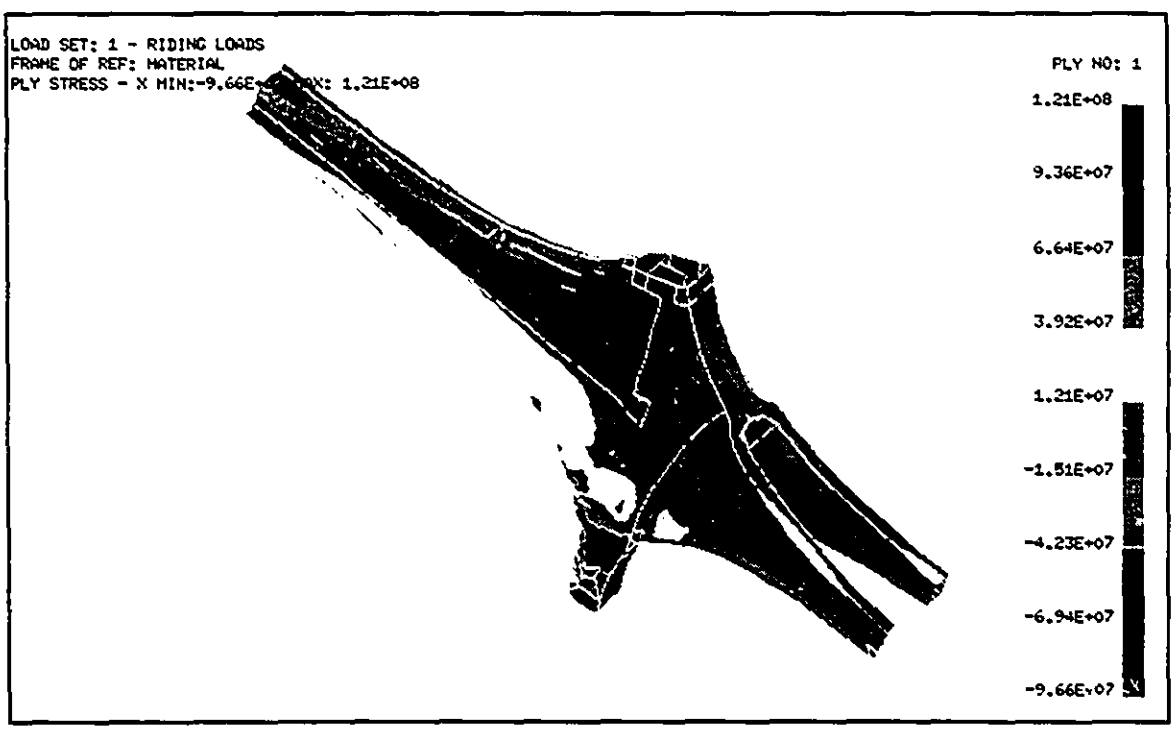

Figure 4.19: Prototype 2 - X-Normal Stress, Layer 1

Figure 4.20 shows the y-stress in ply 1. Most of the frame is subjected to very low y-stress which is again a fiber stress as this is a woven material. The bottom bracket region is again submitted a higher y-stress. From the above discussion, it is immediately evident that the bottom bracket region is the most highly loaded and stressed and that it should be

thoroughly considered both during design and fabrication of the frame. It is a region where geometry, unfortunately does not lend itself to easy material application. This is especially true for this prototype where the bottom bracket region seems attached to the rest of the frame in a way which may not be optimum. Figure 4.21 shows the displacement magnitude contours for prototype 2. Note that the displacement is non-symmetric with respect to the mid-plane and that the maximum occurs again at the bottom bracket.

Figure 4.20: Prototype 2 - Y-Normal Stress, Layer 1

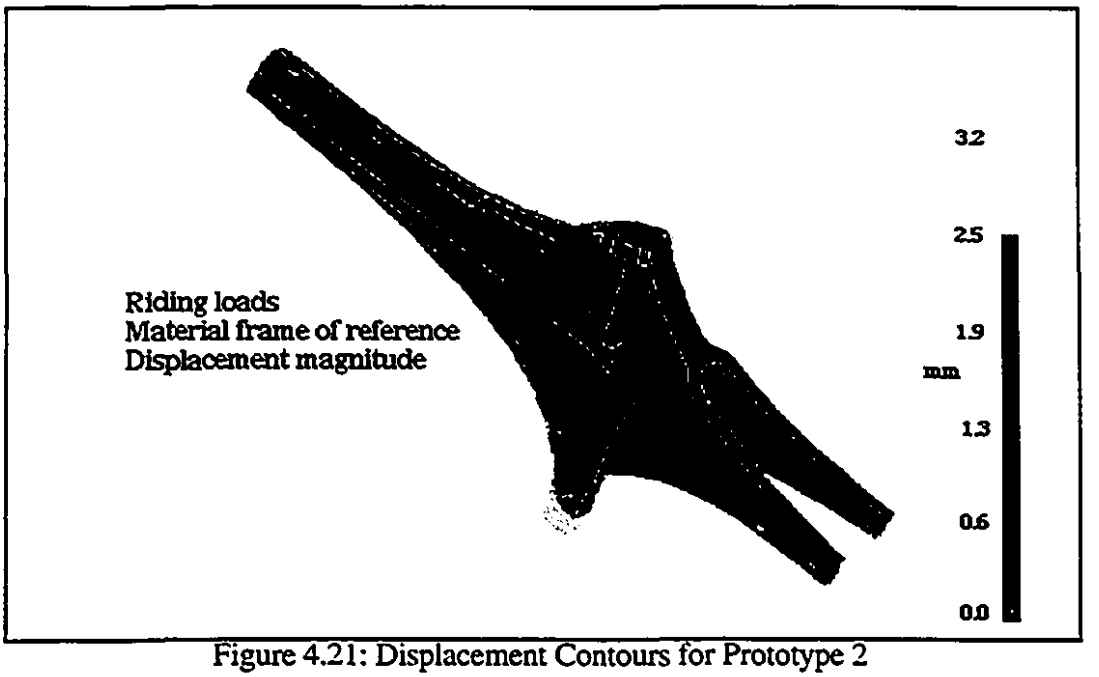

Figure 4.21: Displacement Contours for Prototype 2

Considering the large stress values as seen from Figures 4.18, 4.19 and 4.20, reinforcement was added to the bottom bracket region of prototype 2. Two 45° woven layers were added to the 6 layer laminate already present in this region. This allowed not only the shear stresses to be reduced but also the x and y-normal stresses as well. The shear stress, in particular, reduced by up to 35% in one of the plies. One observation however is that the location of the maximum stress did not change. This confirms that a geometric redesign would be necessary in this area. A bottom bracket geometry like prototype 1 is much more sturdy and hence the stresses there are better distributed.

The addition of the two 45° layers also increased the overall stiffness tremendously as seen by reductions in frame deflections. Table 4.6 shows the displacements at the bottom bracket before and after the addition of the 45° reinforcement. The large X-global (horizontal) displacement is due to the large chain force, and the reinforcement greatly improves the stiffness in this direction. In the Y-global (vertical) direction the displacement is not particularly affected by the laminate change as the vertical displacement is mostly due to the overall flexing of the frame rather then a local effect. The bottom bracket torsional stiffness is much improved with the addition of the reinforcement as can be seen by the reduction of the Z-global (out-of-plane) direction displacement.

	Without reinforcement (mm)	With reinforcement (mm)	Improvement (%)
X_{global}	2.9	1.8	38
Y_{global}	-2.2	-2.0	9.0
Z_{global}	3.0	2.2	27

Table 4.6: Bottom Bracket Displacements With and Without Reinforcement

From the above observations, it should be evident that a carbon fiber frame should be built with as many different laminates which correspond to the different stress regions as the goal should be to have a structure with a uniform stress level throughout. This is achieved with the improved laminate for prototype 2.

4.2.4.3 Prototype 3

For prototype 3, the results of a ply-by-ply analysis were obtained as was performed for prototype 1 and 2, and maximum failure indices are summarized in Table 4.7.

	X tension	Xcomp.	Ytension	Ycomp.	XY shear
Max.F.I.	0.160	0.060	**0.770**	0.224	0.187
Ply #	3	5&6	8	8	2

Table 4.7 : Maximum Failure Index for Each Layer of Prototype 3

Figures 4.22, 4.23, and 4.24 show the maximum X-stress, Y-stress and XY-shear stress contour plots for prototype 3, respectively. Prototype 3 is designed with a $[0_2/90]_s$ unidirectional composite layup in the low load areas and built up to a 10 layer $[0_2/90_2/0]_s$ layup in the higher load areas. As this is unidirectional material, it is expected that the limiting factor will be matrix tension. This is what is observed from Table 4.7. Also, the fact that it occurs in ply 8 could have been expected as it is a 90° layer which is the farthest from the core, hence the layer subjected to the most matrix tension due to bending of the frame. Figure 4.22 shows the fiber stress in ply 3. The magnitude of stresses is high but again the strength of the fibers is correspondingly high resulting in quite low failure indices. The light areas on the frame shown in Figure 4.22 are high tensile stress areas. They correspond mostly to areas of the frame having only 6 layers. These regions show higher stresses as there is less material to take up the load. Note that along the main beam, the line between the two layups coincides with the difference in the two stress levels.

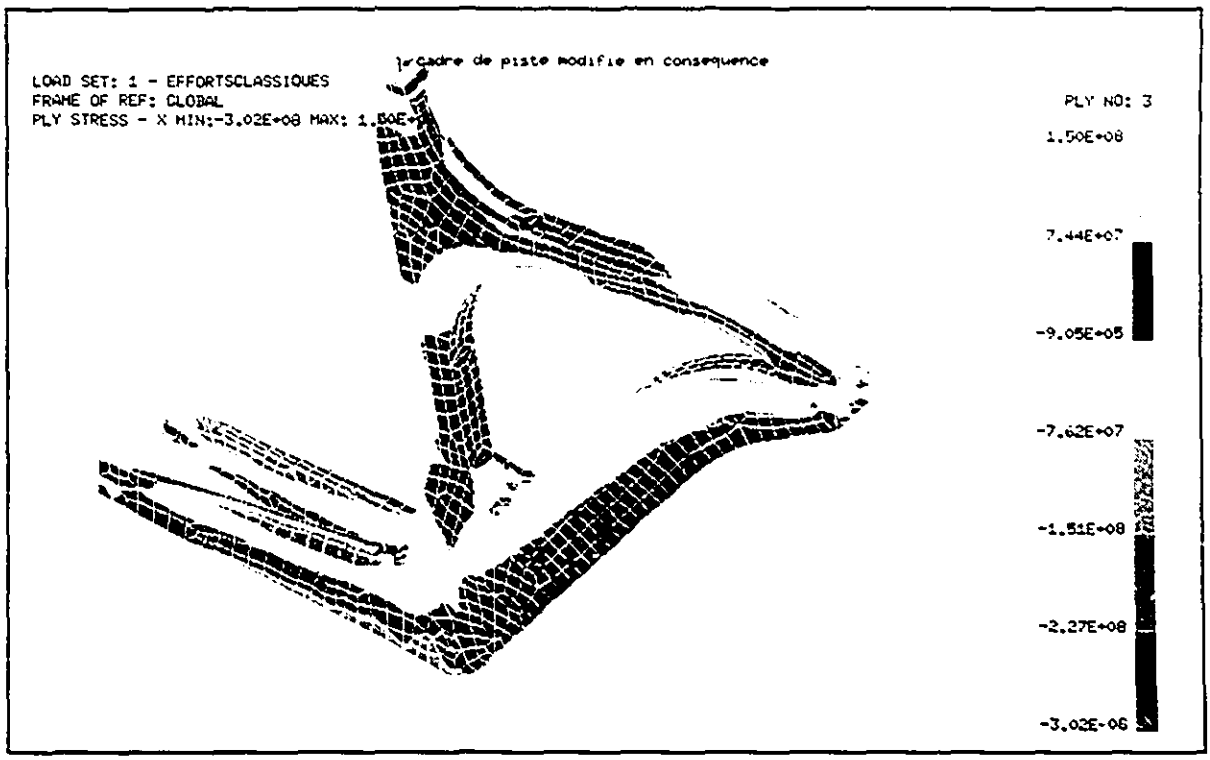

Figure 4.22 : Maximum X-stress for Prototype 3

Figure 4.23 shows the maximum Y-stress for prototype 3 in ply 8. In Figure 4.23, the light regions are regions where no or low stresses exist because in most of the frame there is no ply 8, hence no stress to be displayed. The maximum matrix tension stress is found in the back of the seat beam. Hence as this is the region where the highest failure index exists on the frame, it is the first region where the frame should be reinforced. If we follow the procedure of adding reinforcement to the regions of highest failure index and remove material from regions of low index until a desired failure index value corresponding to the factor of safety is achieved, the lightest frame for this factor of safety will be obtained. Although this proposition is quite true for a given load and boundary condition and quite acceptable in theory, in practice it is completely different. The load case changes continually and hence no perfect theoritical layup will yield a uniform failure index throughout. Even if the loading case was uniform in time, the manufacturing of such a perfect layup with all the combination of layers and orientations would probably be impossible. So, it is impossible to build a frame with a uniform failure index throughout.

Figure 4.24 shows the XY-shear stresses throughout the frame with a maximum near the bottom bracket. Although this bottom bracket region is much more sturdy than for prototype 2, it is expected that the maximum shear stresses will occur in this region.

In conclusion, prototype 3 forms a very efficient structure from a finite-element analysis point of view, but the manufacturing of such a frame by the construction method used might be much more difficult because of the geometry with so many sharp corners. Time constraints combined with this manufacturing problem prevented this frame from being constructed as part of this project.

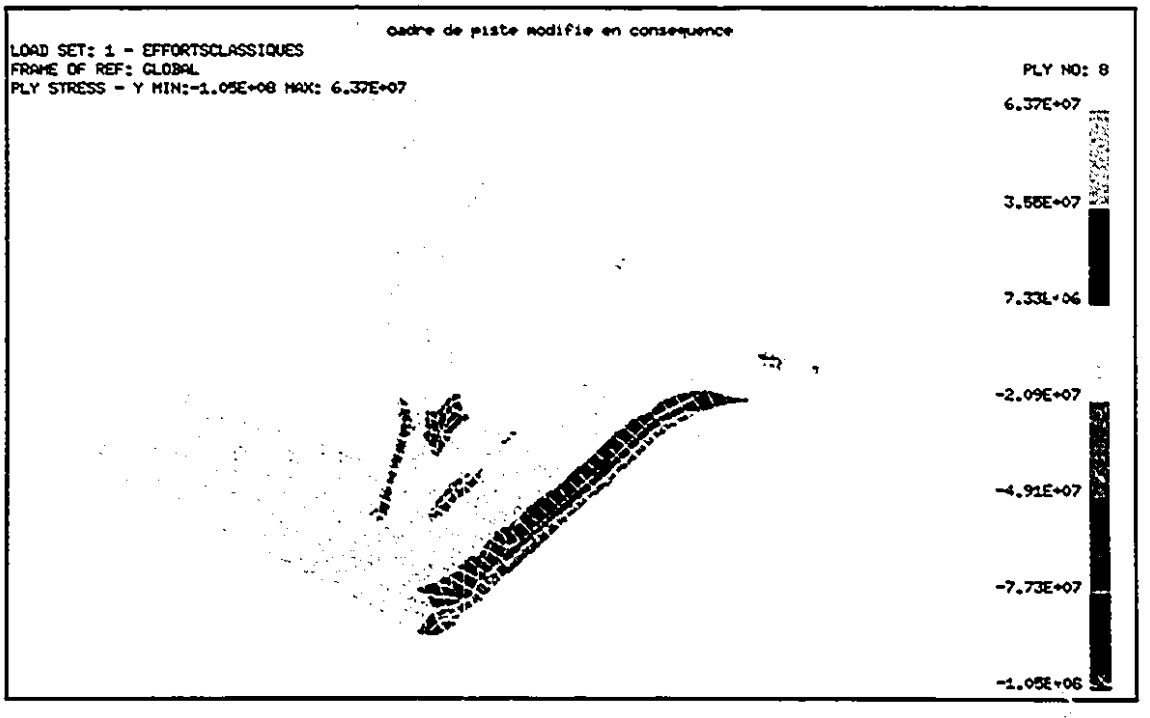

Figure 4.23: Maximum Y-Stress for Prototype 3

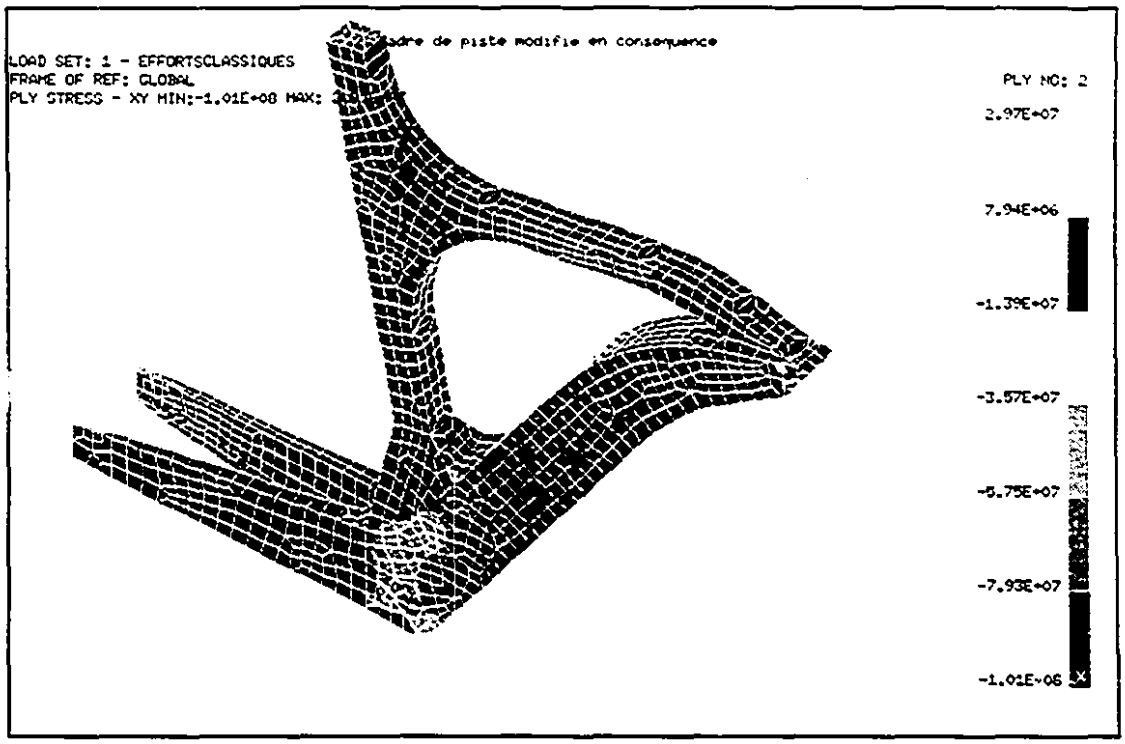

Figure 4.24: Maximum XY-Shear Stress for Prototype 3

Chapter 5

Composite Frame Fabrication and Testing

5.1 Introduction

As previously discussed, the second part of this project includes the construction of two carbon/epoxy monocoque bicycle frames. Prototypes 1 and 2 were constructed. This section will explain in detail the method, instruments, and materials used in the construction of those frames. The final curing of prototypes 1 and 2 took place in September 1994 and June 1995 respectively. The methods used to test the frames will also be explained. The test results for the composite frames will be compared to tests performed on classic metallic frames.

5.2 Rationale for Manufacturing Method

The manufacturing method chosen is the thermoset prepreg-vacuum bagging method outlined in section 2.5.4. It was chosen because as this study is still in the prototyping stage, only one or two models of each frame was initially planned. Hence an expensive aluminum or composite mold would not be appropriate. The thermoset prepreg material was chosen over the wet lay-up and thermoplastic composite because it provides good mechanical properties, the correct fiber to resin volume fraction, an appropriate tackiness for fabrication and a relatively low cost compared to woven or unidirectional thermoplastic prepregs. It is clear that final production of frames, large or small, should use an exterior mold either with an internal bladder or an internal core, both for fabrication time reduction and appropriate surface finish. For the reasons mentioned above, it was clear that the thermoset prepreg-vacuum bagging technique was the best choice for this project.

5.3 Fabrication of Prototype 1

Prototype 1 is the first carbon fiber frame built at McGill University. It is an experimental frame and thus the whole fabrication process was experimental. This prototype was constructed for two main reasons. The first reason was to experiment with the manufacturing technique to see if it yielded acceptable results. The second reason was to verify if the finite-element analysis could closely model the actual situation. Keeping these two reasons in mind, the fabrication should be well understood and appreciated. This frame was not meant for hard racing, and possibly not even for casual riding. The following sections explain in detail the different materials and procedures used in the production of this prototype.

5.3.1 Foam

The core of the frame is made of high performance rigid PVC foam. This was chosen in order to provide a stable platform for shaping at a relatively low weight with appropriate mechanical properties. The properties of the Klegecell R75 foam are shown in Table 5.1.

Density	75 kg/m^3
Compressive Strength	1.29 MPa
Tensile Strength	1.88 MPa
Flexural Strength	1.98 MPa
Shear Strength	1.04 MPa
Elongation at break	3.5%

Table 5.1 : Mechanical Properties of the Foam Used for Prototype 1 [69]

Due to complicated and costly numerical control machining, the foam was shaped using manual labor techniques. A combination of hot-wire, band saw, exacto knives and sand paper was used to shape the 3 foam pieces. The final foam shape was made from three pieces glued together as the thickness of the available foam was not sufficient for the required thickness of the rear part of the model. The final foam shape weighted 901g. Figure 5.1 shows the foam core with the aluminum inserts attached to it.

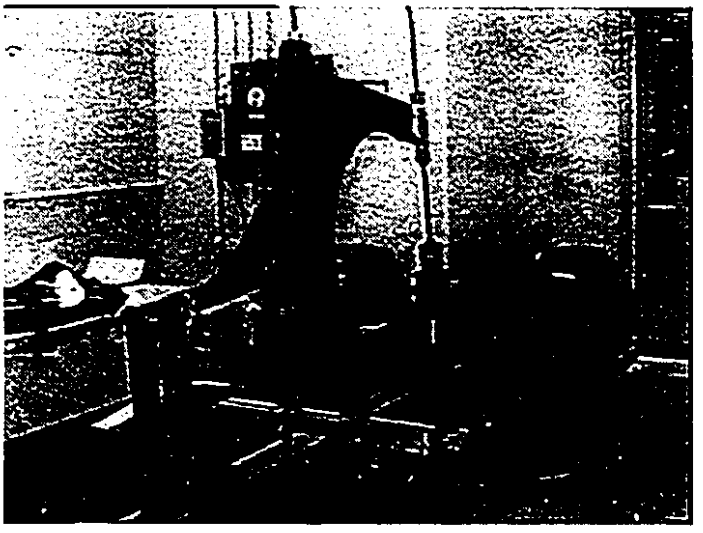

Figure 5.1 : Prototype 1 in the Curing Jig

5.3.2 Foam Adhesive

In order to fabricate the foam model, 3 pieces of foam had to be fastened together. Both the left and right rear stays had to be fastened to the main body. The foam pieces were bonded together using Ciba-Geigy's fastweld epoxy adhesive [69]. This adhesive is fast curing and appropriate for PVC foams.

5.3.3 Inserts

Aluminum inserts were bonded to the foam at different locations. The function of these inserts is to allow the different components to be attached to the carbon frame. These metallic reinforcements were placed between the inner foam core and the exterior layer of composite material. The main purpose of these inserts is to transfer the loads through a large bonding area from the composite material to the external agents. Aluminum inserts were used at the bottom bracket, the rear dropouts, head tube and seat tube. Aluminum was chosen for these parts because of its relatively low weight and ease of machining.

Headset

The headset was designed as a divergent channel with the top open. The exterior of the fitting was horizontally grooved to a depth of 1 mm to allow for a better resistance to vertically applied forces. The grooves allow composite material to become embedded into the insert during the curing process. The headset is shown in Figure 5.2.

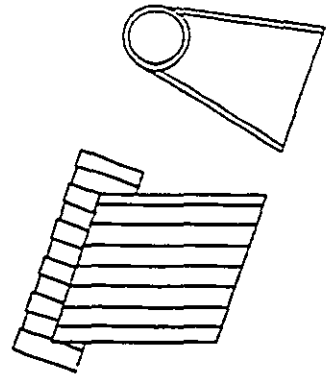

Figure 5.2: Aluminum Headset

The inner diameter of the head tube was machined to fit a standard headset. The headset insert weight was 166g.

Bottom Bracket Insert

The bottom bracket insert consists of 3 pieces. One tube houses the bottom bracket cartridge, and is supported on both sides of the frame by a grooved aluminum plates meant to be embedded in the foam. The bottom bracket arrangement is shown in Figure 5.3. The bottom bracket insert weight was 71g.

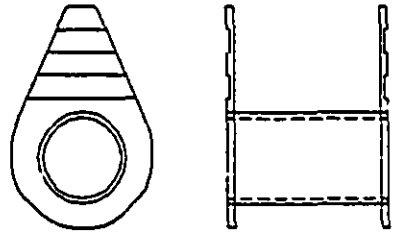

Figure 5.3 : Bottom Bracket

Rear Dropouts

The rear dropouts consist of an open channel closed at one end by the rear axle mount. The 4 pieces of each rear dropout were welded together. The channel is also grooved and the bottom is closed for the same reasons as those described for the headset. Figure 5.4 shows the rear dropout design. The weight of the left dropout was 166g while the right dropout weighed 171g (difference due to welding).

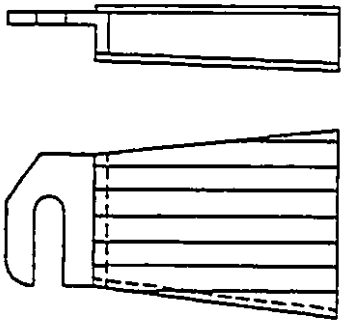

Figure 5.4 : Rear Dropouts

Seat Tube

A seat tube of 28.6 mm external diameter and 26.7 mm internal diameter was inserted to a depth of 5 inches into the foam core. The weight of the seat tube was 33g.

As the carbon fiber is electrically conductive, it is possible that galvanic corrosion may occur at the carbon-aluminum interface. This corrosion produces an oxide that renders the interface weak and less than optimum. Hence in order to minimize the corrosion, etching of the aluminum is performed prior to the bonding with the carbon. This etching process reduces the chances of galvanic corrosion [71].

5.3.4 Curing Jig

In order to install the inserts onto the foam core and also in order to support the frame during the curing process, a special modular jig was designed and constructed [72]. This jig is constructed in such a way as to prevent excessive warping of the frame during curing.

If any of the parts of the frame were to move out of alignment during the curing process, the bike would become unsymmetric and depending on the degree of misalignment, the bike would possibly be useless. This jig was constructed out of steel and aluminum by undergraduate students at McGill [72]. It was designed to be versatile and to be compatible with different frame sizes. The frame is held in the jig by four main attachment points: the pedal shaft, the front tube, the rear forks, and the seat tube. Figure 5.1 shows the foam frame in the jig, ready to be covered with the carbon fiber material. Also, the aluminum inserts can be seen.

5.3.5 Foam-Aluminum Adhesive

After the foam as been correctly shaped, it is fastened with the aluminum inserts and installed on the jig. At this point, it is critical to make sure that the foam, inserts, and jig are in perfect alignment. The aluminum inserts were fastened to the foam core using ADCHEM high strength epoxy (5300A resin, 5300B hardener) [73]. Some properties of this epoxy system are outlined in Table 5.2. The epoxy was allowed to cure for 48 hours before the clamps were removed. Only 22g of adhesive was used to secure the inserts in place.

Boiling Point	260 °C
Tensile Strength	62 MPa
Tensile Modulus	2.3 GPa

Table 5.2: Properties of the ADCHEM High-Strength Epoxy [73]

5.3.6 Carbon Fiber Material

The material used for the construction of this prototype was obtained from The Advanced Composite Group Inc. [61]. Both woven and unidirectional continuous fibers were used. As a very light and stiff structure is required, it is important to use high performance continuous fibers rather than chopped fibers or mats. The woven material is a 4X4 twill weave which uses AKZO HTA carbon fibers [61]. The 4X4 twill weave is referred by the manufacturer as a CFS001 weave and is very drapable, that is it conforms well to double-curvatures. The material is preimpregnated with LTM25 low temperature curing epoxy in a

B-stage. The unidirectional material uses the same fibers and epoxy system as the woven material. The mechanical properties of both the unidirectional material and woven material can be found in Table 4.2. The epoxy system is low temperature curing (56°C) in order to be compatible with the maximum temperature the foam can withstand (77°C). The cured thickness of one layer is 0.28 mm for the woven material and 0.17 mm for the unidirectional material.

5.3.7 Material Orientation

Section 4.2.2.1 gives a detailed account of the material orientations used for the construction of prototype 1.

5.3.8 Vacuum Bagging

After the carbon fiber prepreg had been carefully applied to the foam core, other materials had to be applied to the carbon fiber in order to prepare for curing. A layer of release film (non-porous Teflon) is applied directly on the carbon fibers. This thin film is applied in order to enable the releasing of the vacuum bag from the finished part after curing. Then a breather layer was applied everywhere. The breather material is quite thick and allows the passage of air. This layer helps the vacuum to spread everywhere under the vacuum bag. A vacuum bag was then made around the whole structure. The vacuum bag is sealed all around with vacuum gum. Figure 5.5 shows prototype 1 inside its vacuum bag.

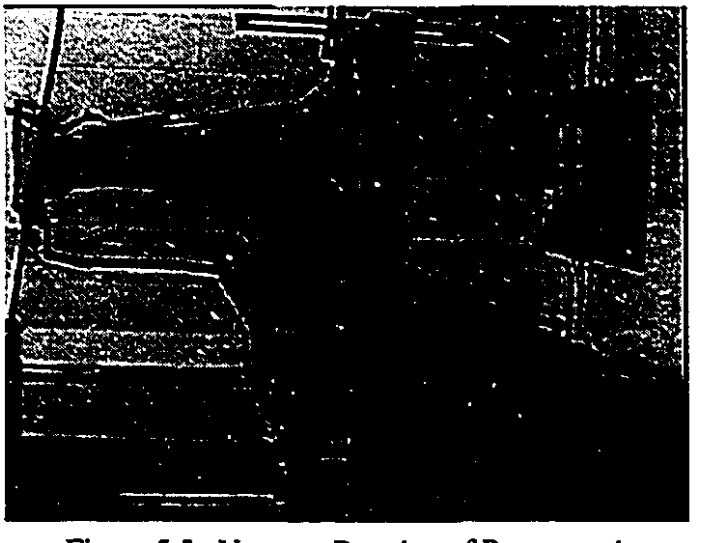

Figure 5.5 : Vacuum Bagging of Prototype 1

A vacuum hose is installed and the vacuum drawn. Some minor air gaps may then be stopped with vacuum gum until an adequate vacuum is obtained. A vacuum pressure of the order of 0.9 atm is achieved.

5.3.9 Curing

After an adequate vacuum is obtained, the frame is ready for curing. The frame was cured in a controlled temperature oven with the prescribed temperature profile shown in Figure 5.6. This curing cycle is the one suggested by the material manufacturer. The slope for the periods of heating and cooling are important as a shallow slope (1/2°C/min.) does not thermally stress the material as much as a steep slope. After curing, the vacuum bag, breather layer and release film are removed to reveal a fully cured carbon monocoque bicycle frame.

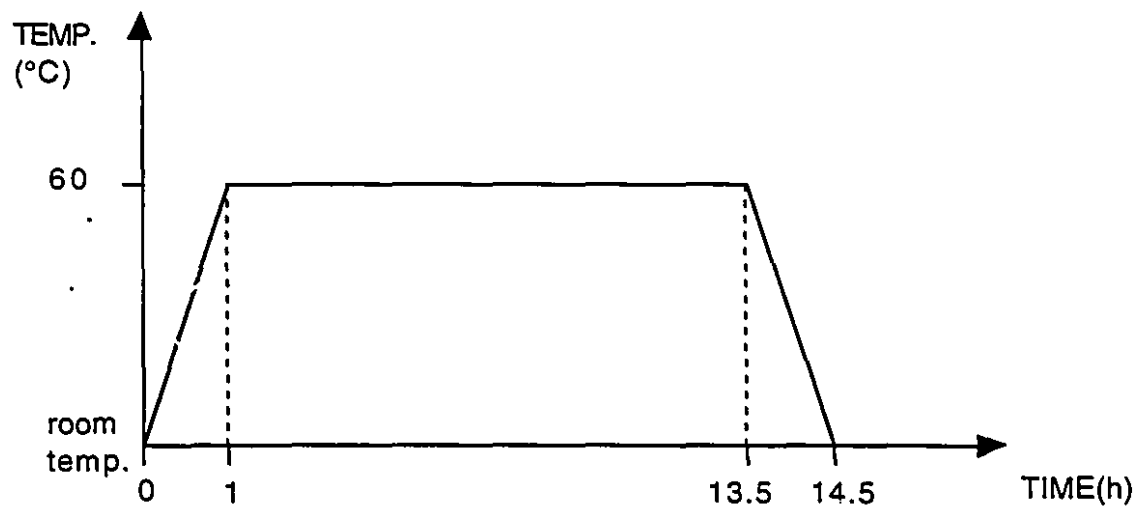

Figure 5.6 : Curing Cycle

After curing, the surface of the composite frame showed some wrinkles. These wrinkles are inevitable and are a result of the imperfect vacuum bag. Some of the wrinkles are minor and are formed from a slight amount of excess resin, while others are a direct wrinkling of the fibers. The resin wrinkles can be sanded off without any loss of structural integrity.

The fiber wrinkles could be grinded off, but weaken the composite frame. The fiber wrinkles appeared evenly throughout the frame. This prototype was not sanded nor painted, as esthetics was not important for this model. Also, not sanding before static testing allows the possibility of examining the effect of the wrinkles against the finite-element model, which of course, does not contain any wrinkles.

5.3.10 Mass Properties of Prototype 1

Table 5.3 shows how much each subgroup contributed to the final weight of prototype 1.

Prototype 1	Weight (g)
Foam	901
Aluminum Inserts	607
Glue and Filler	44
Composite	631
Total	2183

Table 5.3: Summary of Weights for Prototype 1

5.3.11 Conclusions and Recommended Improvements for Prototype 1

As previously specified, this prototype was constructed in an attempt to become familiar with the fabrication method and to validate the finite-element analysis of composite structures of this type. The first and most substantial improvement which resulted from the fabrication of this prototype is the realization that the weight of the aluminum inserts and the foam should be reduced. A weight of 2183g for a composite frame is far too heavy. Another fact realized is that a frame width of 75 mm was too wide. A wide frame is very bad aerodynamically. This frame seemed generally too bulky, hence reduction of the frame thickness was in order. Prototype 2 was built with a nominal thickness of 50 mm. This reduction in width by 33% helped reduce the volume and hence the weight of foam used. Prototype 1 also had another basic problem. It could not be used as a time trial bicycle because there is no possibility for mounting the chain and rear derailleur on the

inside of the rear stays. No rear derailleur can be installed, so the rear sprocket would have to be mounted on the outside of the rear right stay. This is so because the top part of the chain cannot pass from the front chainring to the rear sprocket without being in conflict with the frame itself. As this type of frame can only be of limited use, a frame design allowing both road time trial with rear derailleur and track racing capability is more advantageous. The only way to modify this frame with its rear stay geometry, to be used as a time trial frame, would be to make a hole in the frame at the location where the upper part of the chain meets the frame. The bicycle used by 5 time *Tour de France* champion Miguel Indurain in the time trials built by Pinarello of Italy incorporates this feature. An oval hole is made on the right rear stay in order to allow the chain to go through. Figure 2.16 shows the Pinarello frame with the access hole for the chain.

Another improvement to prototype 1 would be the reduction of the number of wrinkles present on the frame. This would of course result from the use of an exterior mold. Alternatively, greater care in the fabrication of the vacuum bag would allow a reduction in the number of wrinkles. Another way to lower the number of wrinkles is to make sure that all the carbon fiber layers are applied tightly to each other. Loosely applied layers have a greater tendency to wrinkle when compacted by the vacuum pressure.

In summary, the fabrication of prototype 1 was a success for what it was intended to provide. It was the first carbon fiber monocoque frame ever built at McGill, and it yielded encouraging results. It permitted the acquisition of a great deal of experience and hands-on realization of potential problems encountered in composite construction. Figure 5.7 shows prototype 1 as it would look ready for riding (note without pedals or chain).

Figure 5.7 : Completed Prototype 1

5.4 Fabrication of Prototype 2

The fabrication of prototype 2 was intended to yield a rideable, low weight monocoque carbon fiber frame. However, the prepreg-vacuum bag technique is still used and will ultimately yield an imperfect surface finish. This frame could be used as a very decent time trial vehicle. Also, it could be used as a marketing tool for future investors in order to make an association between McGill University and interested bicycle manufacturers. Having gained the experience from two monocoque carbon frames, it would be possible to start a small production of frames with the use of an exterior mold, but still using the same shape. Hence the aim with this prototype is to make a final design which could be rideable and marketable.

5.4.1 Foam

Prototype 2 used a different foam than that used for prototype 1. This decision to change the internal foam material for a lower density material was based on many reasons. The first reason was to reduce the overall weight of the foam core. The internal core weight of 901g for the first prototype was considerably high in order to produce a complete frame with a competitive weight. The foam used for prototype 2 was a very light PVC foam manufactured by Divinycell [74]. Its density of only 45 kg/m^3 is 60% of the foam density used for prototype 1. The second reason for a lower density foam material is an improvement in the dynamic behavior of the frame. It was shown that a lower density internal core improves the dynamic properties by increasing the natural frequencies of the frame [53]. The third reason for reducing the foam weight and hence reducing its material properties is that the finite-element model does not consider the presence of an internal core at all. The foam core is there to separate the left and right shells of the frame, but does not contribute to the structural properties. Based on those 3 reasons, it seems reasonable to reduce the foam density. Hence, any core present even with low mechanical properties will improve the overall integrity of the frame. The new foam was also very easy to shape. The overall foam core had to be made out of 3 pieces as the thickness of the foam was not enough for the required thickness at the rear stays of the frame. The 3 parts are respectively the main body, the left and the right rear stays.

5.4.2 Foam Adhesives

As for prototype 1, the 3 foam pieces were fastened together using Ciba-Geigy's fastweld epoxy adhesive [70]. See section 5.3.2 for further adhesive properties.

5.4.3 Inserts

Aluminum inserts were again used in order to make the interface between the carbon skin and the bicycle's external components. Inserts were machined for the rear dropouts, the headset, the bottom bracket and the seat tube. The goal for prototype 2 was to reduce the overall weight of the frame, hence an effort was made to reduce the weight of all the inserts to a minimum. The total inserts weight on the first prototype was 603g. A goal to reduce the weight of the inserts by 50% was set forward for this second prototype.

As a result of a study on carbon-aluminum-foam interfaces made by undergraduate students [75] it was shown that the required load transfer surface from the carbon skin to the aluminum inserts was much smaller than expected. The design thus concentrated on producing inserts that were very light, while still allowing for adequate bonding and attachment capabilities.

Headset

The headset of prototype 2 is made from two separate pieces. The first piece is a cylindrical section which will accommodate the headset bearings. The second part is a plate which is bent around the cylinder and bonded to it. It is bonded to a recessed portion of the cylinder in order to permit the 0.9 mm plate to be supported from the bottom. The two aluminum pieces were bonded together using Loctite 330 Depend no-mix adhesive [76]. This adhesive is suitable for structural fastening as was required here. As the fastening surface was quite large (approximately 2500 mm^2), the bonding is quite adequate. The total weight of the headset is 58g (30g for the plate and 28g for the cylinder). Figure 5.8 shows the head tube cylinder while Figure 5.9 shows the head tube plate.

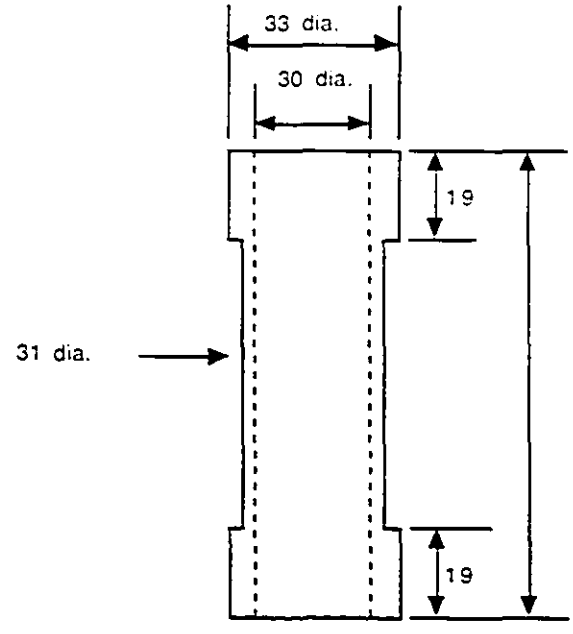

Figure 5.8: Head Tube Cylinder (all dimensions in mm)

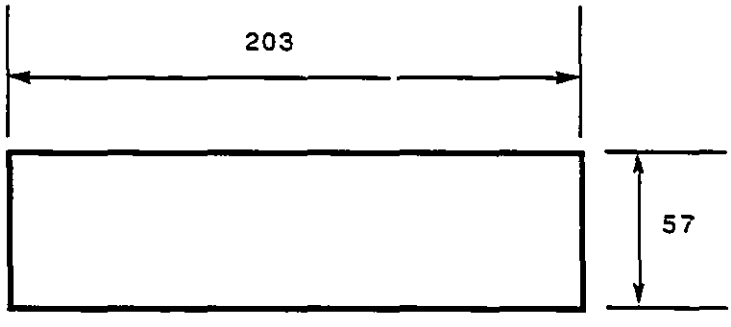

Figure 5.9: Head Tube Plate (all dimensions in mm)

Bottom Bracket

The bottom bracket is made of 3 parts. It contains the bottom bracket cylinder which goes through the frame and one plate recessed in the foam on both sides of the frame in order to secure the cylinder in place. The bottom bracket cylinder is internally threaded with a 1.370X24 left handed thread at one extremity and a right handed thread at the other (standard procedure). These threads were cut in order to meet with the bottom bracket cartridge pedal case. Both bottom bracket plates recessed in the foam were bonded to the

foam using Ciba-Geigy's Fastweld adhesive [70] and bonded to the cylinder using the Loctite 330 Depend adhesive [76]. Figure 5.10 shows the bottom bracket cylinder insert. The weight of the bottom bracket cylinder was 49g while the two end plates weighed 10g each.

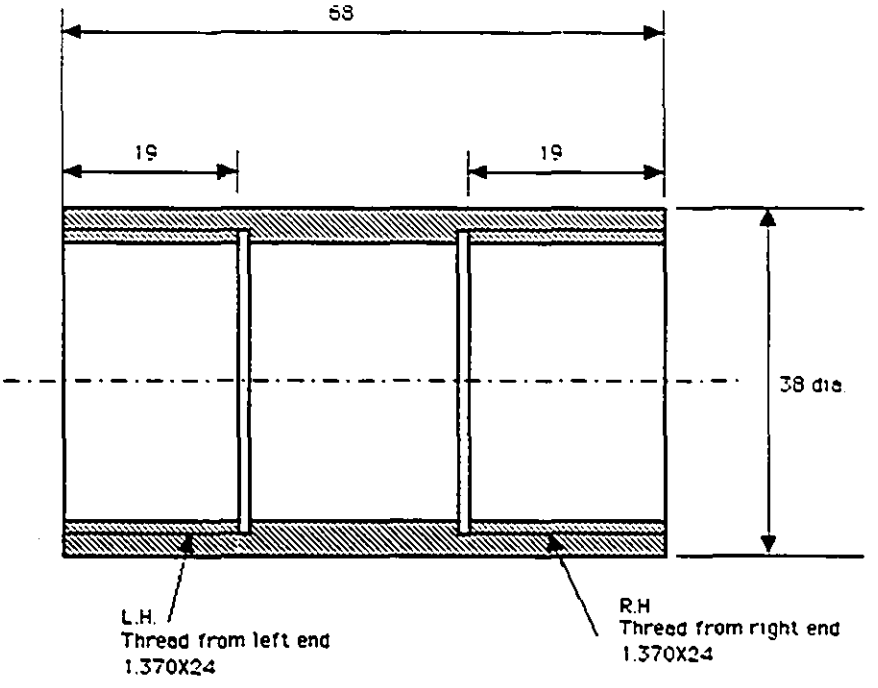

Figure 5.10 : Bottom Bracket Insert

Rear Dropouts

One of the major improvements in the insert design was the rear dropouts. The design for prototype 1 was made by welding 4 aluminum pieces together. The result was a very heavy structure weighing on the order of 170g for each dropout. The rear dropouts for prototype 2 were made by machining one aluminum piece with no welds. It resulted in a much more compact design at a weight of 29g for each dropout.

Seat Tube

A seat tube with an external diameter of 28.6 mm diameter and an internal diameter of 26.7 mm diameter was inserted 360 mm into the foam core. The seat tube was bonded to the foam core using Ciba-Geigy's Fastweld adhesive [70]. The weight of the seat tube was 64g. The seat tube insert is shown in Figure 5.11.

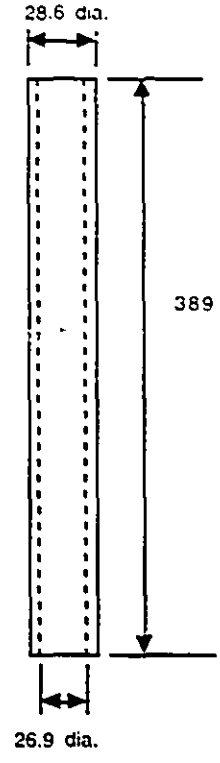

Figure 5.11 : Seat Tube Insert (all dimensions in mm)

5.4.4 Foam-Aluminum Adhesive

Similar to prototype 1, after the inserts had been machined, they were glued to the foam core while the frame was in the curing jig, in order to make sure that the frame and the inserts were in perfect alignment. Before the inserts were glued to the foam core, they were thoroughly etched using West System's aluminum etching kit [71]. This surface treatment for aluminum cleans the surface and applies to it a protective coating which

prevents the oxidation at the aluminum-foam or aluminum-carbon interface. The adhesive used was the Fastweld epoxy by Ciba-Geigy [70].

5.4.5 Internal Shifting Cable

A shifting cable was embedded in the foam core before the application of the carbon fiber material. The purpose of this cable is to activate the rear derailleur from the handlebars. An internal routing method was chosen for both aerodynamic and aesthetic reasons. It was held in place on the foam with Ciba-Geigy's Fastweld epoxy adhesive [70].

5.4.6 Carbon Fiber Material

The material used for the construction of this prototype was woven material obtained from the Advanced Composite Group Inc. [61]. It is the same as was used for prototype 1. However, no unidirectional material was used on this frame. The reason for not using unidirectional material was discussed in section 4.2.2.2.

5.4.7 Material Orientation

The material orientation used for this prototype was consistent with the finite-element model as much as possible. The exact matching of material orientation between the finite-element model and the finished prototype is virtually impossible. If proper patterns are prepared before the lay-up is done, a better match between theory and practice can be achieved. Refer to section 4.2.2.2 for the development of the laminate.

5.4.8 Vacuum Bagging

After the layers of carbon fiber were applied over the frame, the other vacuum bagging materials were applied on the frame. The release film and vacuum bag were thus applied and vacuum drawn from under the bag. Before the introduction in the oven, the last air leaks were removed to in order to assure a proper vacuum. A vacuum of 0.9 atm was obtained under the vacuum bag. Figures 5.12, 5.13 and 5.14 show 3 stages of the layup process

Figure 5.12 : Proto. 2 - Prepreg Application

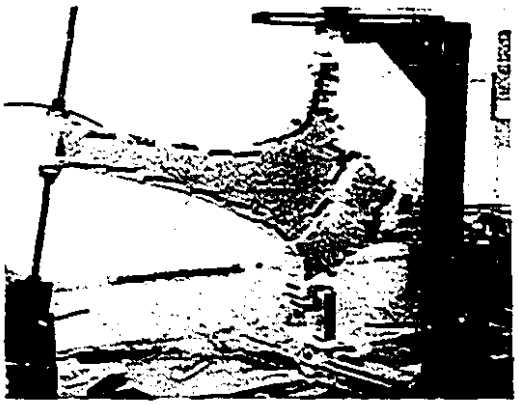

Figure 5.13: Proto 2.- Release Film

Figure 5.14: Vacuum Bag Applied to the Frame

5.4.9 Curing

The curing cycle for prototype 2 was exactly the same as for prototype 1, hence refer to section 5.3.9 and Figure 5.6 for further details.

5.4.10 Final Assembly of Prototype 2

Prototype 2 was completely assembled with standard bicycle components. No front derailleur nor rear brake was mounted on the prototype. The reason for not including these features was to keep the design and manufacturing as simple as possible. As the front brake is mounted directly on the front fork, no provision had to be made for brakes on the frame. The utility of a front derailleur was not completely necessary as the use of this frame is still experimental, thus the 8 speeds provided by the rear cog gears are sufficient for road testing. Table 5.4 gives an account of the components which were mounted on prototype 2.

Front fork	Columbus Foderi Laminati
Front brake	Modolo Sporting
Bottom bracket cassette	Shimano BB UN-51
Seat post	Gipiemme
Seat	Gipiemme
Pedal cranks	Gipiemme
Pedals	Gipiemme
Front wheel	Specialized 3-spoke composite
Rear wheel	Mavic 3G
Front chainring	52 teeth Gipiemme
Rear derailleur	Shimano 600
Cogs	8 speed, 12-23 Shimano 600
Head set	Shimano 105
Handlebars	Profile bars mounted on normal road handlebars
Ergolevers	Shimano 600 shift/brake levers

Table 5.4 : Components

5.4.11 Mass Properties of Prototype 2

Table 5.5 shows how each subgroup contributes to the final weight of prototype 2.

Prototype 2	Weight (g)
Foam	402
Aluminum Inserts	255
Glue and Filler	62
Composite Material	972
Total	1691

Table 5.5 : Summary of Weights for Prototype 2

5.4.12 Improvements and Conclusions for Prototype 2

Prototype 2 was an immense improvement from prototype 1. In addition to the overall structure geometry which is much more efficient at distributing the rider induced loads, the overall design and fabrication of this prototype is very much improved. Prototype 2 has better designed inserts which are much smaller in size and thus lighter. Also, the internal foam core is thinner and made from a lighter material. All in all, there were improvements realized over prototype 1. It is clear that other improvements could be made if other prototypes were built. The main feature which could be improved upon is the surface finish. The vacuum bagging method makes a rather questionable surface finish on pieces of irregular cross section. Also, the use of exterior molds on an internal bladder technique would eliminate the need for a foam core. However, with the resources available, prototype 2 satisfied its goal as being a rideable carbon fiber monocoque frame of acceptable quality. Figure 5.15 shows the finished prototype 2 with all the components attached, ready to be ridden.

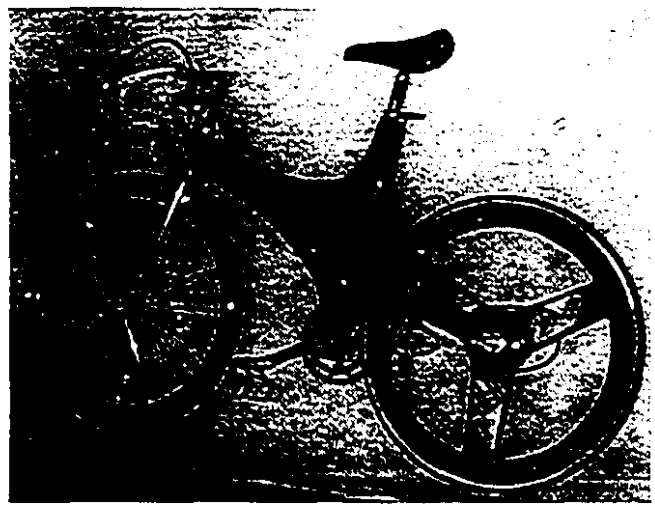

Figure 5.15 : Finished Prototype 2

5.5 Composite Frame Testing

It is essential to test the produced frames in order to assess whether the final constructed product is compatible with the computer elaborated model. To do this, it is essential to chose a method for measuring the similarity or difference between the modeled and constructed versions. It is clear that it is impossible to statically test the constructed prototypes under riding load conditions as too many restraints and loads render this solution impractical. Thus the same tests as those performed on the conventional frames will be performed on the constructed monocoque carbon fiber prototypes. Also, using the same tests will allow comparison between the composite and tubular metallic frames. Hence 2 of the 3 tests described in section 3.3.4 will be performed on the two constructed carbon fiber prototypes.

5.5.1 Prototype 1 Test Results

As mentioned earlier, prototype 1 was not constructed as being a rideable model. It was constructed in order to better understand the finite-element modeling and to familiarize ourselves with the manufacturing aspects. After its construction, prototype 1 was tested in the specially built testing jig shown in chapter 3. Test 1 and 2 were performed on this

prototype. Table 5.6 shows the experimental results obtained for the two different tests combined with the finite-element results obtained for the same load and restraint sets.

Prototype 1	Test 1 (mm)	Test 2 (mm)
FEA	2.70	14.76
Experimental	2.50	14.5
Difference %	8.0	1.8
Tange Prestige (Steel)	0.53	18.6
Trek 1100 (Al.)	1.14	34.1

Table 5.6: FEA and Experimental Results for Prototype 1

From these results, observe that the finite-element results agree surprisingly well with the experimental results. This gives confidence in further finite-element simulation and confidence that the chosen lay-up for further prototypes under the riding case would be appropriate. The error margins for the composite frames are even smaller than for the comparison between the experimental and finite-element results for the tubular frames shown in Table 3.2. This might arise from the fact that shell elements are much better suited to flat skin structures like the composite frames, rather than curved surfaces as those used for modeling traditional frame tubes. The most important observations from this Table are the values obtained for both test 1 and 2 for prototype 1 compared to the best aluminum and steel frames tested. Prototype 1 is 28% stiffer in the out-of-plane direction (test 2) than the Rocky Mountain frame and 4.7 times more compliant in the in-plane direction as shown by test 1. From these results, we can observe that some of the initial goals were obtained. Prototype 1 is made from an internal foam core 75 mm thick. This large thickness assures rigidity in the out of plane direction. Hence, for this particular prototype, because of its thickness, the design shifts from being stiffness-based to being strength-based as the extra internal core thickness allows for an increased out-of-plane rigidity.

5.5.2 Prototype 2 Test Results

As for prototype 1, prototype 2 was experimentally tested. Table 5.7 shows the results of test 1 and 2 performed both using the FEA approach and experimentally. The Table also includes, for comparison purposes, the results for prototype 1, the best steel frame and the aluminum frame.

Prototype 2	Test 1 (mm)	Test 2 (mm)
Prototype 2-FEA	2.69	14.36
Prototype 2- Exp.	2.54	13.73
Difference (%)	5.9	4.6
Steel-Tange Prestige	.53	18.6
Aluminum-Trek 1100	1.14	34.1
Prototype 1- Exp.	2.5	14.5

Table 5.7 : FEA and Experimental Results for Prototype 2

Note again that the experimental and FEA results agree quite well. As a result of the experimentation with prototype 1, and the fact that the same care was taken for the study of prototype 2, it is not surprising that close results were obtained between the experimental and FEA study. Prototype 2 shows an out-of-plane rigidity 5.6% better than prototype 1 even though prototype 2 is 33% thinner and has an overall weight almost 500g less than prototype 1. Also, it shows an in-plane resilience very similar to prototype 1. The most important aspect to remember from this Table, which is basically a summary of this research, is that it is possible to design a monocoque composite frame using FEA which corresponds closely to the fabricated prototype. In addition, this constructed frame can, at a lower weight, exhibit more desirable features than the conventional traditional tubular frames.

5.6 Summary

The first part of this chapter has shown the procedure for the construction of the two carbon fiber monocoque frames. Although the fabrication procedure chosen could only apply to the construction of prototypes, it has shown to be very appropriate for this purpose. The weight and surface finish of both prototypes could be improved with the use of another production method. Using another production method, such as an internal bladder technique, could reduce the weight of the frames to the range of the lightest on the market (1.2kg) while still showing excellent stiffness attributes compared to other light frames which are usually extremely flexible.

The second part of chapter 5 was concerned with the testing of the fabricated frames and comparison with metallic tubular frames tested under the same conditions using the same apparatus. The results have shown the composite frames to be stiffer in the out-of-plane direction and more resilient in the in-plane direction, two attributes which are beneficial for a bicycle frame. It is thus encouraging to observe that the initial goal set forth has been met: to produce a carbon fiber monocoque frame with directionally tailored properties.

Chapter 6

Conclusion

The methodology for designing composite bicycle frames illustrates the importance of using finite-element analysis as a way of minimizing the cost and time required for different designs. The analysis can be effective for determining both geometry and laminate design to obtain better strength and stiffness characteristics than traditional tubular frames. The three carbon fiber monocoque frame designs presented are a result of this design process. From these designs, it is evident that a carbon fiber frame should be built using many different laminates which correspond to the different stress regions as the goal should be to have a structure with a uniform stress level throughout. The addition of local reinforcement has been shown to reduce local stresses. Local reinforcement can be added to the frame with a minimum increase in overall weight.

Finite-element analysis was also used to numerically compute frame stiffnesses in order to compare with experimental results performed on tubular and composite frames. Frame stiffness is important when attempting to design the frame for performance and rider comfort. When discussing the stiffness of frames, it is actually the directional stiffness that the designer should be concerned with as torsional stiffness is desirable while in-plane stiffness is not. While frame stiffness is inherently involved in the process, it is the interaction of the biomechanical characteristics of the individual rider with the bicycle that ultimately determines whether the bicycle has a feel that is too "soft" or too "stiff". Determination of how the quantifiable frame stiffness characteristics relate to the qualitative description of what the rider senses is an important factor to consider further. It has been successfully shown that with simple tests, different important frame stiffnesses can be measured and can be used to quantify the quality of different frames.

The preliminary static testing of traditional frames was essential to this research as it permitted the development of the testing methods which would be used for the carbon fiber prototypes both experimentally and numerically. The traditional frames produced results which were found to be invaluable for comparison with the constructed carbon fiber prototypes. As a result of this testing, it was shown that the constructed carbon fiber frames showed stiffness attributes which were clearly superior to the best traditional frames examined. It is important to note that this improvement was predicted with the finite-element analysis even before the first carbon fiber frame was constructed.

The second part of this research was the development of a manufacturing technique for composite material bicycle frames. The method chosen provided, at low costs, the most flexible means of producing prototypes. The hand layup of prepreg carbon/epoxy material to an internal foam core was ideal for prototype modeling. The main inconveniences which resulted from this method are the final surface finish, which is clearly inappropriate for a marketable product, and the impossibility of removing the internal core after curing. In a production situation, it would be essential to remove the internal core since in the prototypes it contributes 25 to 40% of the finished frame weight. Prototype 1 achieved its goal of being a trial prototype for the finite-element method, fabrication method and to develop the testing procedures. Prototype 2 also matched its goal of being a rideable and adequate pre-production prototype.

In addition to its high strength and stiffness properties, it is the versatility of carbon fiber which makes it an excellent material for lightweight structures. Bicycle frames are an excellent example of successful application of this material.

Chapter 7

Recommended Further Research

As future and complementary research, several other aspects of composite bicycle design should be examined in order to obtain a complete study. With respect to the finite-element modeling, it would be interesting to model the frame using solid elements for the internal core. A more detailed analysis could be performed on the metal/composite interfaces at the joint locations. This could include consideration of titanium as a more compatible material for use as inserts. Also, in addition to the use of reinforcement, geometric redesign of certain regions should be considered in order to reduce the stresses to a minimum. Both finite-element and experimental dynamic loading should be performed in order to assure the structural integrity, for example, due to high rate impact. Experimental fatigue testing should be performed on the frames in order to assure long term structural integrity even though carbon fiber is known to have excellent fatigue resistance. The complete series of standards bicycle tests should be imposed on the prototypes in order to assure that the production models would respect those standards.

This study was focused on the bicycle frame structural design, but aerodynamic testing should be performed in order to reduce the frame drag. Minute changes to structural cross-sections may produce a huge reduction in aerodynamic drag.

Further research and work on the fabrication method to be used should be performed. Both the fabrication method of the prototypes and the fabrication method for large scale production should be further examined. An appropriate, low cost moulding procedure should be devised.

Last but not least, there is a potential for further research in non-conventionnal composite frame building materials. It seems that a thermoplastic matrix combined with new fibers such as Vectran or Dynema could potentially revolutionize frame building, both in the quality of the products and in the marketing appeal which would emanate from the use of these new materials.

Different geometries and loading cases could also be elaborated for different types of uses such as mountain biking, triathlon, olympic pursuit and even touring.

Analysis of the complete frame as part of a complete dynamic system comprising of all other components such as the front fork and wheels. A study of this type would fully characterize the response of a frame in a realistic situation with the interaction of all the components.

Publications Resulting from this Work

A) Patrick L. Lizotte, Larry B. Lessard, James A. Nemes, "Design of Advanced Bicycle Frames", ATMAM 1994, Montreal, August 10-12 1994, pp. 90-97.

B) Larry B. Lessard, James A.Nemes, Patrick L.Lizotte, "Utilization of FEA in the Design of Composite Bicycle Frames", *Composites*, Vol 26, Number 1, pp 72-74, 1995.

C) Patrick L. Lizotte, Larry B. Lessard, James A. Nemes, "Stress and Failure Analysis of Composite Bicycle Frames", ICCM-10, Whistler B.C., August 14-18 1995, Vol.III, pages 701-708 .

References

1- Perry, D.B., Bike Cult, Four Walls Eight Windows, New-York and London, 1995.

2- Rowland, F.W., and Wilson, D.G.,Bicycling Science, Second Edition, MIT Press, Cambridge Massachusetts, 1982, p. 6.

3- Rowland, F.W., and Wilson, D.G., Bicycling Science, Second Edition, MIT Press, Cambridge Massachusetts, 1982, p. 9.

4- Rowland, F.W., and Wilson, D.G., Bicycling Science, Second Edition, MIT Press, Cambridge Massachusetts, 1982, p. 14.

5- Rowland, F.W., and Wilson, D.G., Bicycling Science, Second Edition, MIT Press, Cambridge Massachusetts, 1982, p. 19.

6- Rowland, F.W., and Wilson, D.G., Bicycling Science, Second Edition, MIT Press, Cambridge Massachusetts, 1982, p. 20.

7- Rowland, F.W., and Wilson, D.G., Bicycling Science, Second Edition, MIT Press, Cambridge Massachusetts, 1982, p. 259.

8- Kukoda, J., "Steel", *Bicycling*, August 1993, pp. 80-83.

9- Editors of Mountain Bike and Bicycling Magazine, Bicycling Magazine Complete Guide to Bicycle Maintenance and Repair, Rodale Press, Emmaus, Pennsylvania, 1994, p.14.

10- Editors of Mountain Bike and Bicycling Magazine, Bicycling Magazine Complete Guide to Bicycle Maintenance and Repair, Rodale Press, Emmaus, Pennsylvania, 1994, p.16.

11- Rowland, F.W., and Wilson, D.G., Bicycling Science, Second Edition, MIT Press, Cambridge Massachusetts, 1982, p. 262.

12- Kukoda, J., "Tubing Tutorial", *Bicycling*, 1991, pp. 120-123.

13- Kukoda, J., "Titanium: The Miracle Metal", *Bicycling*, July 1989, pp. 110-114.

14- Kukoda, J., "Titanium", *Mountain Bike*, November 1990, pp. 5-7.

15- Lessard, L.B., Composite Materials Class Notes, McGill University, 1993, p. 4.

16- Rowland, F.W., and Wilson, D.G., Bicycling Science, Second Edition, MIT Press, Cambridge Massachusetts, 1982, p. 244.

17- Gould, R., "The Bike Built to Win", *New Scientist*, June 30 1990, pp. 49-51.

18- Kukoda, J., "Materials Update", *Bicycling*, May 1988, pp. 90-96.

19- Hult, J., "The Itera Plastic Bicycle", *Social Studies of Science*, **22**, 1992, pp. 373-385.

20- Mallick, P.K., Fiber Reinforced Composites, Second Edition, Marcel Dekker Inc. New-York, 1993.

21- Roosa, D., "A Taste of the Future", *Bicycle Guide*, August 1987, pp. 20-29.

22- "The 1994 Guide to Carbon Fiber Bikes", *Mountain Bike Action*, April 1994, pp. 44.

23- Lai, G., "Aegis", *Bicycle Guide*, November 1994, pp. 34-37.

24- Gruenwedel, E., "Truly World Class", *Winning*, 1992, pp. 62-63.

25- Barnett, J., "Carbon Fiber: Is the Future Here", *Cyclist*, September 1994, pp.26-29.

26- Kestrel 1991 Pre-Saison Dealer Catalog, 1991.

27- Trimble, B.J., *Bicycle Frame*, U.S. Patent #4,513,986, April 30 1985.

28- Trimble, B.J., *Bicycle Frame*, U.S. Patent # Re 33,295, August 14 1990.

29- Trimble, B.J., *Composite Bicycle Frames and Methods of Making Same*, U.S. Patent # 4,889,355, December 26 1989.

30- Trimble, B.J., *Tubular Bicycle Frame*, U.S. Patent # 4,941,674, July 17 1990.

31- Roosa, D., "Graphite Technology Racingbik", *Bicycle Guide*, April 1990, pp. 82-84.

32- Kim, I., "Racers, Rough Riders and Recumbents", *Mechanical Engineering*, May 1990, pp. 52-59.

33- Riedy, M., "Corima Road", *Bicycle Guide*, November 94, pp. 22-26.

34- Zinn, L., "Boardman's World Hour Record Bike", *Velonews*, August 30 1993, p. 22.

35- "Zipp 2001 Road Bike", *Road Bike Action*, November 93, pp. 13-19.

36- "Lemond", Winning, January-February 1994, p. 23.

37- Lai, G., "Beam Bikes", *Bicycle Guide*, September 1994, pp. 29-36.

38- "Mike Burrough's Red Giant", *Bicycle Guide*, November 94, pp. 17-18.

39- Associated Press, "Indurain Sets Record for Distance in Hour", *Montreal Gazette*, Saturday September 3 1994.

40- Guiness, R., "Indurain Breaks 53km Hour Record Barrier", *Velonews*, October 3 1994, p. 21.

41- Whittle, J., "The Final Frontier", *Winning*, November 94, pp. 66-69

42- Vroomen, G., "Design of an Aerodynamic Time Trial Bicycle", Final Year Project, Eindhoven University of Technology, The Netherlands, 1995.

43- "Hotta Time Trial Champ", *Road Bike Action*, March 1995, pp. 56-61.

44- Bolourchi, F., Hull, M.L., "Bicycle Frame Stress by Means of Finite Element Analysis", *ASME DES. ENG. DIV. PUBL. DE.*, Vol.11, 61-72, 1987.

45- Redcay, J., "CAD Comes to Cycling", *Bicycling Science*, April, 105-115, 1986.

46- Peterson, L.A., Londry, K.J., "Finite Element Structural Analysis: a New Tool for Bicycle Frame Design", *Bike Tech*, Vol.5, No.2, 1-9, 1986.

47- Lizotte, P.L., Lessard, L.B., Nemes, J.A., "Design of Advanced Bicycle Frames", *ATMAM 1994*, Montreal August 10-12, 1994.

48- Davis, R.R., Hull, M.L., "Design of Aluminum Bicycle Frames", *Journal of Mechanical Design*, vol.103 no.4, 901-907.

49- ISO 4210 Bicycle Standard, Organisation Internationale de Normalisation, Geneva, Switzerland, 1993.

50- JSA 9401 Bicycle Standard, Frame-Fork Assembly for Bicycles, *Japanese Standards Association*, Tokyo, Japan,1995.

51- Committee for Bicycling Standards, ASTM (American Society for Testing and Materials), Philadelphia, PA, established 1995.

52- Flanagan, T.M., Dyer, R.M., "Composite Monocoque Bicycle", *38th International SAMPE Symposium, Anaheim California*, May 10-13 1993, pp. 293-305.

53- Castejon, L., et al., "Composite Monocoque Frame for a Mountain Bicycle: Testing and Calculations", *Applied Composite Materials*, **1**, pp. 247-258, 1994.

54- Macmartin, B., "Carbon Fiber Monocoque Frame Design for Mountain Bikes", Bulletin d'Information, CACSMA, Vol. 7, no.1, March 1994, p. 4.

55- Eckold, G., Design and Manufacture of Composite Structures, McGraw-Hill Inc., New-York, 1994, p.268.

56- SDRC I-DEAS version 6, Integraded Design Engineering Software, user manual, Structural Dynamics Research Corporation, Milford, OH, 1991.

57- Roy, M., Chabot, G., and Lavin, A., "Bicycle Frame Testing Jig", Design 3 Final Report, McGill University, 1994.

58- SDRC I-DEAS version 6, Integraded Design Engineering Software, user manual, Structural Dynamics Research Corporation, Milford, OH, 1991.

59- Devallée, R., and Tizi, J-P., "Conception et Calcul de Structure d'un Velo en Matériaux Composite", Projet de Fin d'étude, Ecole National d'Ingénieurs de Metz, France, Juin 1993.

60- Union Cycliste International, Rule 49, May 1994.

61- The Advanced Composite Group, Technical Manual, Tulsa, Ok, 1994.

62- Hull, M.L., Bolourchi, F., "Contribution of Rider Induced Loads to Bicycle Frame Stress", *ASME DES. ENG. DIV. PUBL. DE.*, vol.1, 25-28, 1986.

63- "Pour la Science", February 1984, pp. 69-72

64- Rowland, F.W., and Wilson, D.G., Bicycling Science, Second Edition, MIT Press, Cambridge Massachusetts, 1982, p. 281.

65- Rowland, F.W., and Wilson, D.G., Bicycling Science, Second Edition, MIT Press, Cambridge Massachusetts, 1982, p. 37.

66- Rowland, F.W., and Wilson, D.G., Bicycling Science, Second Edition, MIT Press, Cambridge Massachusetts, 1982, p. 52.

67- Rowland, F.W., and Wilson, D.G., Bicycling Science, Second Edition, MIT Press, Cambridge Massachusetts, 1982, p. 46.

68- Tsai, S.W., and Hahn, H.T., "Introduction to Composite Materials", Technomic, 1980.

69- Dufresne, S., Godin, S., Munger, S., "Analysis, Testing and Sampling of a Composite Bicycle Frame", Mechanical Laboratory II Final Report, McGill University,April 1993.

70- Formulated Systems Group, Ciba-Geigy Corporation, Araldite Fastweld Adhesive, East Lansing, Mi.

71- Gougeon Brothers Inc, 1994 West System Technical Manual, 860-8 Aluminum Etching Kit, Bay City, Mi.,1994.

72- Grégoire, S., Jones, A., Kiley, L., Lavergne, N., and Nour, S., "Curing Jig", Design III Final Report, McGill University, 1994.

73- Adchem Corporation, Adbond High-strength Adhesive, 5300 A resin and 5300 B hardener.

74- Divinycell International, Technical Specifications, H-grade, De Soto, Texas.

75- Gervasi, P., Bégin, P-A., and Rahman, T., "Manufacturing and Experimental Investigation of a Composite Beam Under Pure Bending & Torsion", Mechanical Laboratory II Final Report, McGill University, April 1994.

76- Loctite Corporation, Depend 330 Technical Sheet, Mississauga, Ontario.